Electronic Supplementary Information for "On the interactions between RNA and titrateable lipid layers: Implications for RNA delivery with lipid nanoparticles"

Jennifer Gilbert,[ab] Inna Ermilova,[c] Marco Fornasier[a], Maximilian Skoda[d], Giovanna Fragneto[ef], Jan Swenson[c] and Tommy Nylander[abg*]

[a] *Division of Physical Chemistry, Department of Chemistry, Naturvetarvägen 14, Lund University, 22362 Lund, Sweden.* [b] *NanoLund, Lund University, Professorsgatan 1, 223 63 Lund, Sweden.* [c] *Department of Physics, Chalmers University of Technology, 412 96 Gothenburg, Sweden.* [d] *ISIS.* [e] *ILL.* [e] *ESS.* [g] *Lund Institute of Advanced Neutron and X-Ray Science, Scheelevägen 19, 223 70 Lund, Sweden.*
[*] *Corresponding author: tommy.nylander@fkem1.lu.se*

Contents

1 General information

1.1 Neutron reflectometry

For plots with qualitative comparison of data sets from different samples, all data was rescaled so that the critical edge in D_2O was 1 and the H_2O and CMSi contrasts for the sample were rescaled with the corresponding D_2O scale factor. For fitting, the scale parameter was allowed to vary to account for this.

1.1.1 Calculation of scattering length density (SLD)

All atomic scattering lengths were taken from Sears[1].

Lipid	Molecular volume (Å^3)	SLD (10^{-6}Å^{-2})
MC3	1290*[2]	0.09
MC3 Head	274**	0.69
MC3 Tail	1016***[3]	-0.07
DOPC	1295[4]	0.30
DOPC Head	319[5]	1.88
DOPC Tail	976****	-0.21

Table S1 Lipid (partial) molecular volumes and SLDs. *Calculated from density in Arteta et al.[2]. **Calculated by subtracting volume of tail from volume of lipid. ***Calculated using component volumes from Armen et al.[3] ****Calculated by subtracting volume of head group from volume of lipid from Greenwood et al.[4].

Contrast	polyA 10^{-6}Å^{-2}	polyU 10^{-6}Å^{-2}	EPO mRNA 10^{-6}Å^{-2}
H2O	3.56	3.27	3.45
CMSi	3.93	3.55	3.87
CMRNA	4.20	3.75	4.16
D_2O	4.55	4.00	4.55

Table S2 Nucleic acid SLDs were calculated using the Biomolecular Scattering Length Density Calculator (http://psldc.isis.rl.ac.uk/Psldc/) assuming 100% exchange and 0% deuteration.

1.1.2 Fitting and model description

The substrate was described as a silica layer (slab described with a thickness (fitted), SLD (fixed = 3.47 x 10^{-6}Å^{-2}), substrate roughness (fitted), hydration (fitted)) with a silicon backing. All models described below include this silica layer with parameters fixed from separate fitting of the bare substrate. All models were simultaneously fit using at least 3 solvent contrasts: D_2O = 100% D_2O, CMSi = 38% D_2O, H_2O = 0% D_2O, with an additional CMmRNA contrast (= 35% D_2O) for 15% MC3 pH6 samples after incubation with polyA or polyU. Common model parameters were constrained to the same in each contrast, including certain slab parameters and the scale([lower bound = 0.9, upper bound = 1.1]) and the SLD of the solvent was allowed to vary within a reasonable range to account for contamination/incomplete buffer exchange (D_2O SLD: [5.8, 6.36], CMSi SLD: [1.6, 2.2], H_2O SLD: [-0.56, 0]). The background was allowed to fit independently for each contrast (bkg: [-1x10^{-6}, 1x10^{-5}]). After fitting, if the parameter values were very close to or hit any limits in the fitting range (which could be observed in the Bayesian posterior distributions), the fit was run again with wider limits as long as this was physically reasonable.

Lipid leaflet based bilayer model. The lipid leaflet model contains four slabs corresponding to inner leaflet head groups (slab 1), inner leaflet tails (slab 2), outer leaflet tails (slab 3) and outer leaflet head groups (slab 4). The slab parameters are constrained by physical lipid parameters, including lipid area per molecule (APM: [50, 120]) to ensure the correct stoichiometry between the head group and tail slabs and molecular volume of the lipids and water and number of waters per lipid head or tail (WPLH: [0, 30], WPLT: [0, 20]) to fit the volume fraction of solvent (vf) and thickness. The SLD of the slab was defined by the weighted average of the SLDs of the (parts of the) lipids in each slab. The roughness ([3, 25]) was constrained to be the same for each lipid leaflet slab. This model assumes a symmetric bilayer.

Bilayer + water layer. In addition to the model described above, an additional slab to describe a water interlayer was included between the silica layer and the inner leaflet head group slab. The interlayer slab was described by a vf (fixed = 1), roughness (fixed = roughness of silica layer) and thickness (fitted, [0, 20]). This model assumes a symmetric bilayer.

Three slab. This model has three slabs and is more general with the aim to model something more similar to the simulation results for the uncharged MC3, therefore does not require the MC3 and DOPC head groups to be in the same slab. The fitting ranges for the slab SLDs and thicknesses were defined by the highest/lowest SLD of the expected components in the slab (assuming slabs 1 and 3 are similar to lipid head groups: SLD = [1, 1.88], thickness = [0, 15] and slab 2 is similar to the hydrophobic region: SLD = [-0.4, 0], thickness = [20, 45]) and the vf was allowed to vary from 0 to 1. The roughness ([0, 20]) was constrained to be same for each slab. This model does not assume slab 1 = slab 3.

Four slab. In addition to the 3 slabs described above, an additional slab was included between slab 2 and 3 (from the 3 slab model) to describe the hydrophobic region with the same parameter ranges as slab 2 (from the 3 slab model except thickness = [10,25]). This does not assume that any of the slabs are the same.

Mixed area model: Bilayer + stack A mixed area model is a linear combination of the two models with the contribution from each model (i.e. the area they cover) described using a scale factor. This mixed area model is a combination of the bilayer model described above and a repeating stack of 2 slabs. This model was fit to samples where a broad peak was observed after incubation of the lipid layer with an NA. For the mRNA samples where this peak was observed (10 and 15% MC3 in pH6 and 15% MC3 in pH7), the NR curves overlap well except at high q for 15% MC3 pH7 where this difference was already observed in the NR curve for the lipid alone (see Figure S28). This indicates that the lipid layer structure is not strongly affected in the non-multilayer regions, therefore the lipid leaflet parameters were fixed to those determined from fitting the lipid layer alone. For both slabs in the stack, the vf was allowed to vary over the full range of 0 to 1, the thickness ([1, 80]) between 1 and approximately the repeat distance calculated from the peak position (76 Å) and the roughness was constrained to be the same for both slabs and allowed to vary (minimum = substrate roughness, [3, 20]). The SLD range was based on the assumption of an mRNA rich layer ([0.5, 4.55]) and a lipid rich layer ([-0.2, 2.0]) from prior knowledge and initial manual fitting. It was assumed that the vf of the slab described SLD change of the NA in different solvent contrasts due to exchangable hydrogens.

Bilayer (fixed) + slab This model was aiming to describe the 15% MC3 pH6 sample after incubation with polyA, where a clear increase in adsorbed mass was observed in QCM-D (Figure 7) but there is very little change observed in the NR curve (i.e. the multilayer peak is not clearly observed). This model consists of a bilayer (fixed to the fitted parameters for the lipid layer alone) with a single slab on top. The single slab parameters were the same as described above assuming an mRNA rich layer.

Mixed area model: Bilayer (varying) + slab This mixed area model is a combination of a bilayer model (fixed to the fitted parameters for the lipid layer alone) and a bilayer (varying within the bounds stated previously for this model) with a single slab on top. The single slab parameters were the same as described above assuming an mRNA rich layer. This model takes into account the possible changes to the bilayer structure induced by the adsorbed polyA.

1.2 Lipid models: partial atomic charges

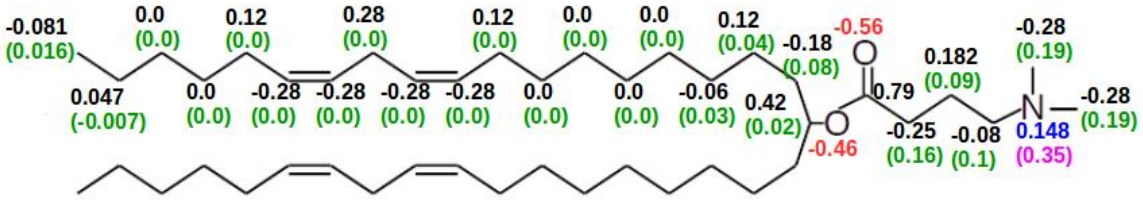

Figure S1 Partial atomic charges for ionized DLin-MC3-DMA. Colors of charges: black - carbons, green - hydrogens, red - oxygens, blue - nitrogen, magenta - charged hydrogen. Charges are represented in electron charge units. The second lipid tail has the same charges as the first one. The total charge of the lipid is equal to +1.

2 Lipid layer

2.1 QCM-D

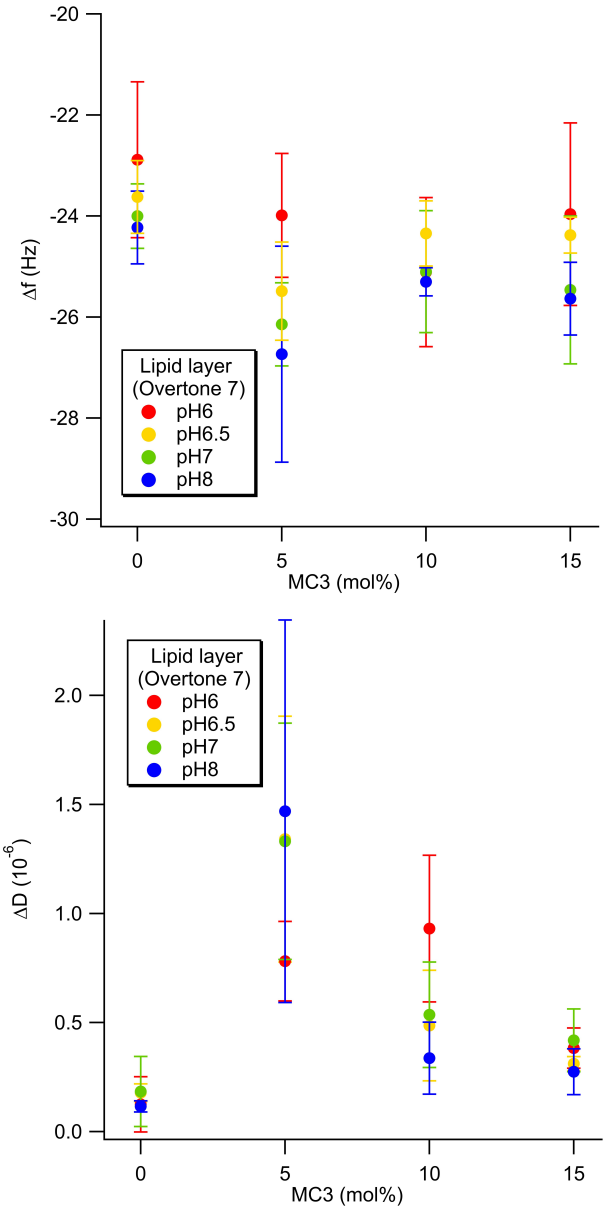

Figure S2 The change in frequency (top) and dissipation (bottom) for the 7th overtone after equilibration for the lipid layers before incubation with nucleic acids.

2.2 Simulation: Mass density profiles

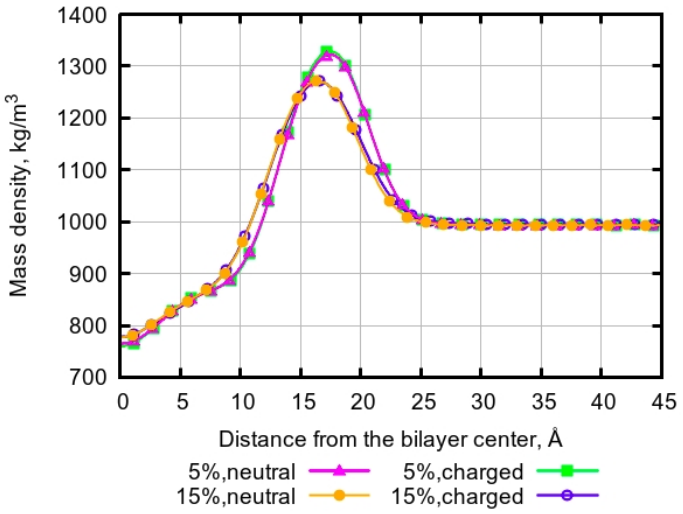

Figure S3 Mass density profiles for simulations without NA.

2.3 NR: Model comparison

2.3.1 Lipid layer in pH 6 samples: Bilayer vs Bilayer + water layer

For the 5, 10 and 15% MC3 lipid layers in pH6 buffer, two models were compared; bilayer and bilayer + water layer. For all of the lipid compositions in pH6 buffer, adding a water layer did not result in an improvement of the global χ^2 (Table S5) compared to the bilayer fit. The fitted water layer thickness was 0 Å or almost 0Å for all samples. Except for WPLH, for both 10 and 15% MC3, the fitted parameters values were the same for the bilayer and bilayer + water layer fit within error, whereas for 5% MC3, the WPLH and roughness changed. As expected, adding the water layer mostly affected the parameters describing the silica-lipid head group interface. Additionally, a correlation can consistently be observed between water thickness and WPLH (and APM to a lesser extent) in the Bayesian posterior distributions (Figures S9, S10, S11). For the 10% MC3 sample, introducing the water layer resulted in bimodal posterior distributions in the Bayesian analysis indicating that there are 2 structures that fit the data. This can be seen for the following parameters: roughness, WPLT, WPLH, APM and water thickness. (Figure S10), whereas for the bilayer fits for all pH6 samples these distributions were monomodal (Figures S6, S7, S8). Unsurprisingly when plotted, both fits are almost indistinguishable (Figure S4).

The volume fraction profiles for each sample were plotted for the bilayer model fit in Figure S5 and were similar for all of the lipid layers in pH 6 buffer. The main difference was observed between the 5% MC3 layer to the higher %MC3, as the slightly higher WPLH and bilayer roughness for the 5% MC3 layer resulted in a higher volume fraction of solvent in the head group (Figure S5(a)).

Bilayer	5% MC3 pH6	10% MC3 pH6	15% MC3 pH6
WPLH	11.0 ± 0.4	9.5 ± 0.4	10.6 ± 0.4
APM	68.0 ± 0.4 Å^2	69.2 ± 0.4 Å^2	68.1 ± 0.3 Å^2
WPLT	0.1 ± 0.1	0.1 ± 0.1	0.02 ± 0.03
Bilayer roughness	4.4 ± 0.2 Å	3.7 ± 0.2 Å	3.1 ± 0.1 Å
Scale	0.931 ± 0.004	0.913 ± 0.004	0.959 ± 0.003

Table S3 Bilayer fit parameters for 5, 10 and 15% MC3 lipid layers in pH6 buffer.

Bilayer + water layer	5% MC3 pH6	10% MC3 pH6	15% MC3 pH6
WPLH	9.7 ± 0.6	5 ± 4	9 ± 1
APM	68.6 ± 0.4 Å^2	70.2 ± 0.8 Å^2	68.6 ± 0.5 Å^2
WPLT	0.9 ± 0.2	0.5 ± 0.3	0.06 ± 0.07
Bilayer roughness	3.2 ± 0.2 Å	3.9 ± 0.7 Å	3.1 ± 0.1 Å
Water layer thickness	0.1 ± 0.1 Å	1 ± 2 Å	0.5 ± 0.4 Å
Scale	0.929 ± 0.003	0.913 ± 0.004	0.958 ± 0.003

Table S4 Bilayer + water layer fit parameters for 5, 10 and 15% MC3 lipid layers in pH6 buffer.

Model	5% MC3			10% MC3			15% MC3		
	D_2O	CMSi	H_2O	D_2O	CMSi	H_2O	D_2O	CMSi	H_2O
Bilayer	2.2	2.2	2.1	1.7	2.6	2.1	1.6	2.1	3.4
Bilayer+WL	2.4	2.0	2.3	1.8	2.5	2.2	1.7	1.9	3.4

Table S5 Comparison of normalised χ^2 values for fitting with a bilayer model or a bilayer + water layer (WL) model for 5, 10 and 15% MC3 lipid layers in pH6 buffer.

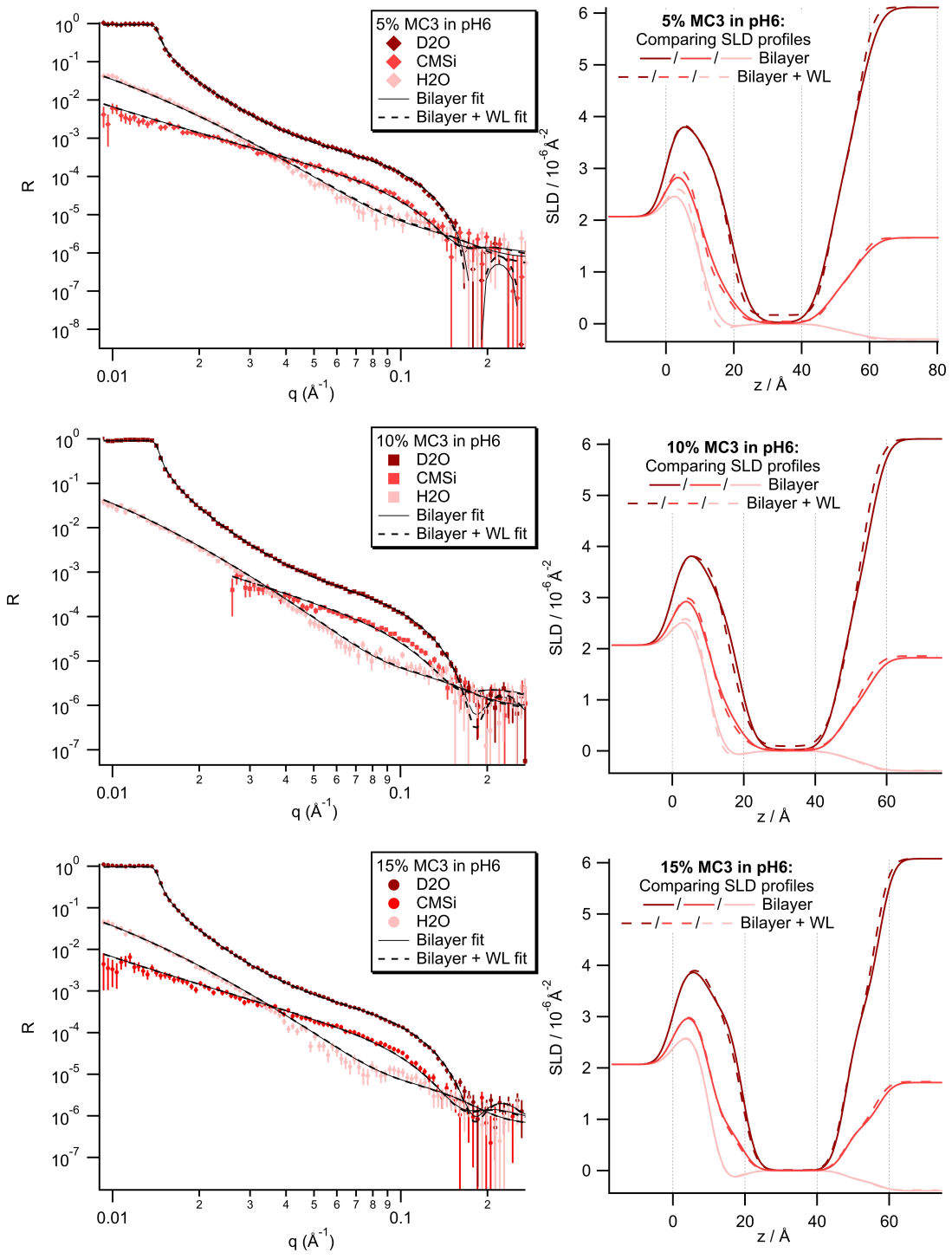

Figure S4 Comparing data for 5, 10 and 15% MC3 lipid layers in pH6 buffer to the bilayer model fit (solid line) and bilayer + water layer model fit (dashed line). The fits and SLD profiles are almost indistinguishable.

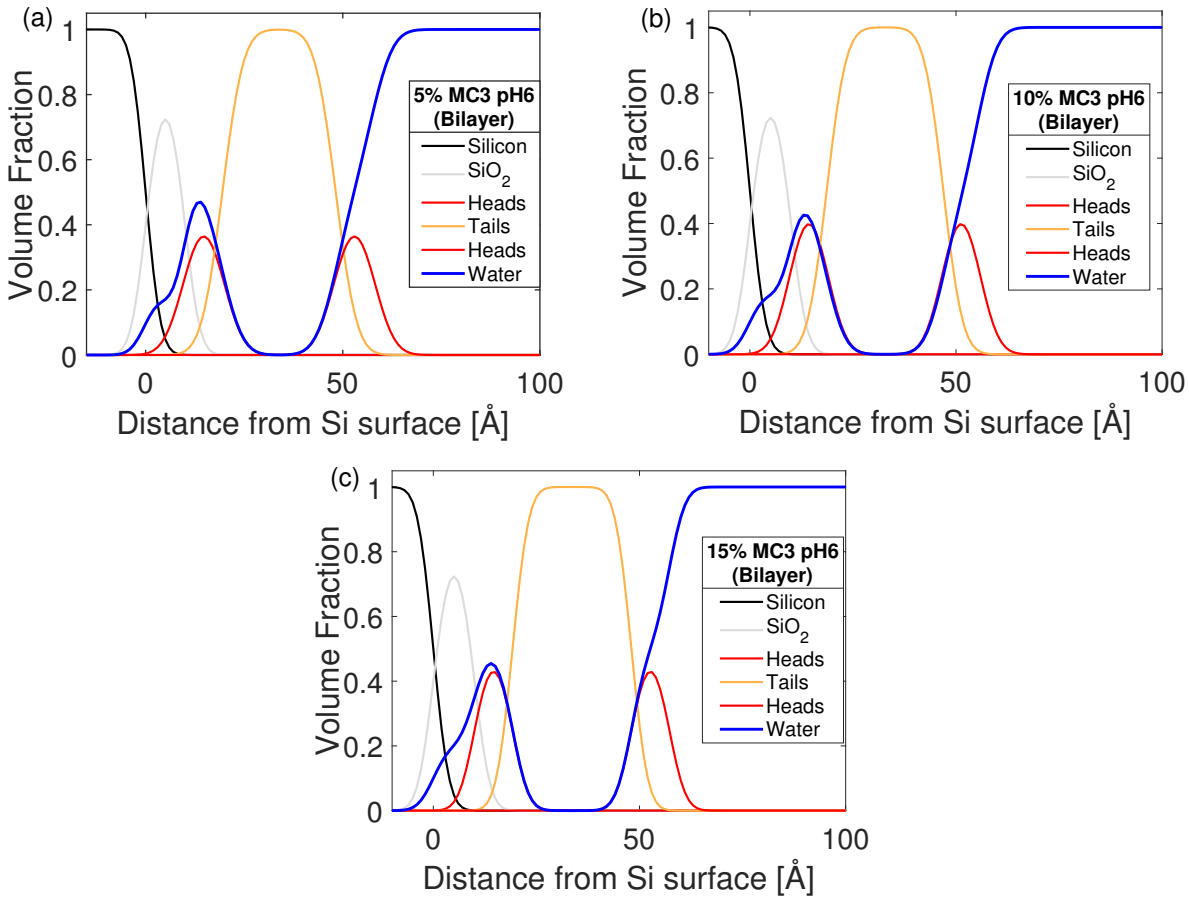

Figure S5 Plots of the volume fraction of different components calculated for the bilayer models for the 5% (a), 10% (b), and 15% (c) MC3 lipid layers in pH6 buffer.

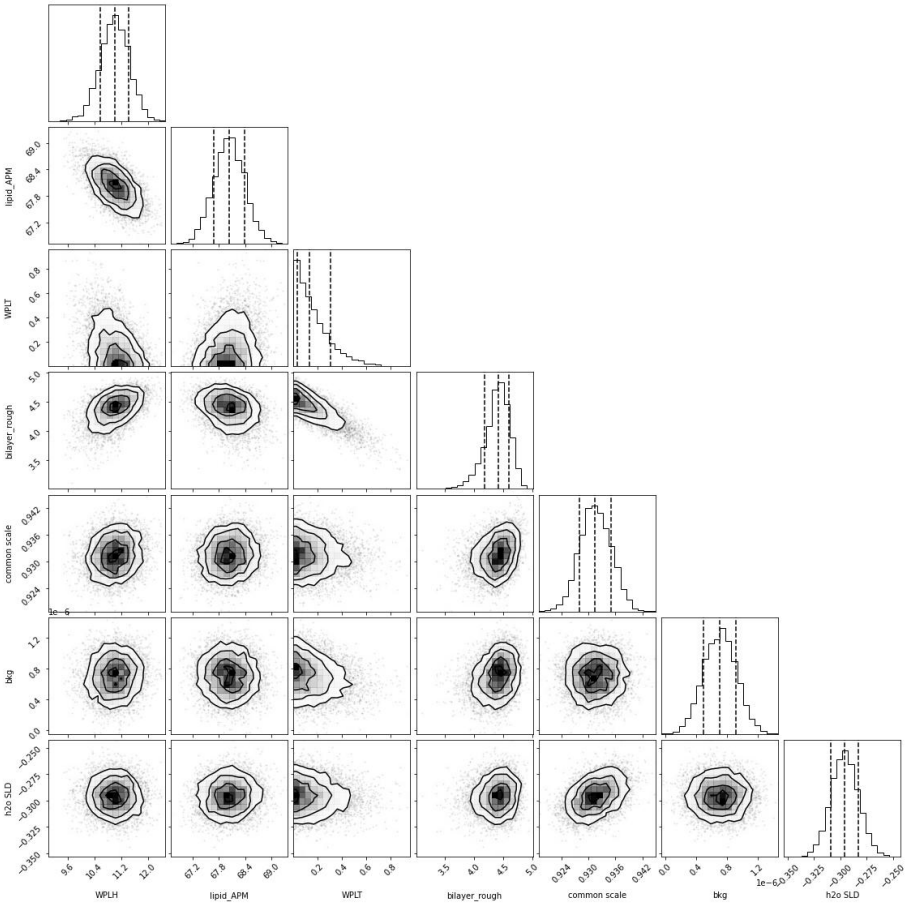

Figure S6 Corner plot of parameter posterior distributions from Bayesian analysis for a bilayer model fit for the 5% MC3 layer in pH6 buffer.

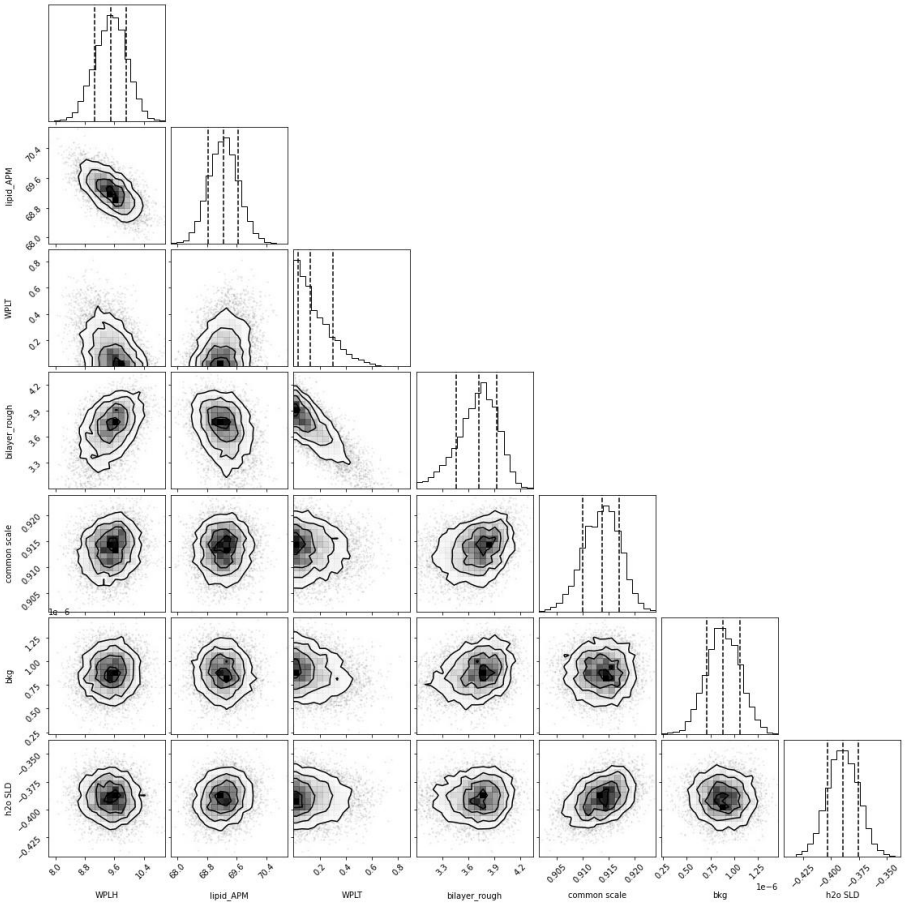

Figure S7 Corner plot of parameter posterior distributions from Bayesian analysis for a bilayer model fit for the 10% MC3 layer in pH6 buffer.

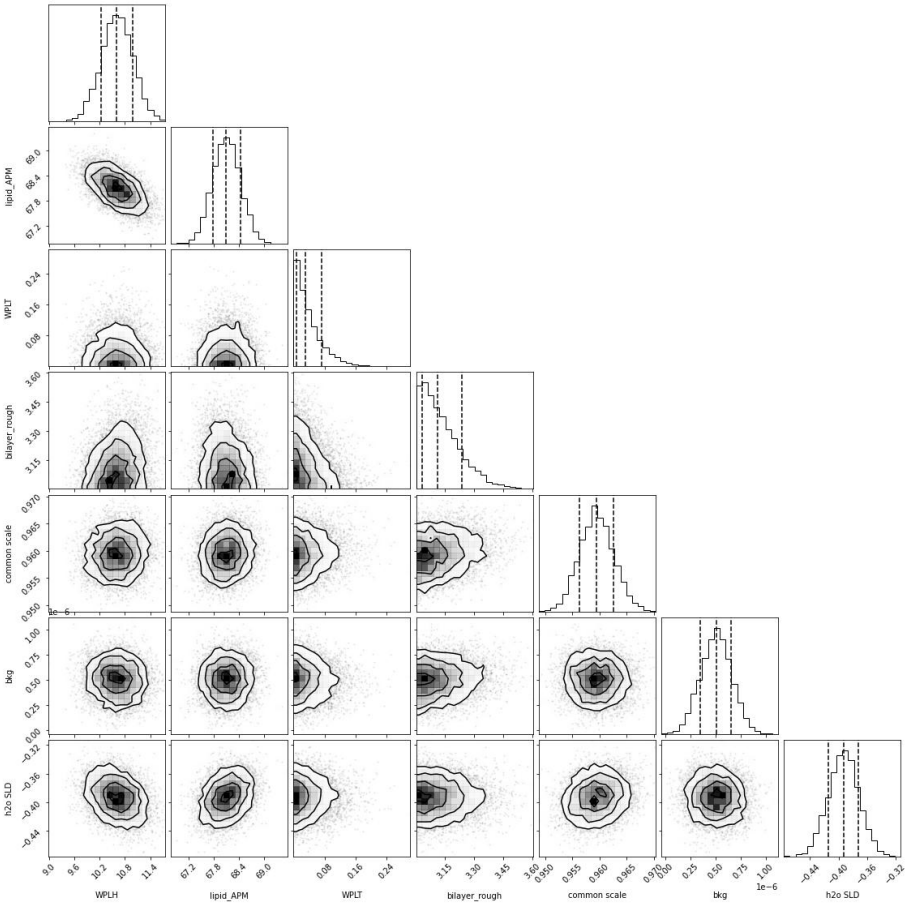

Figure S8 Corner plot of parameter posterior distributions from Bayesian analysis for a bilayer model fit for the 15% MC3 layer in pH6 buffer.

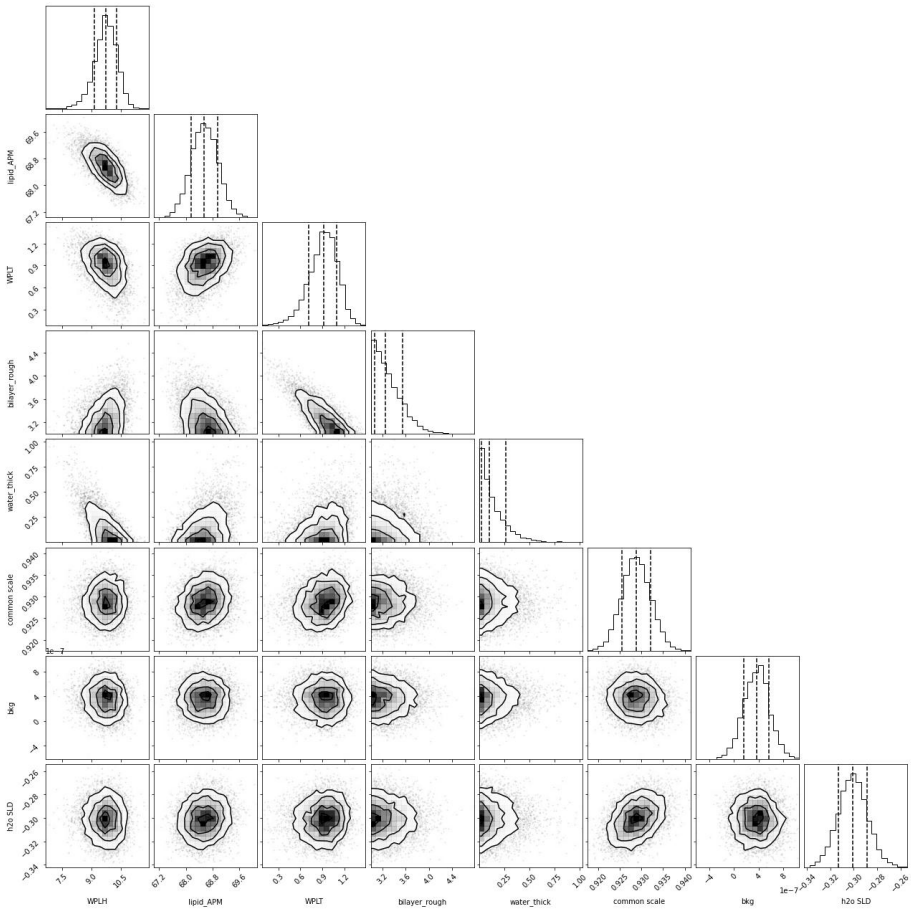

Figure S9 Corner plot of parameter posterior distributions from Bayesian analysis for a bilayer + water layer model fit for the 5% MC3 layer in pH6 buffer.

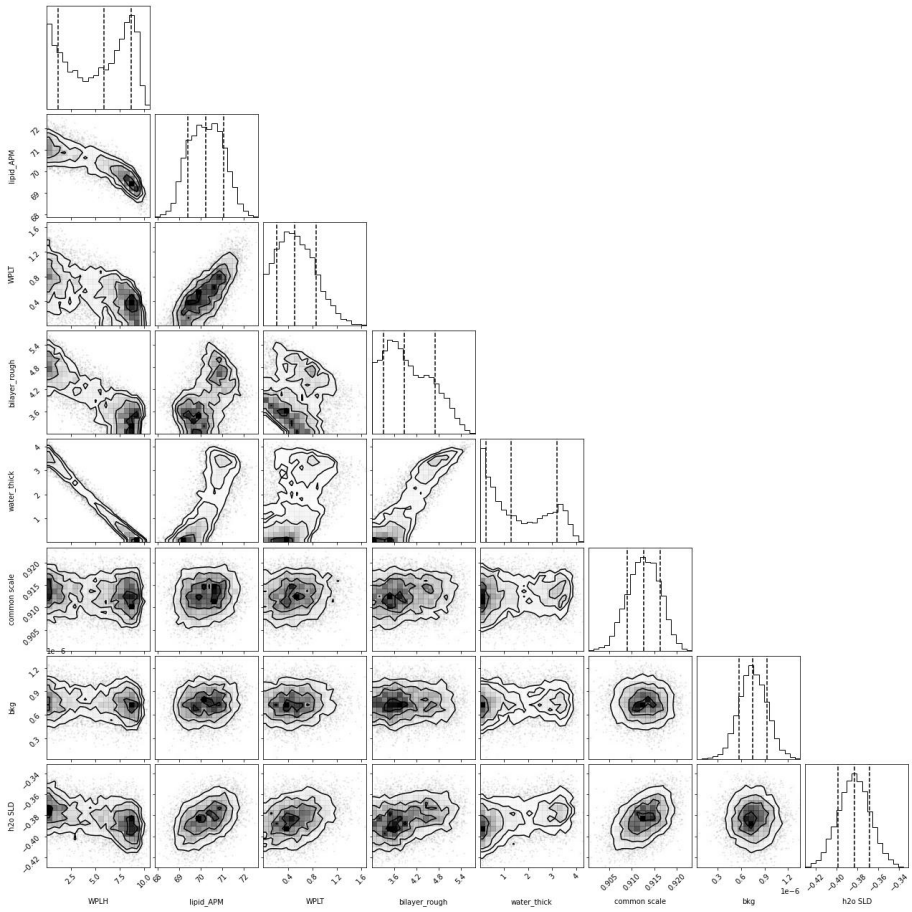

Figure S10 Corner plot of parameter posterior distributions from Bayesian analysis for a bilayer + water layer model fit for the 10% MC3 layer in pH6 buffer.

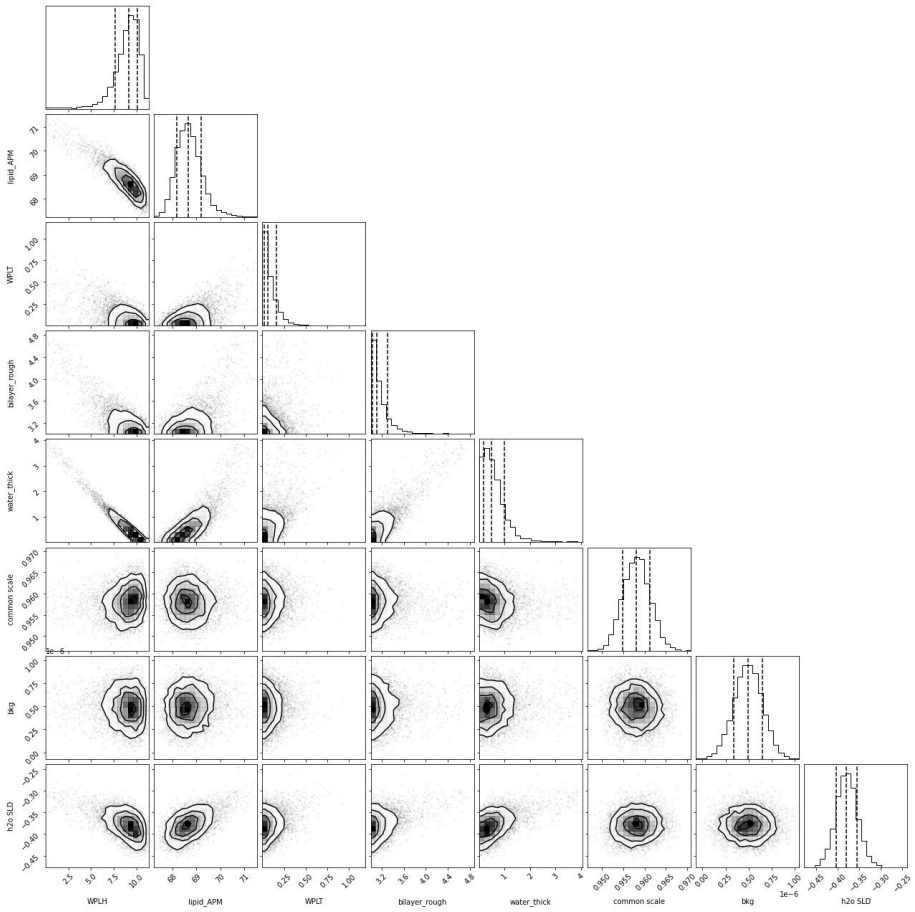

Figure S11 Corner plot of parameter posterior distributions from Bayesian analysis for a bilayer + water layer model fit for the 15% MC3 layer in pH6 buffer.

2.3.2 Lipid layer in pH 7 samples

For the 5 and 15% MC3 lipid layers in pH7 buffer, four models were compared; bilayer, bilayer + water layer, three slabs and four slabs.

When compared to the bilayer model, adding the water layer does not improve the fit for 5 or 15% MC3 lipid layers in pH7 buffer (see Table S10), as the thickness of the water is again 0 Å or close to 0 Å here. As also seen for the lipid layers in pH6 buffer, the main difference between fitted parameters values can be seen for the bilayer roughness and WPLH.

Comparing the three slab and four slab models, it can be concluded that the extra slab does not improve the description of the data as slabs 2 and 3 in the four slab model are approximately equivalent to slab 2 in the three slab model and the global χ^2 is higher for the four slab model than the three slab model.

Comparing the bilayer and three slab models for this samples, it can clearly be observed that an improvement in fit can be observed with the three slab model (see Figure S12 and Table S10), especially in the CMSi and H_2O contrasts. Looking at the model parameters, both models produce the same tail thickness and the same or very similar inner head group thickness but the main differences lie in the higher head group layer hydration and asymmetry observed in the three slab model. The bilayer model is set up to be symmetric, however in the three slab model, where all slabs can vary independently, a difference can be seen between the inner and outer head group thicknesses, which is further highlighted by comparing the respective volume fraction profiles for the different samples (Figure S13), especially for 15% MC3 (Figure S13(c,d)).

However, the same trends in roughness and hydration can be observed with the bilayer model and three slab model with respect to the pH6 samples and between the pH7 samples, and the 3 slab model still fails to describe deviation from fit in CMSi data around 0.09 $Å^{-1}$ (see Figure S12), therefore it does not improve understanding of the system enough to justify extra fit parameters.

Bilayer	5% MC3 pH7	15% MC3 pH7
WPLH	22.8 ± 0.4	14 ± 0.5
APM	66.7 ± 0.3 $Å^2$	65.9 ± 0.4 $Å^2$
WPLT	0.05 ± 0.06	0.4 ± 0.3
Bilayer roughness	4.0 ± 0.2 Å	5.9 ± 0.3 Å
Scale	0.927 ± 0.003	0.930 ± 0.003

Table S6 Bilayer fit parameters for 5 and 15% MC3 lipid layers in pH7 buffer.

Bilayer + water layer	5% MC3 pH7	15% MC3 pH7
WPLH	21.7 ± 0.4	12.0 ± 0.8
APM	66.9 ± 0.3 $Å^2$	66.3 ± 0.6 $Å^2$
WPLT	0.5 ± 0.1	1.7 ± 0.4
Bilayer roughness	3.1 ± 0.1 Å	4.4 ± 0.6 Å
Water layer thickness	0.07 ± 0.09 Å	0.1 ± 0.2 Å
Scale	0.924 ± 0.003	0.926 ± 0.003

Table S7 Bilayer + water layer fit parameters for 5 and 15% MC3 lipid layers in pH7 buffer.

3 slab	5% MC3 pH7	15% MC3 pH7
S1 thickness	14.9 ± 0.2 Å	13.9 ± 0.9 Å
S2 thickness	29 ± 1 Å	29 ± 1 Å
S3 thickness	12 ± 1 Å	12 ± 2 Å
S1 SLD	1.86 ± 0.02 x $10^{-6}Å^{-2}$	1.79 ± 0.9 x $10^{-6}Å^{-2}$
S2 SLD	-0.01 ± 0.01 x $10^{-6}Å^{-2}$	-0.30 ± 0.07 x $10^{-6}Å^{-2}$
S3 SLD	1.1 ± 0.2 x $10^{-6}Å^{-2}$	1.7 ± 0.2 x $10^{-6}Å^{-2}$
S1 vf	0.57 ± 0.02	0.42 ± 0.03
S2 vf	0.010 ± 0.009	0.01 ± 0.01
S3 vf	0.5 ± 0.1	0.5 ± 0.1
Bilayer roughness	4.2 ± 0.6 Å	7.6 ± 0.5 Å
Scale	0.939 ± 0.004	0.943 ± 0.003

Table S8 Three slab fit parameters for 5 and 15% MC3 lipid layers in pH7 buffer.

4 slab	5% MC3 pH7	15% MC3 pH7
S1 thickness	14.8 ± 0.2 Å	13 ± 1 Å
S2 thickness	14 ± 3 Å	15 ± 3 Å
S3 thickness	15 ± 4 Å	14 ± 3 Å
S4 thickness	8 ± 2 Å	8 ± 2 Å
S1 SLD	1.85 ± 0.04 x 10^{-6}Å^{-2}	1.7 ± 0.1 x 10^{-6}Å^{-2}
S2 SLD	-0.03 ± 0.04 x 10^{-6}Å^{-2}	-0.3 ± 0.1 x 10^{-6}Å^{-2}
S3 SLD	-0.06 ± 0.08 x 10^{-6}Å^{-2}	-0.3 ± 0.1 x 10^{-6}Å^{-2}
S4 SLD	1.2 ± 0.2 x 10^{-6}Å^{-2}	1.6 ± 0.2 x 10^{-6}Å^{-2}
S1 vf	0.56 ± 0.02	0.44 ± 0.05
S2 vf	0.02 ± 0.02	0.02 ± 0.02
S3 vf	0.02 ± 0.02	0.03 ± 0.03
S4 vf	0.4 ± 0.1	0.3 ± 0.2
Bilayer roughness	4.9 ± 0.6 Å	7.6 ± 0.5 Å
Scale	0.944 ± 0.004	0.938 ± 0.004

Table S9 Four slab fit parameters for 5 and 15% MC3 lipid layers in pH7 buffer.

Model	5% MC3			15% MC3		
	D_2O	CMSi	H_2O	D_2O	CMSi	H_2O
Bilayer	3.1	3.1	1.8	4.5	4.1	1.7
Bilayer + water layer	3.3	2.9	2.0	4.5	3.6	2.3
3 slab	2.8	1.1	1.0	4.0	2.5	1.2
4 slab	2.7	1.1	0.9	4.7	2.7	1.0

Table S10 Comparison of normalised χ^2 values for fitting with a bilayer model, a bilayer + water layer model, a three slab model and a four slab model for 5 and 15% MC3 lipid layers in pH7 buffer.

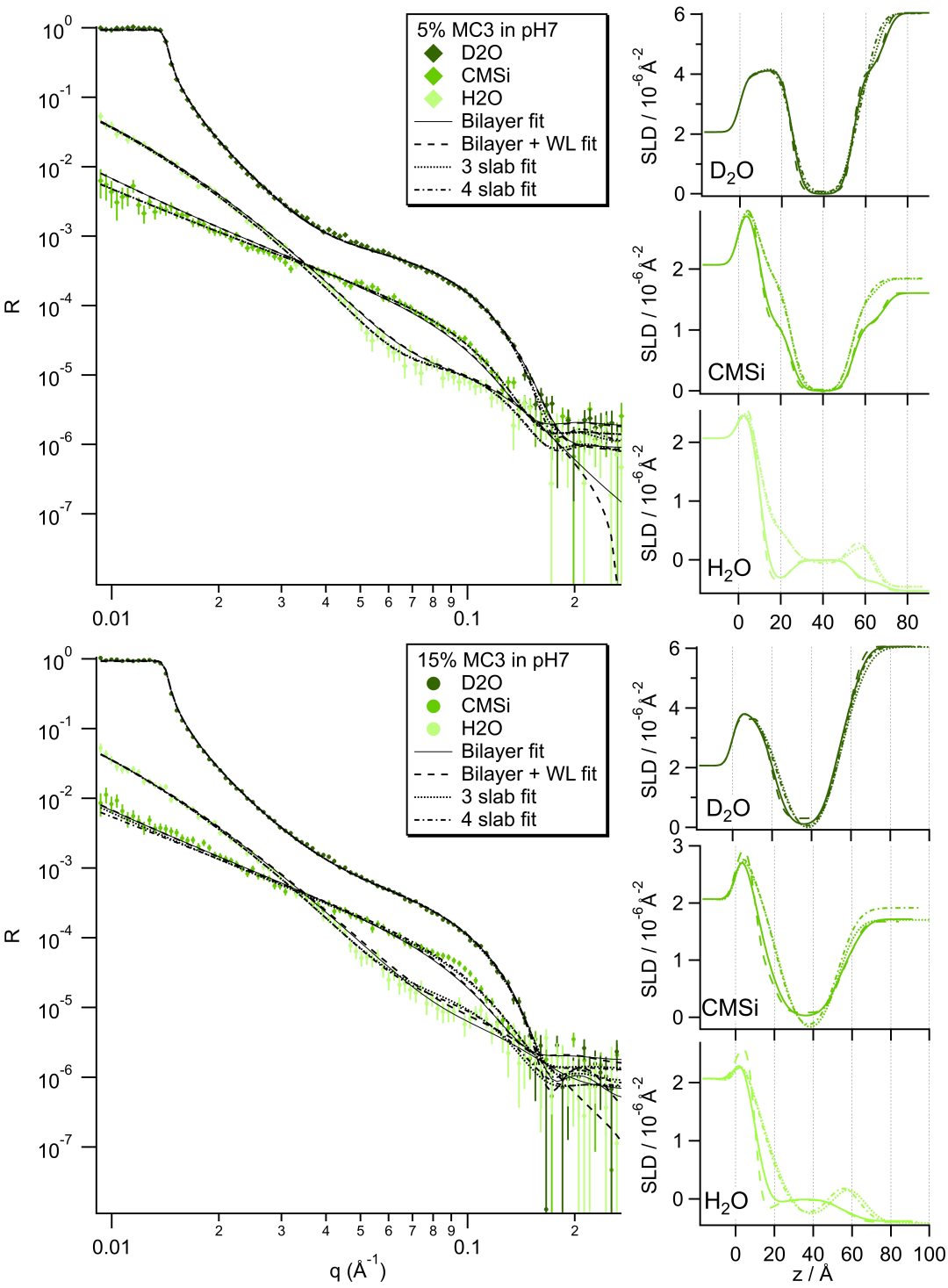

Figure S12 Comparing data for 5 and 15% MC3 lipid layers in pH7 buffer to the bilayer model fit (solid line), bilayer + water layer model fit (dashed line), three slab model fit (dotted line) and four slab model fit (dash-dotted line).

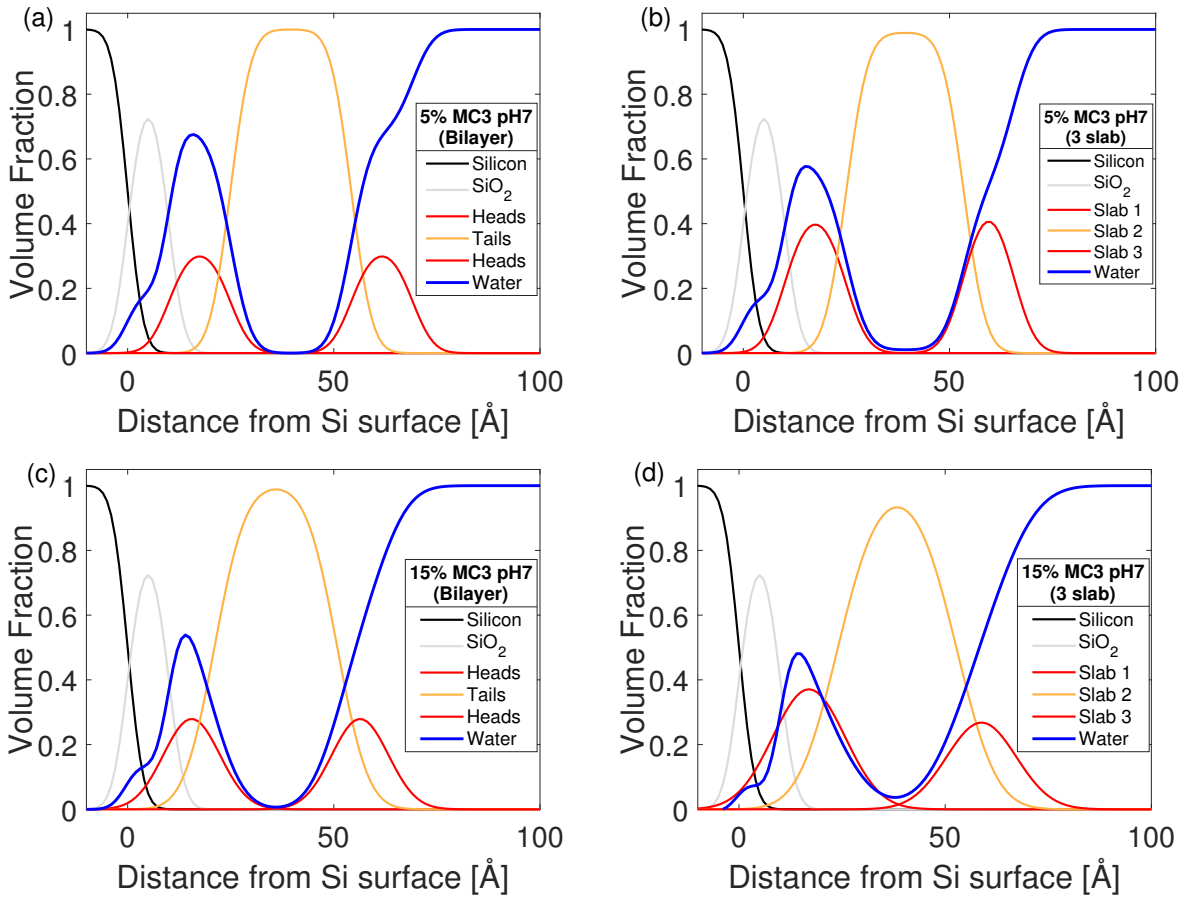

Figure S13 Plots of the volume fraction of different components calculated for the bilayer and 3 slab models for the 5% (a,b) and 15% (c,d) MC3 lipid layers in pH7 buffer.

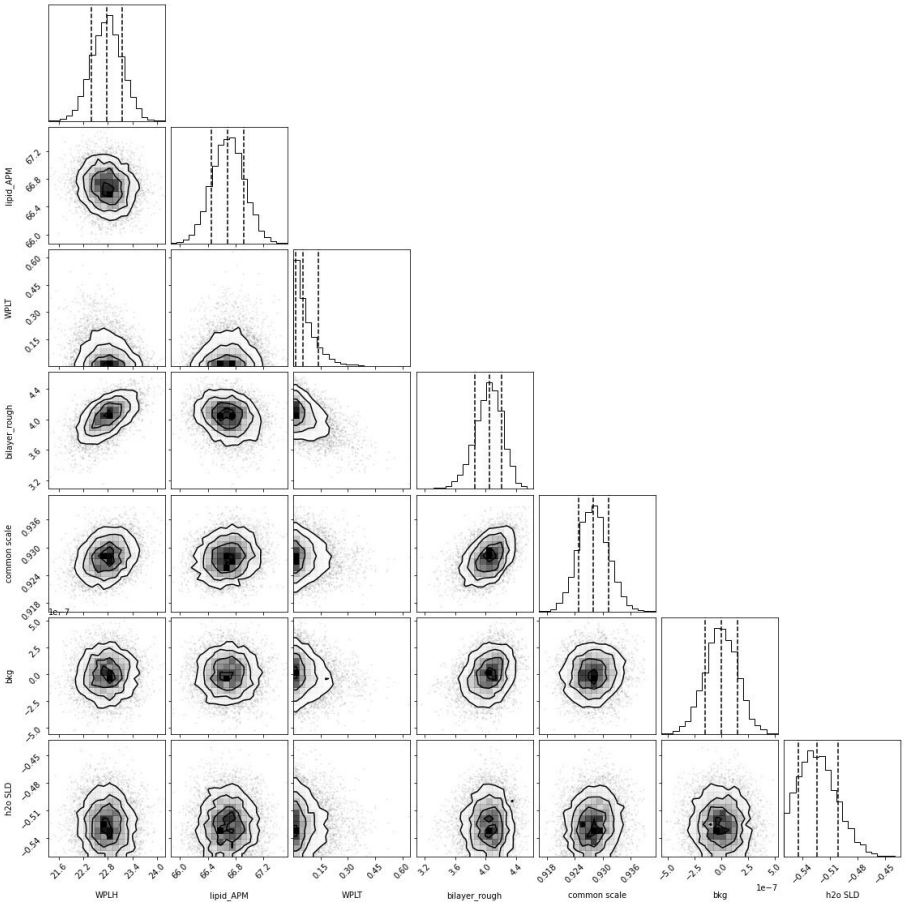

Figure S14 Corner plot of parameter posterior distributions from Bayesian analysis for a bilayer model fit for the 5% MC3 layer in pH7 buffer.

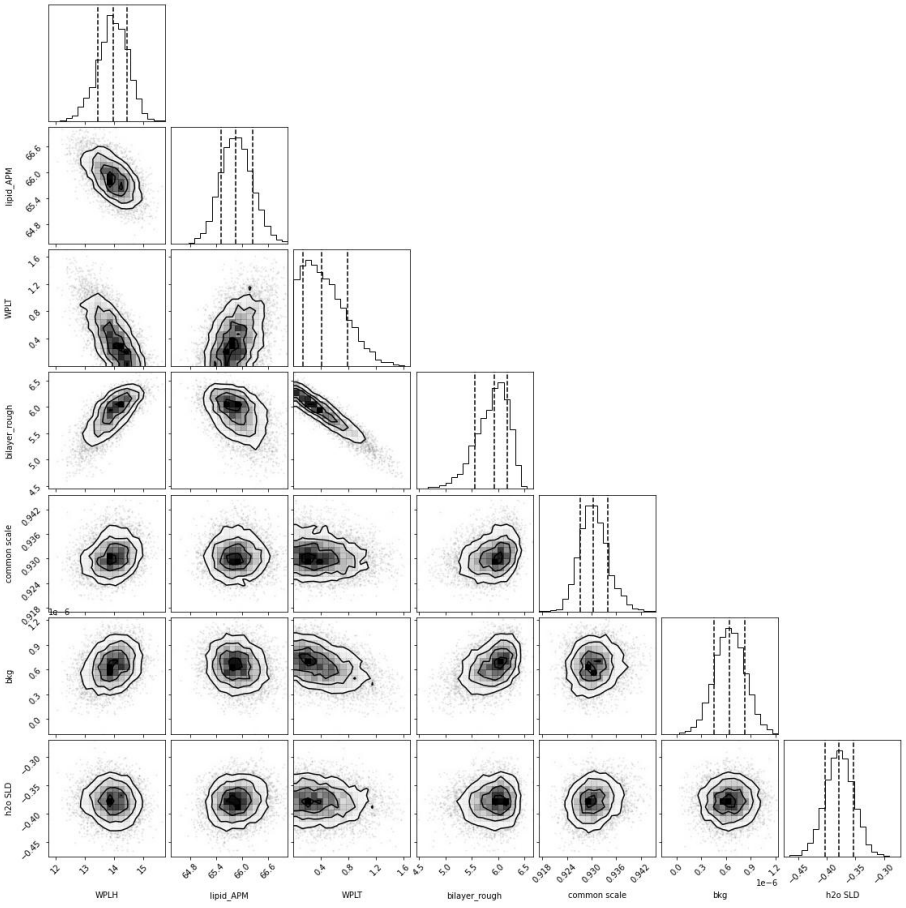

Figure S15 Corner plot of parameter posterior distributions from Bayesian analysis for a bilayer model fit for the 15% MC3 layer in pH7 buffer.

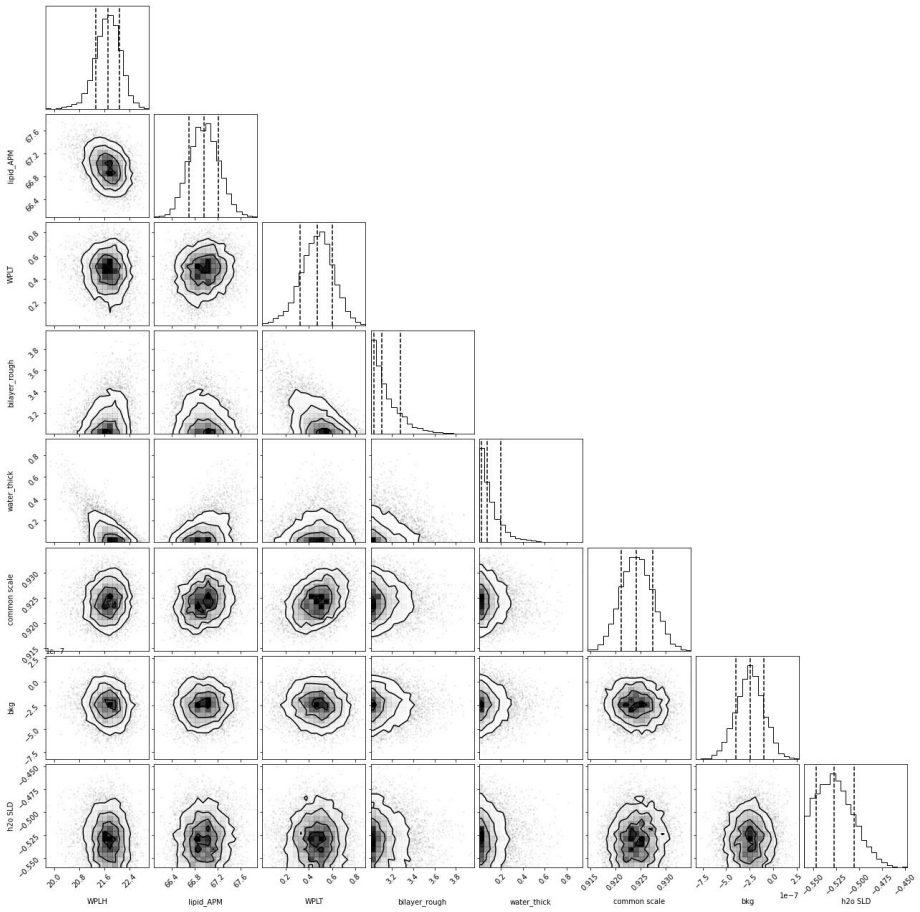

Figure S16 Corner plot of parameter posterior distributions from Bayesian analysis for a bilayer + water layer model fit for the 5% MC3 layer in pH7 buffer.

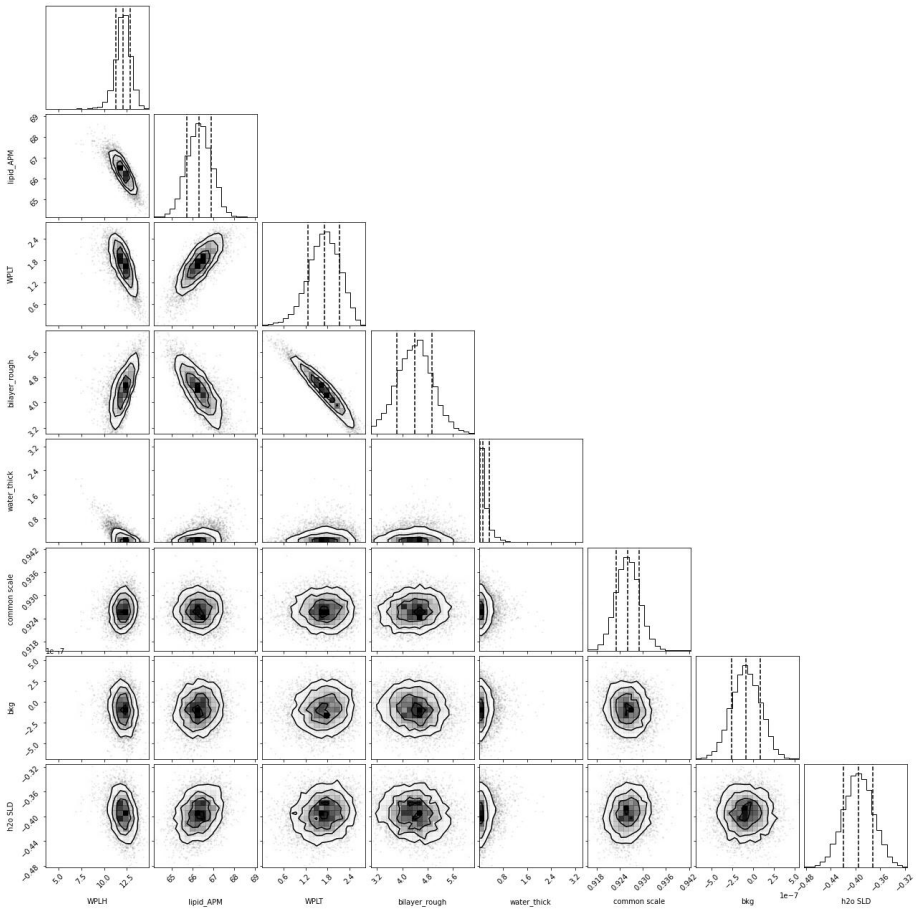

Figure S17 Corner plot of parameter posterior distributions from Bayesian analysis for a bilayer + water layer model fit for the 15% MC3 layer in pH7 buffer.

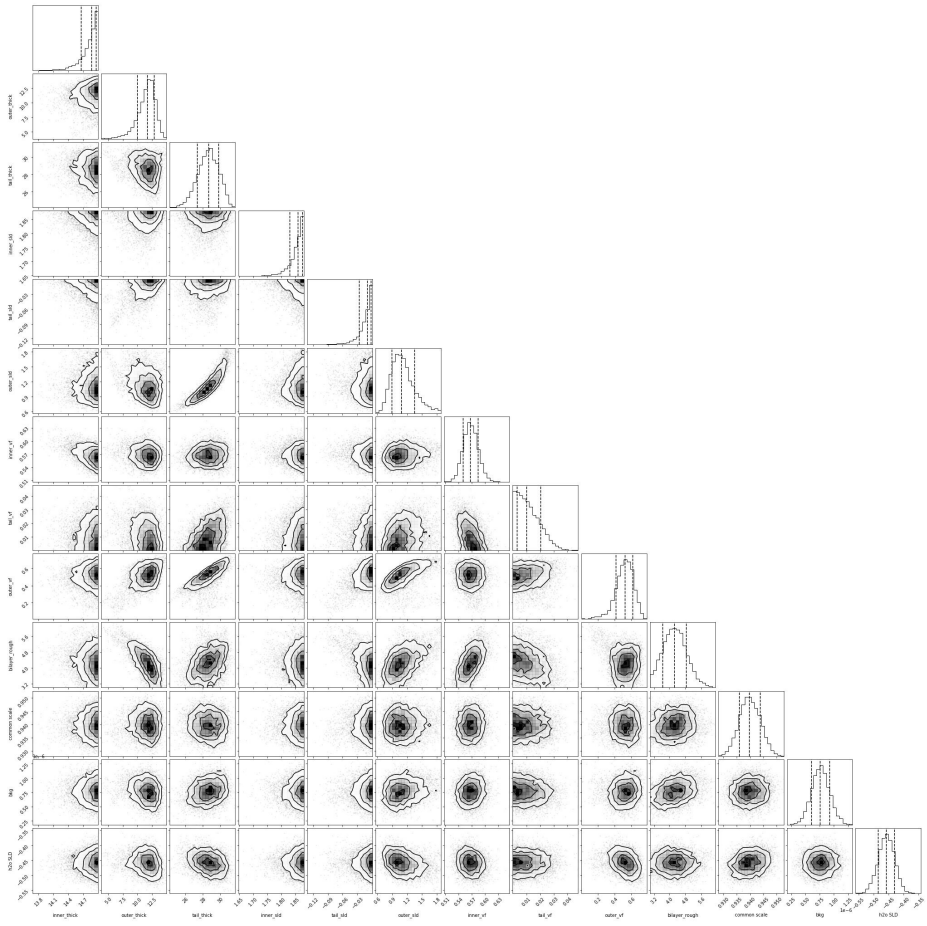

Figure S18 Corner plot of parameter posterior distributions from Bayesian analysis for a three slab model fit for the 5% MC3 layer in pH7 buffer.

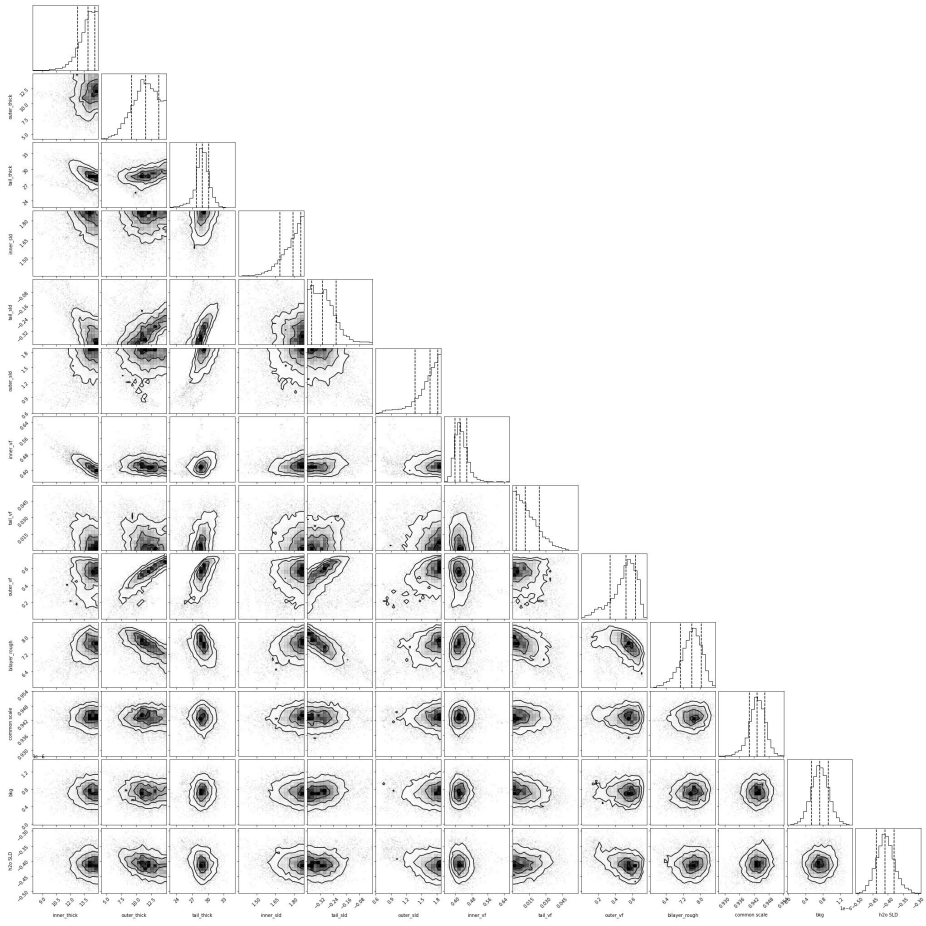

Figure S19 Corner plot of parameter posterior distributions from Bayesian analysis for a three slab model fit for the 15% MC3 layer in pH7 buffer.

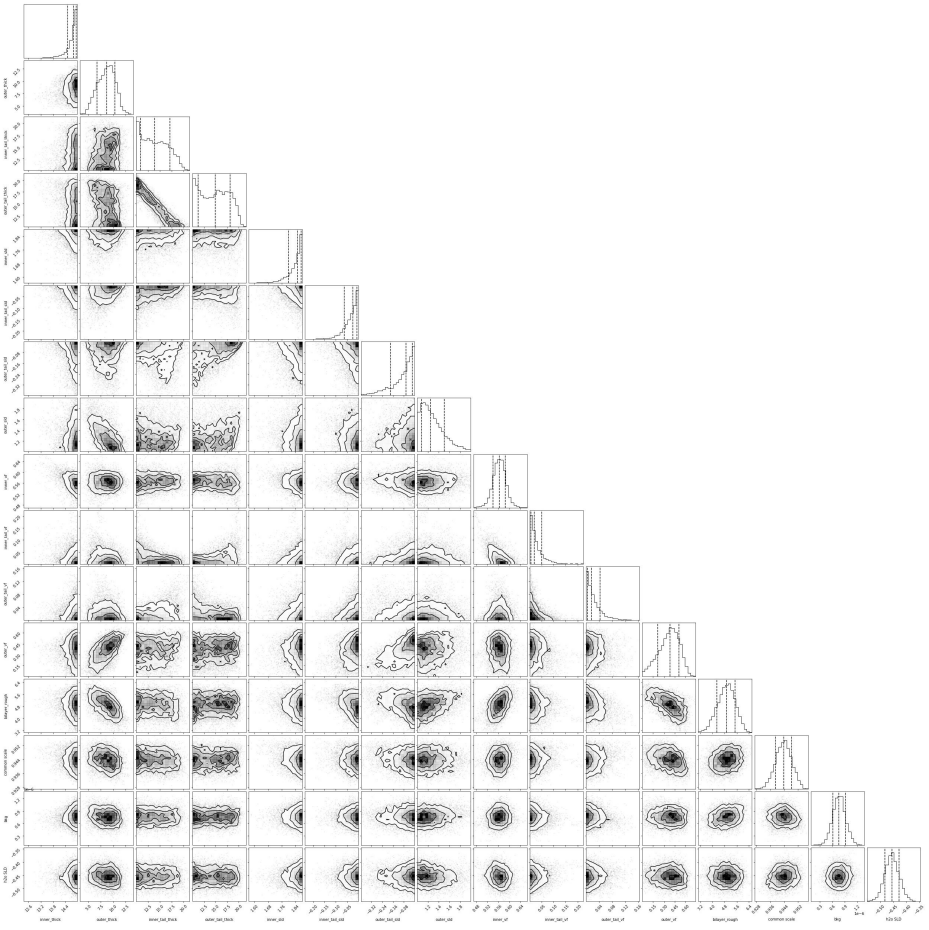

Figure S20 Corner plot of parameter posterior distributions from Bayesian analysis for a four slab model fit for the 5% MC3 layer in pH7 buffer.

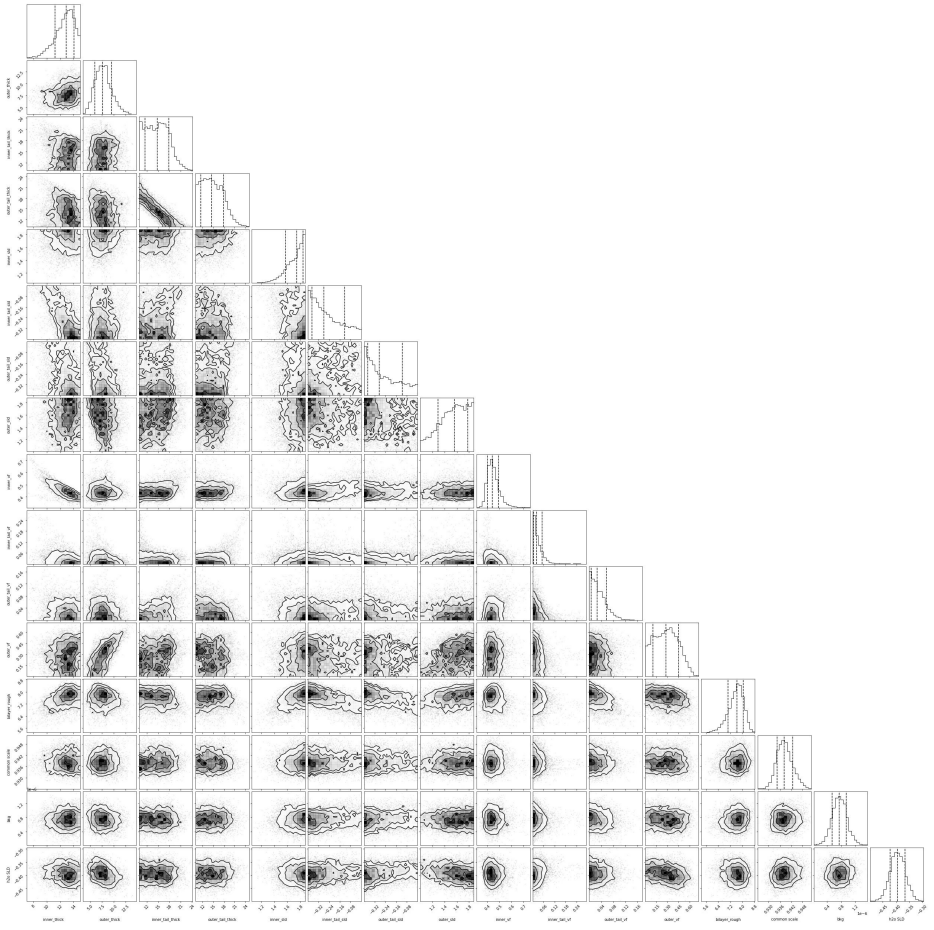

Figure S21 Corner plot of parameter posterior distributions from Bayesian analysis for a four slab model fit for the 15% MC3 layer in pH7 buffer.

3 Addition of nucleic acids

3.1 QCM-D

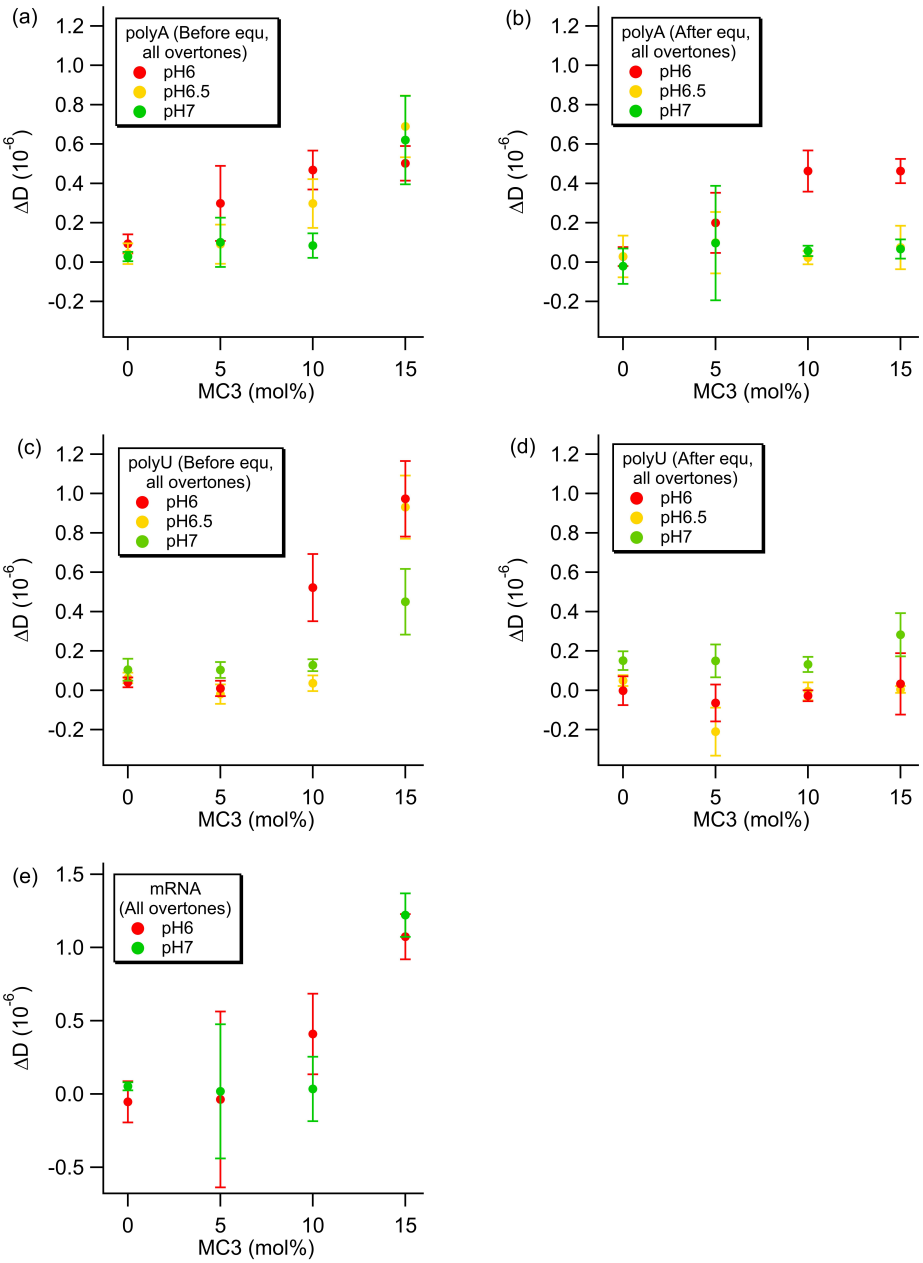

Figure S22 The change in dissipation before and after equilibration is shown for polyA (a, b) and polyU (c,d). For mRNA in all conditions, the dissipation remained the same after equilibration (e). Change in dissipation before equilibration was calculated using the difference in dissipation between the lipid layer and the initial maximum after addition of the NA. Dissipation after equilibration was calculated using the difference in dissipation between the lipid layer and the plateau after equilibration and rinsing.

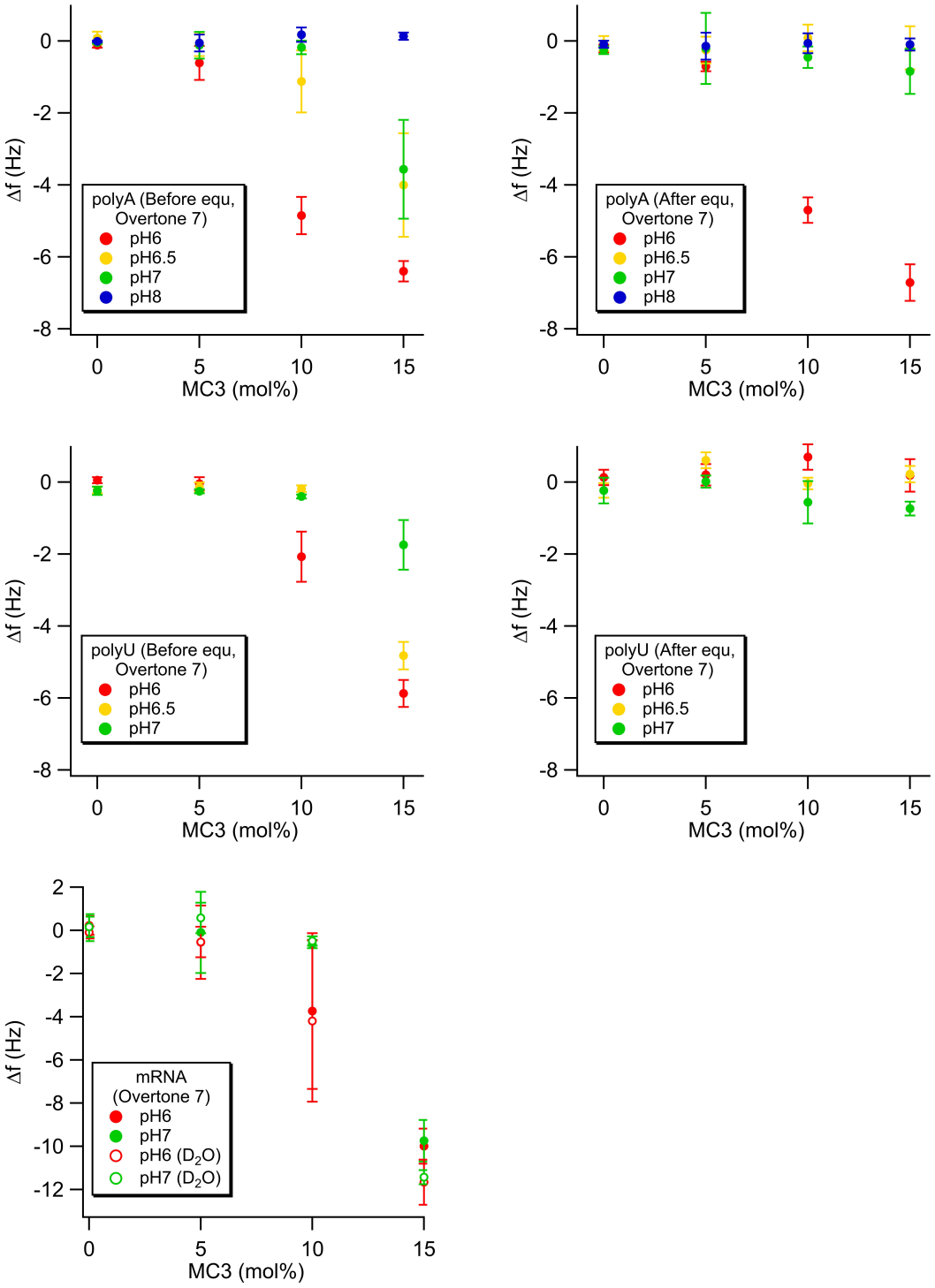

Figure S23 The change in frequency before and after equilibration of the 7th overtone for polyA (a, b) and polyU (c,d). For mRNA in all conditions, the frequency remained the same after equilibration (e). Note the different axis range for the mRNA measurements.

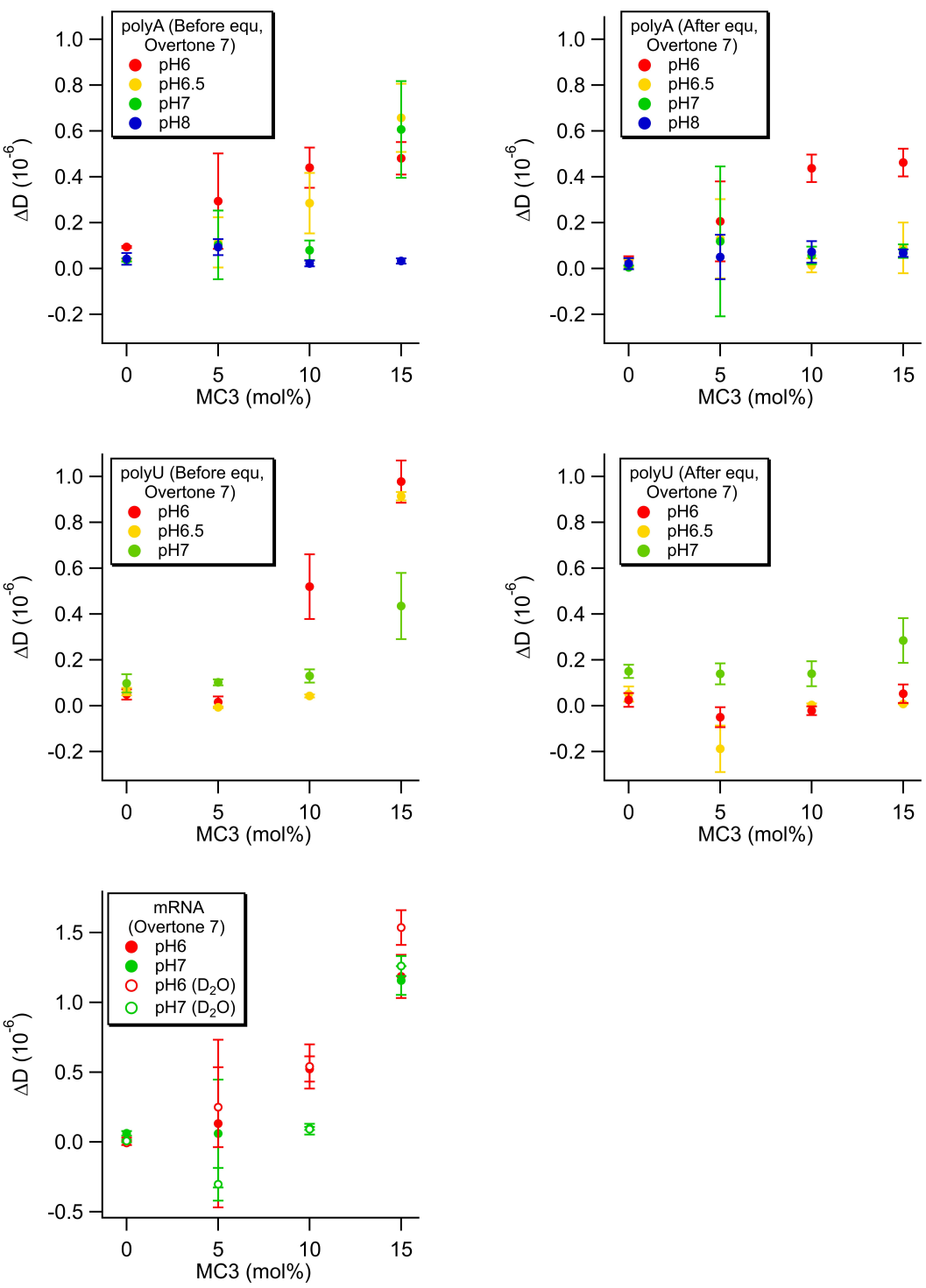

Figure S24 The change in dissipation before and after equilibration of the 7th overtone for polyA (a, b) and polyU (c,d). For mRNA in all conditions, the dissipation remained the same after equilibration (e). Note the different axis range for the mRNA measurements.

3.2 NR model comparison

3.2.1 mRNA: No adsorption

For the 5% MC3 samples in both pHs, no change was observed in the QCM-D upon addition of mRNA and very minor changes were observed in the reflectometry curves after incubation with mRNA (see Figure 6). These samples were therefore fit again with a bilayer model (Figure S25), where an increase in roughness and minor changes in WPLH and APM were observed for both pHs.

[H]

Bilayer	5% MC3 pH6	5% MC3 pH7
WPLH	17.7 ± 0.4	22.6 ± 0.4
APM	66.0 ± 0.3 Å^2	70.4 ± 0.3 Å^2
WPLT	0.05 ± 0.06	0.1 ± 0.1
Bilayer roughness	5.7 ± 0.2 Å	6.9 ± 0.3 Å
Scale	0.901 ± 0.001	0.922 ± 0.004

Table S11 Bilayer fit parameters for 5% MC3 layer in both pH6 and 7 buffers after incubation with mRNA

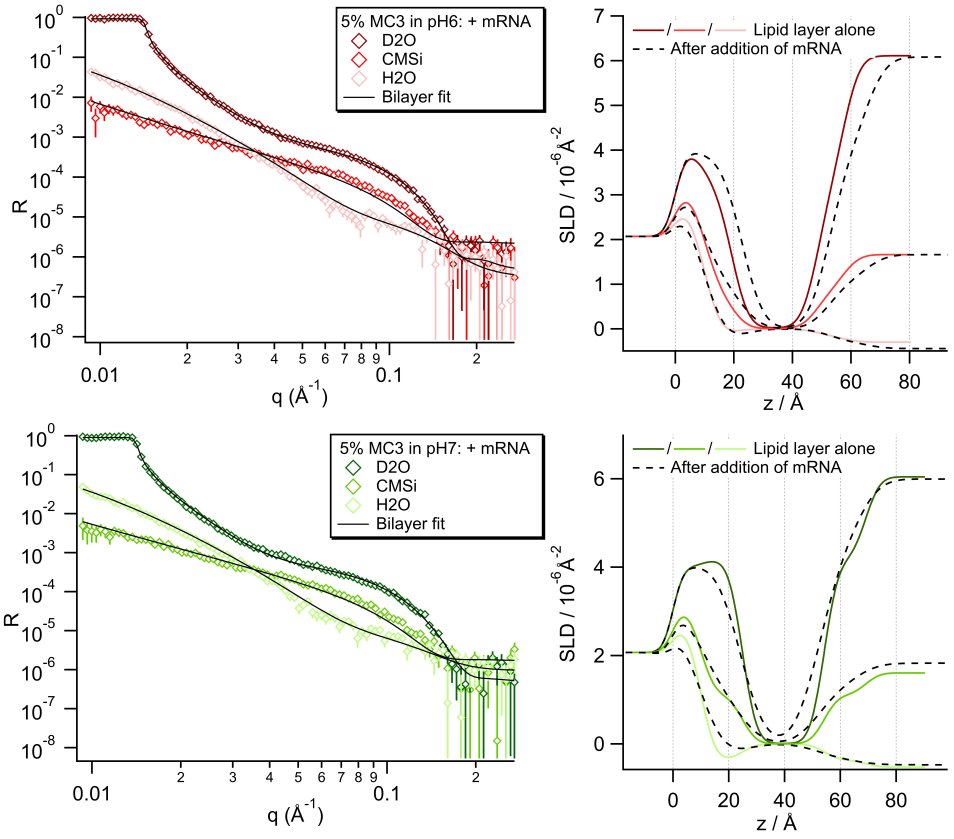

Figure S25 Comparing data for for 5% MC3 layers in pH6 and pH7 after incubation with mRNA to the bilayer model fit (solid line).

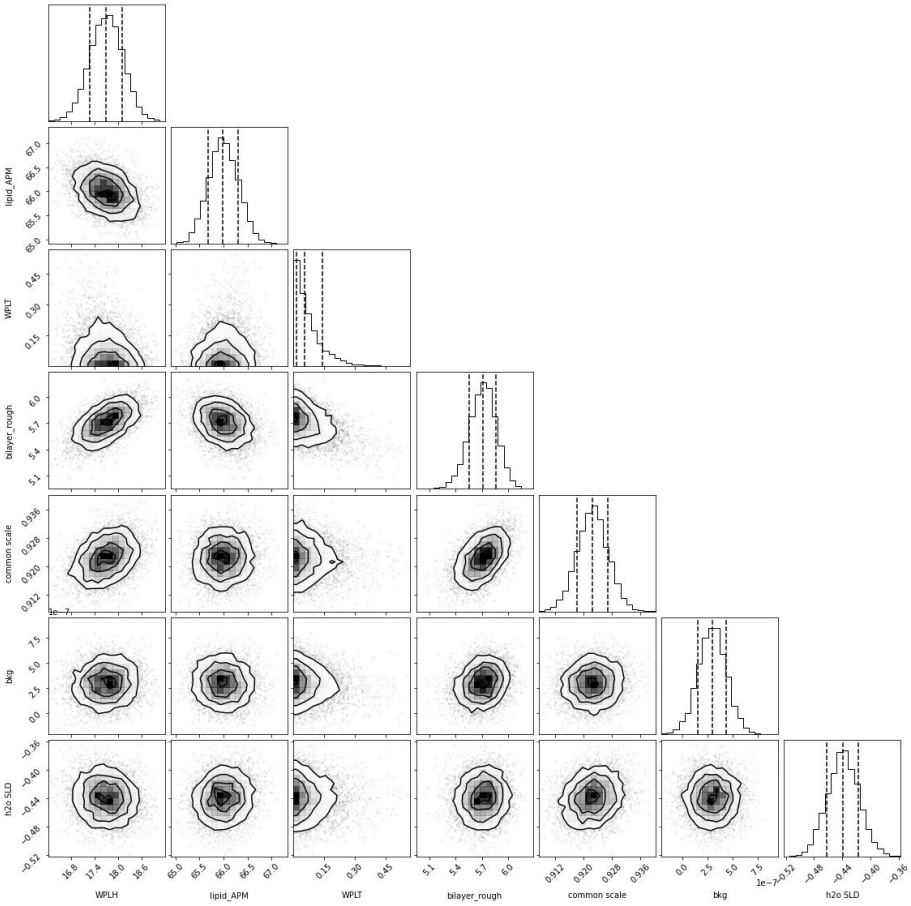

Figure S26 Corner plot of parameter posterior distributions from Bayesian analysis for a bilayer model fit for the 5% MC3 layer in pH6 buffer after incubation with mRNA.

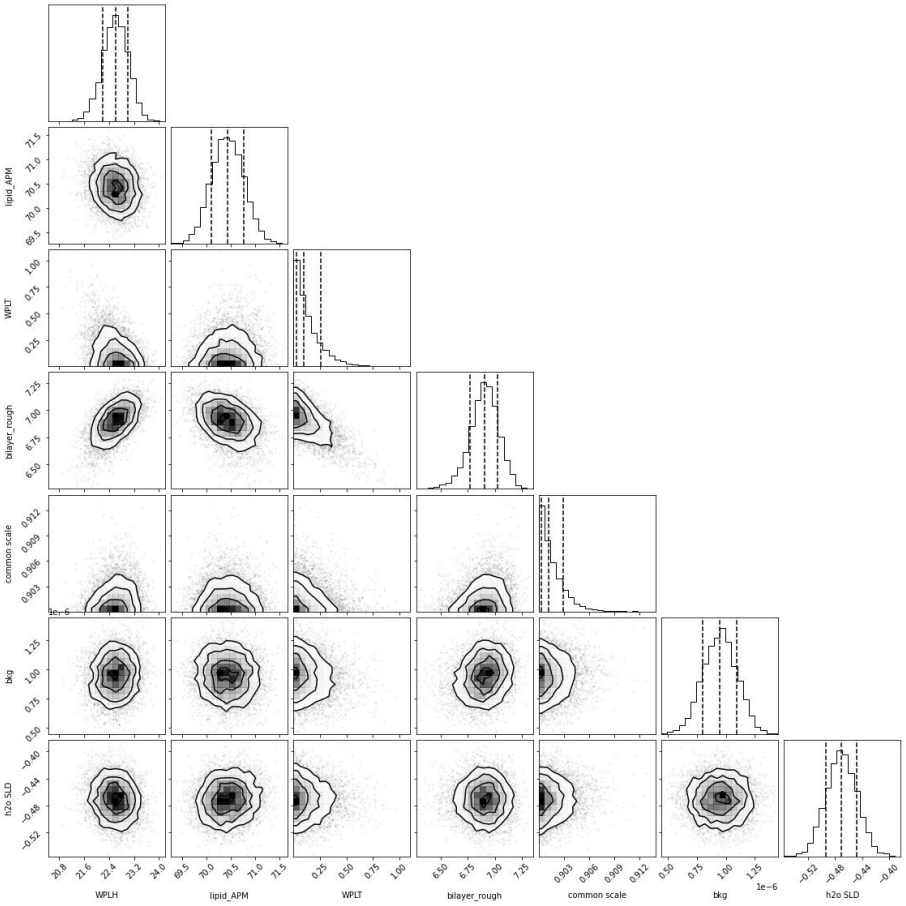

Figure S27 Corner plot of parameter posterior distributions from Bayesian analysis for a bilayer model fit for the 5% MC3 layer in pH7 buffer after incubation with mRNA.

3.2.2 mRNA: Adsorption

For the 10% MC3 in pH6 and 15% MC3 in both pHs, a peak appears in the reflectometry data after incubation with mRNA, indicating the formation of a multilayer structure (Figure 6). Initially a fit using a mixed area model of a bilayer and bilayer with a multilayer stack on top was also attempted (data not shown), but this could not describe the peak. This data was, therefore, fitted using a mixed area model with a bilayer (fixed) and a multilayer stack (as described in section 1.2.5). From the fitted SLDs, it can be deduced that the first, thicker slab (closest to the Si layer) is lipid rich with a very low hydration and the second, thinner slab is mRNA rich with a higher hydration (Table S12).

For all samples, in the Bayesian distributions (Figures S30, S31, S32), there is a strong correlation between the thickness of the 2 slabs, which is expected, as these thicknesses need to reproduce the repeat distance given by the peak. There is also a strong correlation between the scale factors for the bilayer model and the multilayer model, as these need to reproduce the critical edge in the D_2O contrast. For the Bayesian analysis for 15% MC3 sample in pH6, the posterior distributions are not so well defined, resulting in some bimodel distributions, indicating that there are 2 structures describe the data (Figure S10).

Multilayer stack	10% MC3 pH6	15% MC3 pH6	15% MC3 pH7
ML1 Thickness	44 ± 1 Å	40 ± 3 Å	40 ± 3 Å
ML2 Thickness	28 ± 2 Å	30 ± 3 Å	31 ± 3 Å
ML1 SLD	1.14 ± 0.09 x 10^{-6}Å^{-2}	1.0 ± 0.1 x 10^{-6}Å^{-2}	0.2 ± 0.2 x 10^{-6}Å^{-2}
ML2 SLD	4.4 ± 0.1 x 10^{-6}Å^{-2}	4.4 ± 0.2 x 10^{-6}Å^{-2}	4.3 ± 0.2 x 10^{-6}Å^{-2}
ML1 vf	0.004 ± 0.005	0.006 ± 0.007	0.07 ± 0.04
ML2 vf	0.57 ± 0.02	0.52 ± 0.2	0.65 ± 0.02
Roughness	9.2 ± 0.6 Å	7.1 ± 0.9 Å	9 ± 1 Å
Bilayer scale	0.688 ± 0.009	0.78 ± 0.01	0.720 ± 0.008
ML scale	0.19 ± 0.01	0.14 ± 0.01	0.13 ± 0.01

Table S12 Mixed area model with bilayer and multilayer stack fit parameters for the 10% MC3 (pH6 buffer) and 15% MC3 (pH6 and 7) lipid layers after incubation with EPO mRNA. Bilayer parameters were fixed from the previous fit for these lipid layers without mRNA.

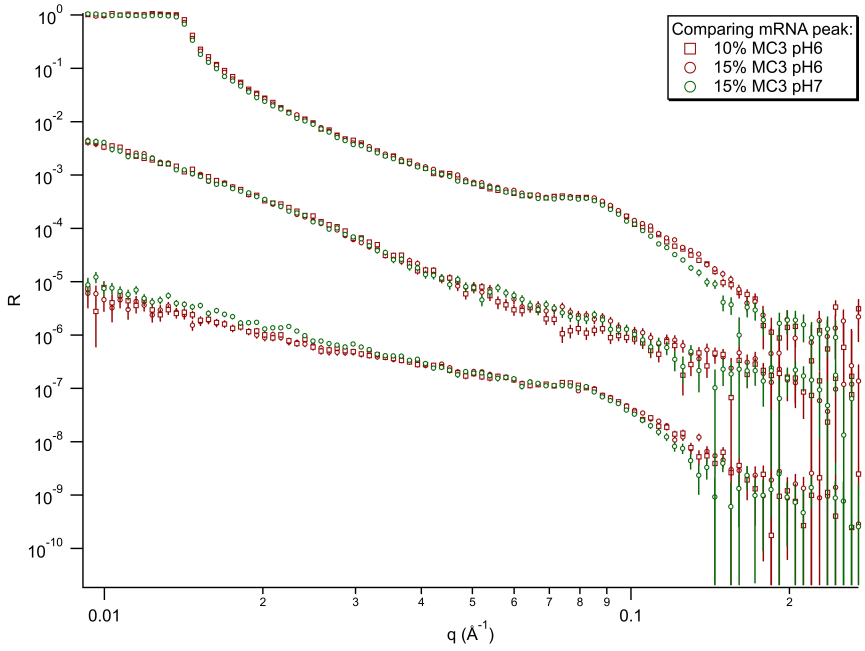

Figure S28 Data for the 10% MC3 (pH6 buffer) and 15% MC3 (pH6 and 7) lipid layers after incubation with EPO mRNA are overlaid here to demonstrate the similarity between the peak position in these data sets. The main differences are observed at high q, where they are also observed for the pure lipid layers.

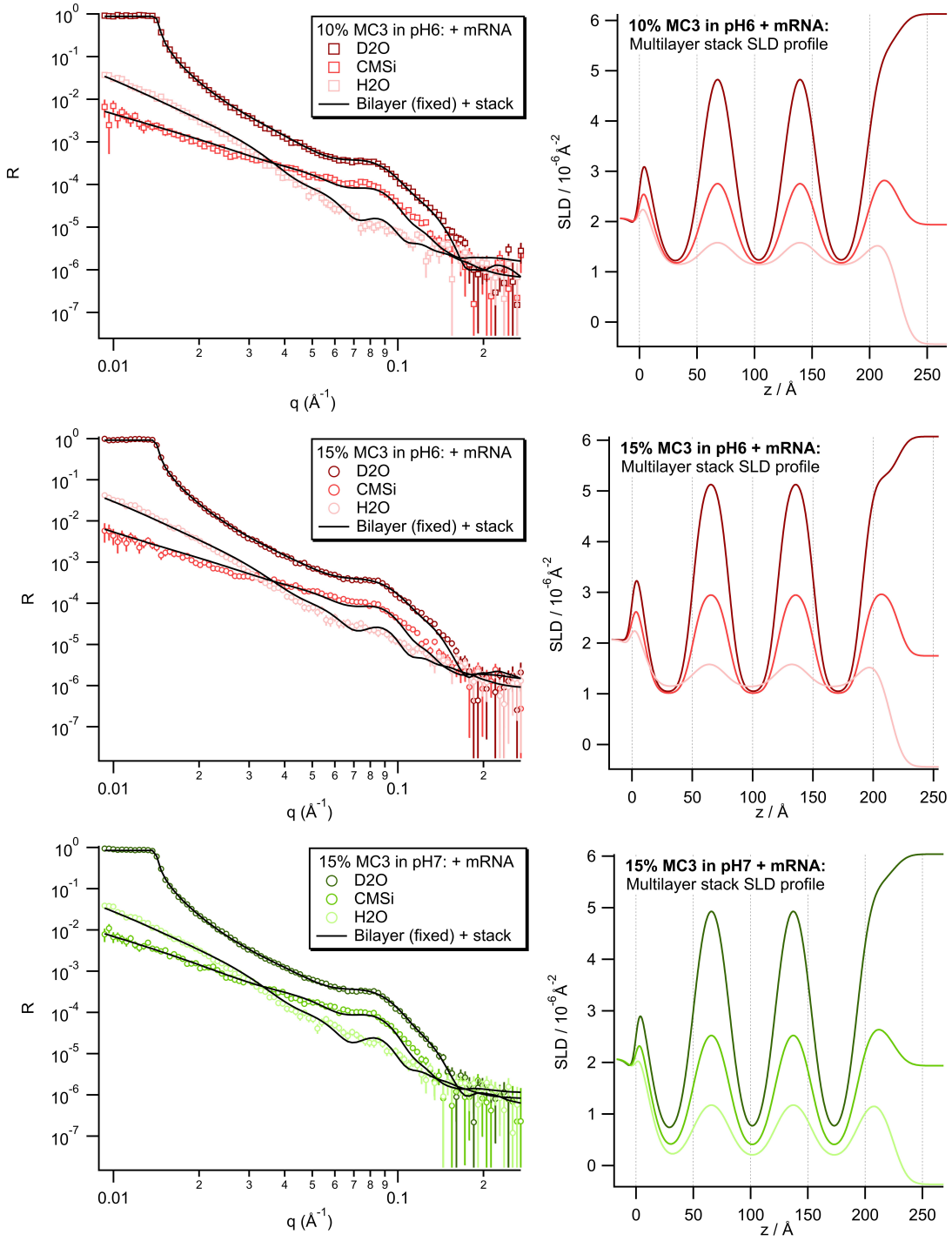

Figure S29 Comparing the data for the 10% MC3 (pH6 buffer) and 15% MC3 (pH6 and 7) lipid layers after incubation with EPO mRNA to the mixed area model with bilayer and multilayer stack fit.

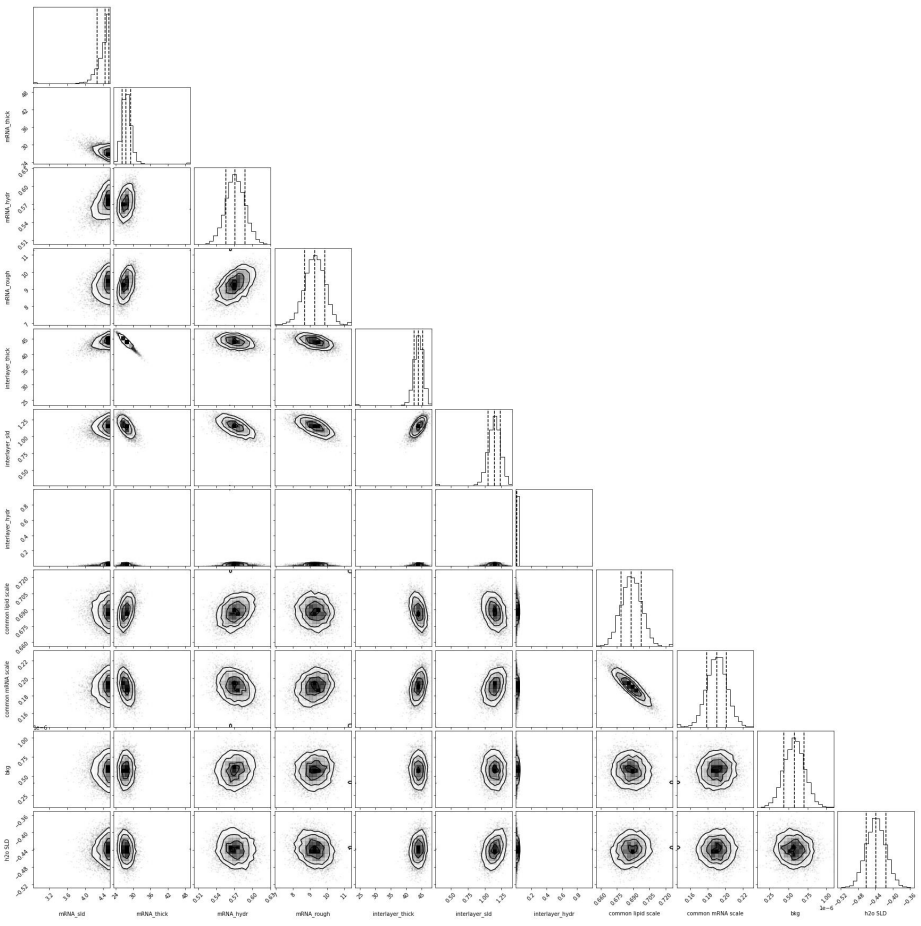

Figure S30 Corner plot of parameter posterior distributions from Bayesian analysis for a mixed area model with bilayer and multilayer stack fit for the 10% MC3 layer in pH6 buffer after incubation with mRNA.

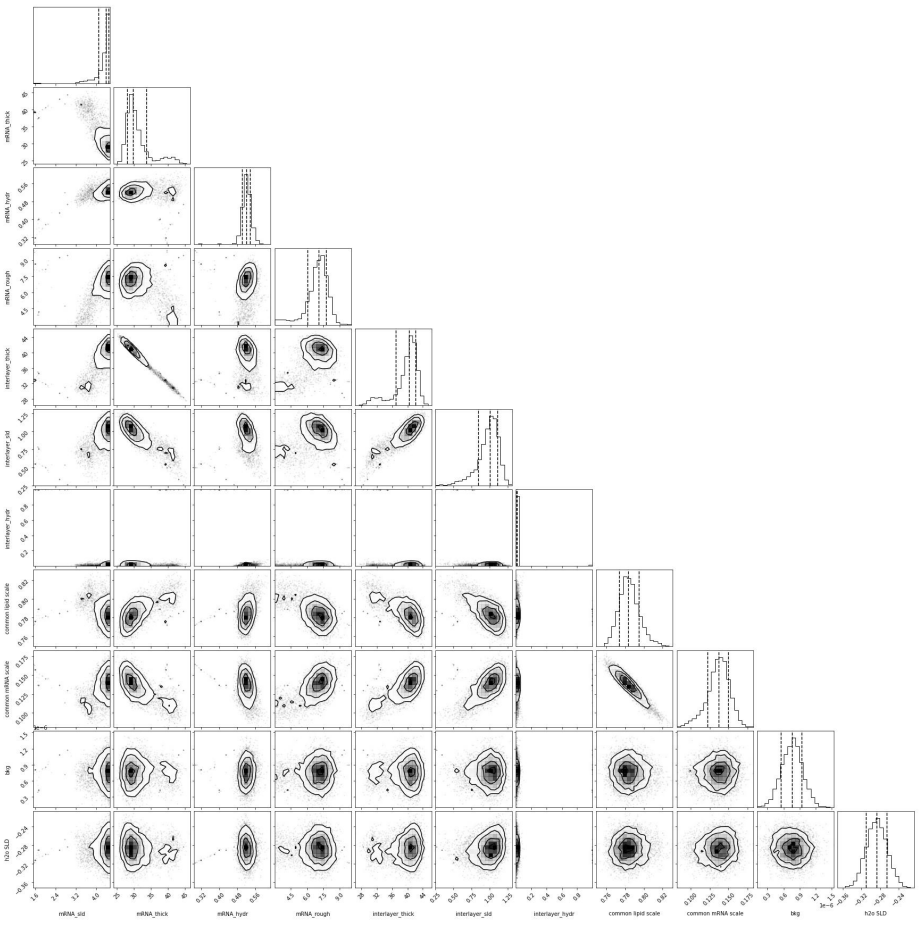

Figure S31 Corner plot of parameter posterior distributions from Bayesian analysis for a mixed area model with bilayer and multilayer stack fit for the 15% MC3 layer in pH6 buffer after incubation with mRNA.

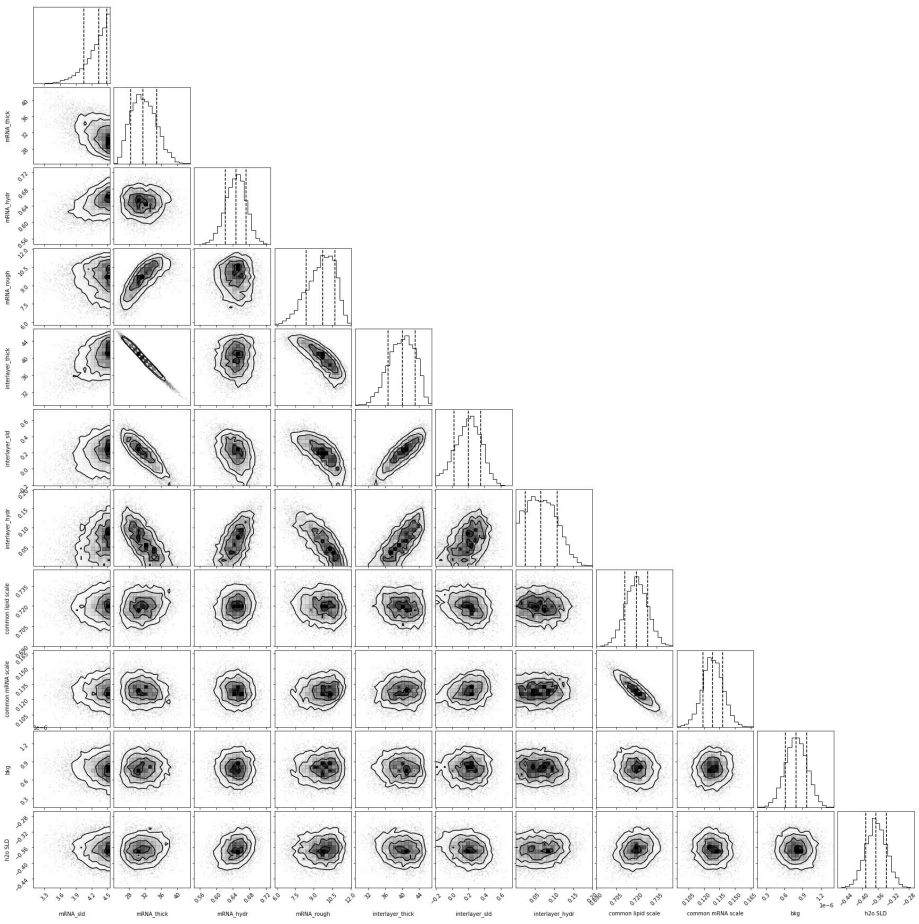

Figure S32 Corner plot of parameter posterior distributions from Bayesian analysis for a mixed area model with bilayer and multilayer stack fit for the 15% MC3 layer in pH7 buffer after incubation with mRNA.

3.2.3 polyU/polyA: Adsorption

For the 15% MC3 pH6 samples incubated with polyA and polyU, a much smaller difference was observed after incubation, compared to the corresponding mRNA samples.

For the polyU samples the fit parameters for the multilayer were very similar to those observed for the 10 and 15 % MC3 samples in pH6 where a broad peak was observed after addition of EPO mRNA. The fit, however, still does not really capture this broad peak at approximately 0.09 $Å^{-1}$ in the D_2O contrast very well, therefore it is possible that the fit is not not sensitive enough to describe it (see Figure S33).

Here, for the sample with polyA, there is no clear peak formation, therefore it is assumed that a multilayer is not formed. It is especially hard to compare the samples qualitatively before and after incubation, as there is a shift in the critical edge in the D_2O contrast (see Figure 6). This data set was therefore fit using some different models: a bilayer and a bilayer with a single slab on top with the bilayer parameters either fixed from the lipid layer fit (single area model) or varying (mixed area model). The polyA sample was additionally fit with a bilayer model due to the minimal change observed.

The best fit was achieved with a mixed area model of a bilayer and a bilayer with a single slab on top with the bilayer parameters varying. Although the fits are quite similar for the D_2O, CMmRNA and CMSi contrasts, the bilayer model and the mixed area model of a bilayer (fixed) and a slab do not describe the H_2O contrast as well as the mixed area model of a bilayer (varying) and a bilayer with a single slab (see Figure S35). As the largest difference is in the H_2O contrast, this implies that the change is in the head group region of the layer. This can further be seen in the high roughness of the slab for this model, as the roughness is higher than the thickness of the slab, indicating that the interface between the layers is very poorly defined and there is likely a wide distribution of polyA chain lengths making up this 'layer'.

Multilayer stack	polyU
ML1 Thickness	39.5 ± 0.2 Å
ML2 Thickness	18.7 ± 0.3 Å
ML1 SLD	1.69 ± 0.1 x $10^{-6}Å^{-2}$
ML2 SLD	3.99 ± 0.02 x $10^{-6}Å^{-2}$
ML1 vf	0.0003 ± 0.0005
ML2 vf	0.560 ± 0.008
Roughness	3.6 ± 0.2 Å
Bilayer scale	0.730 ± 0.002
ML scale	0.199 ± 0.003
Repeats	2.44

Table S13 Fit parameters for mixed area model of a bilayer (fixed) and a multilayer stack for 15% MC3 lipid layers in pH6 buffer after incubation with polyU. Bilayer parameters were fixed from fit for the lipid layer without NA.

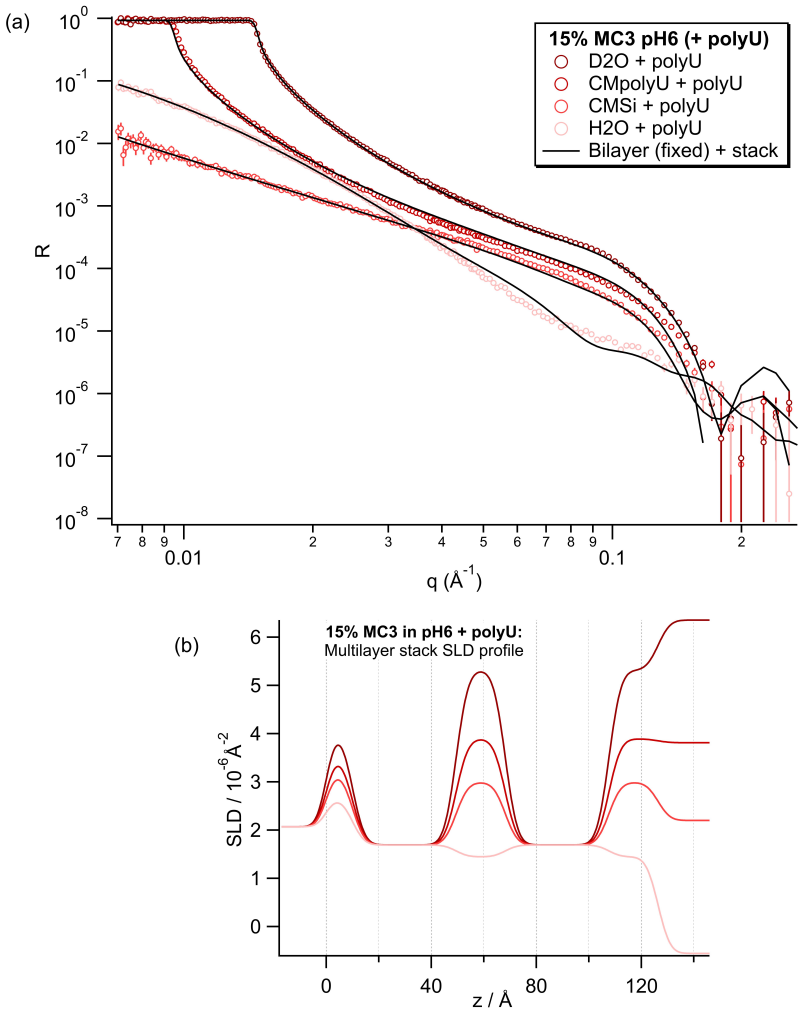

Figure S33 (a) The data for the 15% MC3 lipid layer in pH6 buffer after incubation with polyU was fitted with a mixed area model of a bilayer (fixed) and a multilayer stack (solid line). (b) SLD profiles for the multilayer stack.

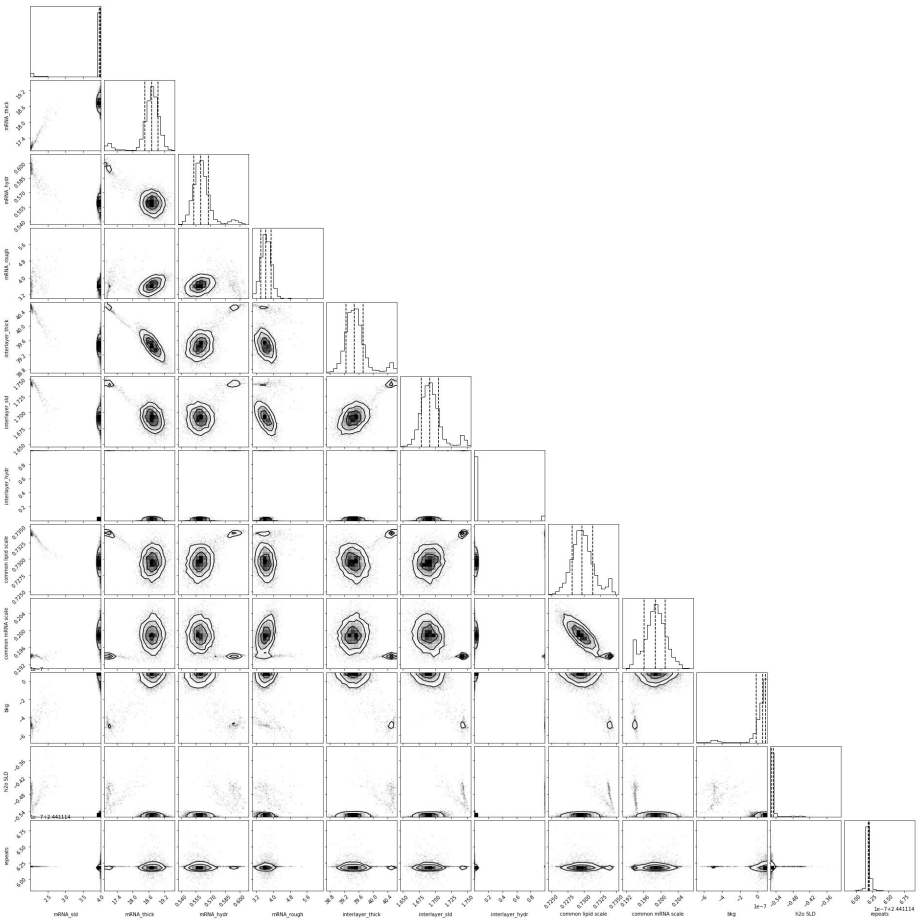

Figure S34 Corner plot of parameter posterior distributions from Bayesian analysis for a mixed area model of a bilayer (fixed) and a multilayer stack fit for 15% MC3 lipid layer in pH6 buffer after incubation with polyU.

Bilayer	polyA
WPLH	7.7 ± 0.1
APM	74.86 ± 0.07 Å^2
WPLT	0.001 ± 0.001
Bilayer roughness	3.002 ± 0.002 Å
Scale	0.9474 ± 0.0008

Table S14 Bilayer fit parameters for 15% MC3 lipid layers in pH6 buffer after incubation with polyA.

Slab with fixed bilayer	polyA
SL1 Thickness	62.3 ± 0.4 Å
SL1 SLD	1.47 ± 0.02 x 10^{-6}Å^{-2}
SL1 vf	0.887 ± 0.002
Roughness	22.6 ± 0.3 Å
Scale	0.972 ± 0.001

Table S15 Fit parameters for a bilayer (fixed) and a single slab for 15% MC3 lipid layers in pH6 buffer after incubation with polyA. Bilayer parameters were fixed from the fit for the lipid layer without NA.

Slab with varying bilayer	polyA
WPLH	7.8 ± 0.1
APM	75.87 ± 0.07 Å^2
WPLT	0.006 ± 0.009
SL1 Thickness	2.13 ± 0.04 Å
SL1 SLD	4.54 ± 0.02 x 10^{-6}Å^{-2}
SL1 vf	0.003 ± 0.005
SL1 roughness	9.8 ± 0.3 Å
Bilayer roughness	3.04 ± 0.03 Å
Bilayer scale	0.003 ± 0.005
SL scale	0.967 ± 0.005

Table S16 Fit parameters for mixed area model of a bilayer (varying) and a single slab for 15% MC3 lipid layers in pH6 buffer after incubation with polyA.

Model	polyA			
	D_2O	CMmRNA	CMSi	H_2O
Bilayer	39	42	8	32
Bilayer (fixed) + slab	57	44	9	33
Bilayer (varying) + slab	32	43	4	2

Table S17 Comparison of normalised χ^2 values for fitting with a bilayer model, a bilayer (fixed) and a single slab or a mixed area model of a bilayer (varying) and a single slab for 15% MC3 lipid layers in pH6 buffer after incubation with polyA.

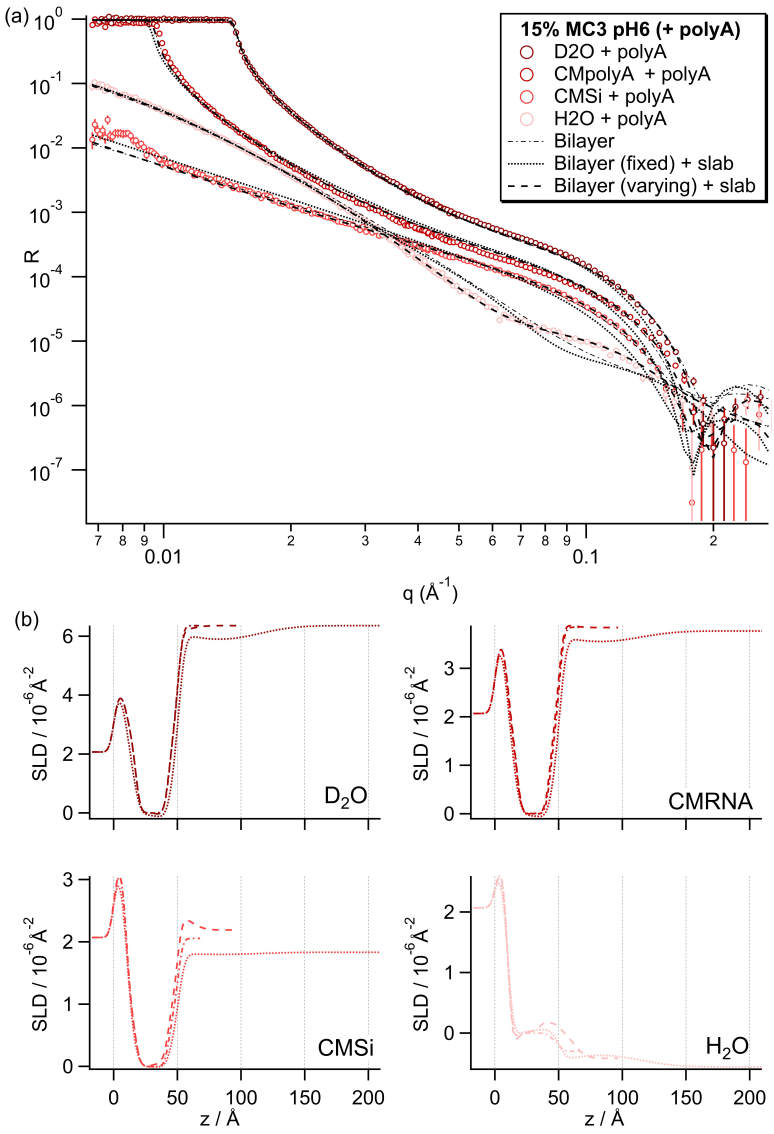

Figure S35 (a) Comparing data for the 15% MC3 lipid layer in pH6 buffer after incubation with polyA to fits with a bilayer model (polyA only, dash-dotted line), a bilayer (fixed) and a single slab (dotted line) and a mixed area model of a bilayer (varying) and a single slab (dashed line). (b) Corresponding SLD profiles for the fits. The data for the 15% MC3 lipid layer in pH6 buffer after incubation with polyU was fitted with a mixed area model of a bilayer (fixed) and a multilayer stack (solid line).

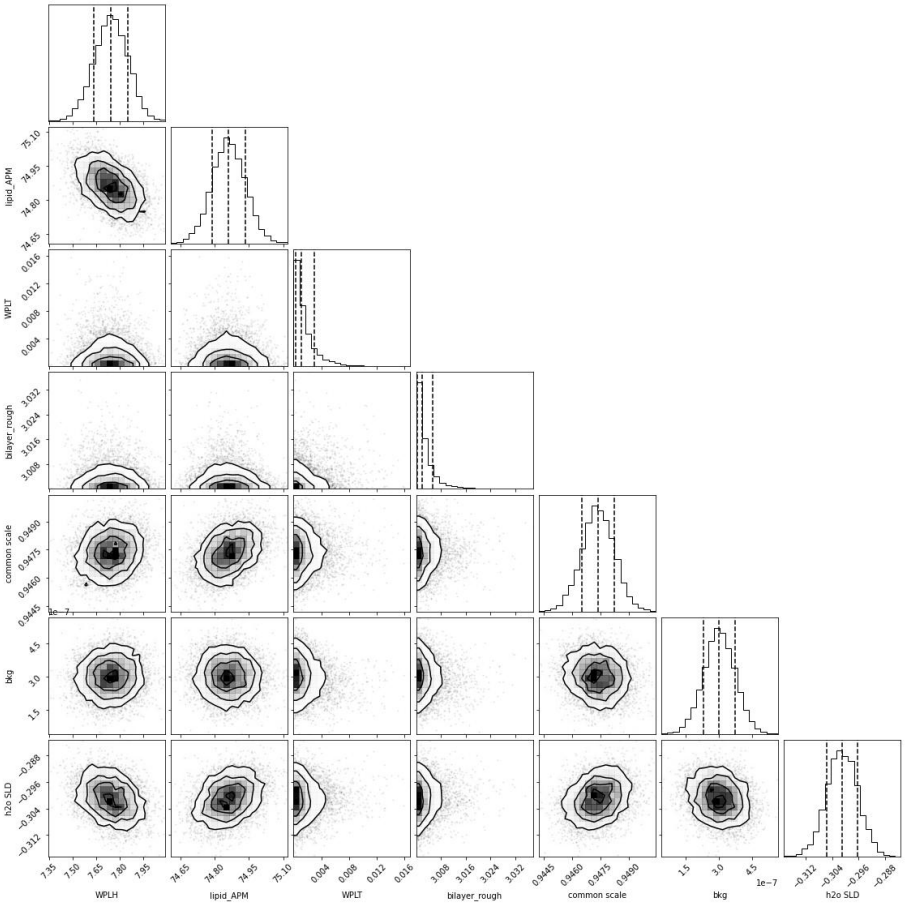

Figure S36 Corner plot of parameter posterior distributions from Bayesian analysis for a bilayer model fit for 15% MC3 lipid layer in pH6 buffer after incubation with polyA.

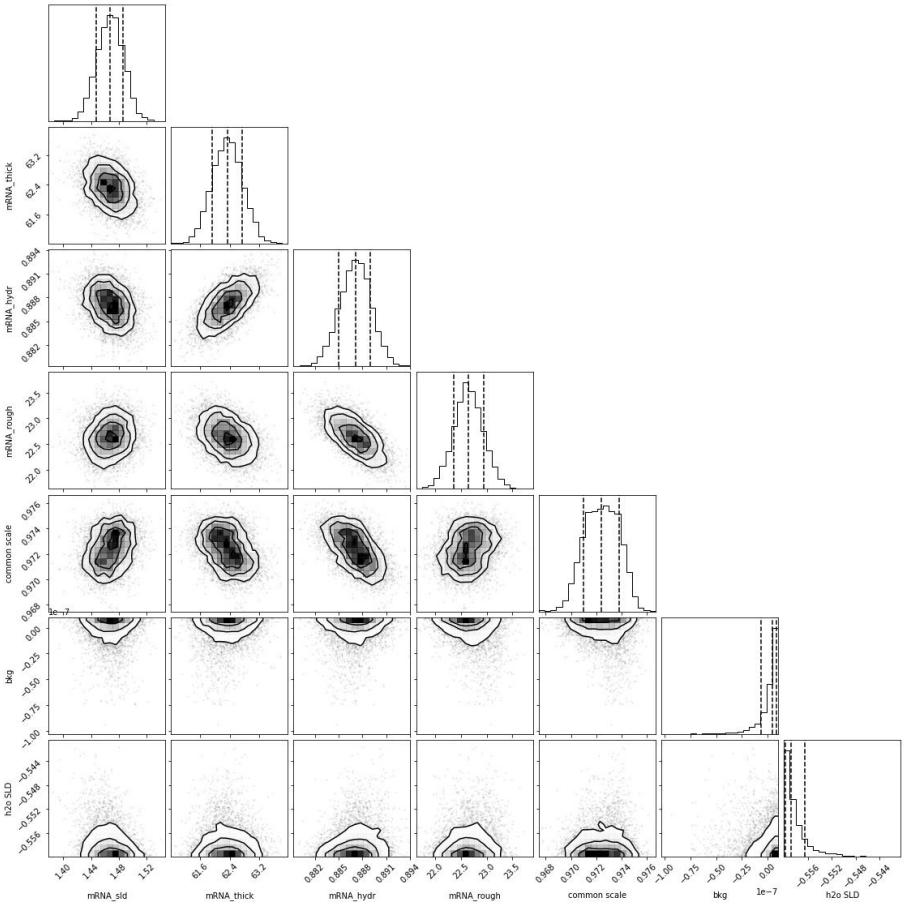

Figure S37 Corner plot of parameter posterior distributions from Bayesian analysis for a mixed area model of a bilayer (fixed) and a single slab fit for 15% MC3 lipid layer in pH6 buffer after incubation with polyA.

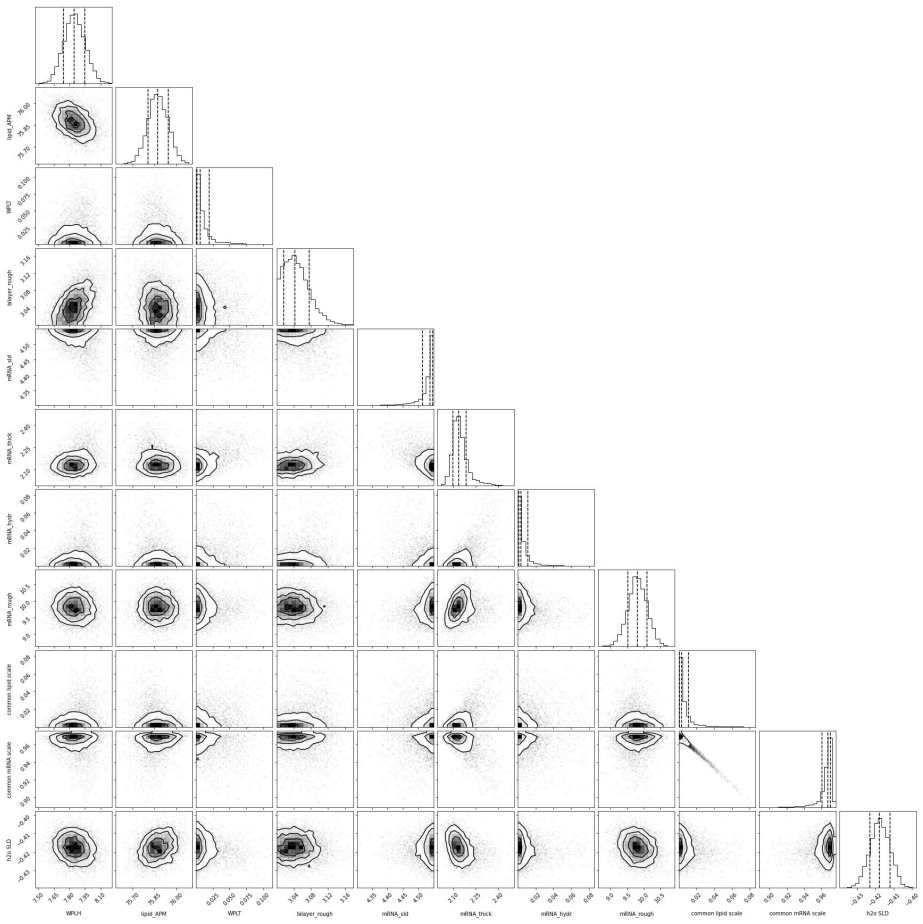

Figure S38 Corner plot of parameter posterior distributions from Bayesian analysis for a mixed area model of a bilayer (varying) and a single slab fit for 15% MC3 lipid layer in pH6 buffer after incubation with polyA.

3.3 Full mass density profiles

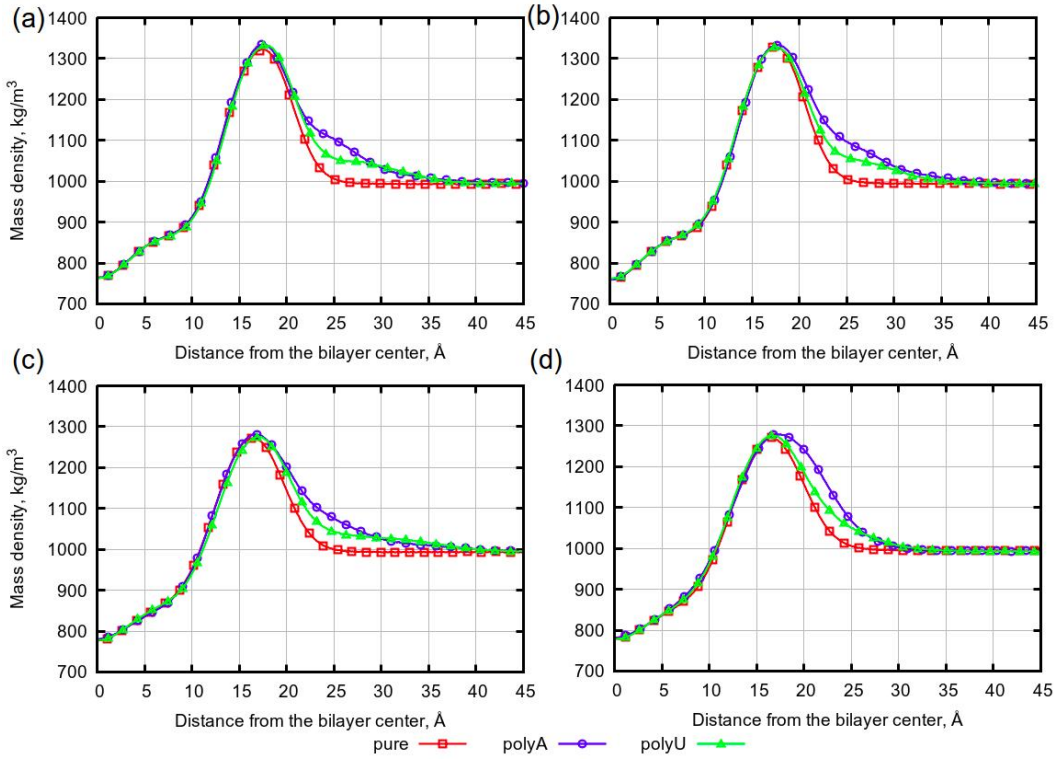

Figure S39 Mass density profiles computed over last 400 ns of simulation. (a) Systems with 5% of neutral DLin-MC3-DMA. (b) Systems with 5% of ionised DLin-MC3-DMA. (c) Systems with 15% of neutral DLin-MC3-DMA. (d) Systems with 15% of ionised DLin-MC3-DMA. "Pure" means that there were no polynucleotides in the system.

3.4 Snapshots

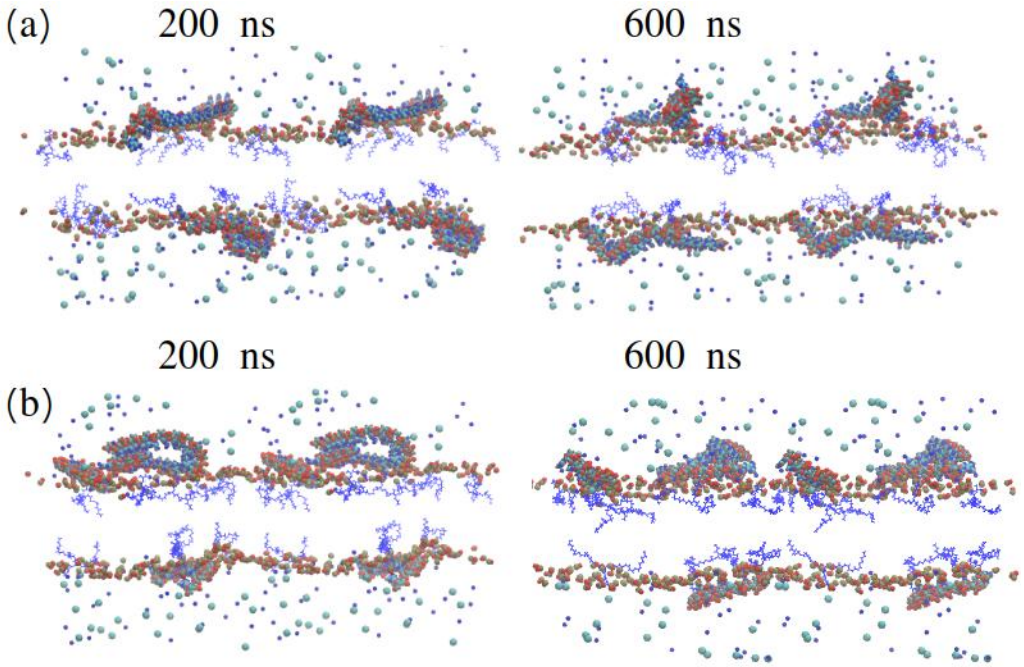

Figure S40 Snapshots of simulated systems containing with NA and 5% of DLin-MC3-DMA. (a) System with polyA and neutral DLin-MC3-DMA at 200 and 600 ns. (b) System with polyA and ionized DLin-MC3-DMA at 200 and 600 ns. Water and DOPC are omitted for the clarity. Only phospatic groups of DOPC are kept in order to show intersections of locations with polyA and shown with red-yellow colors. Visualization: blue lines - DLin-MC3-DMA, big and fat molecules on top are polyA, light blue and cyan balls are ions of salt.

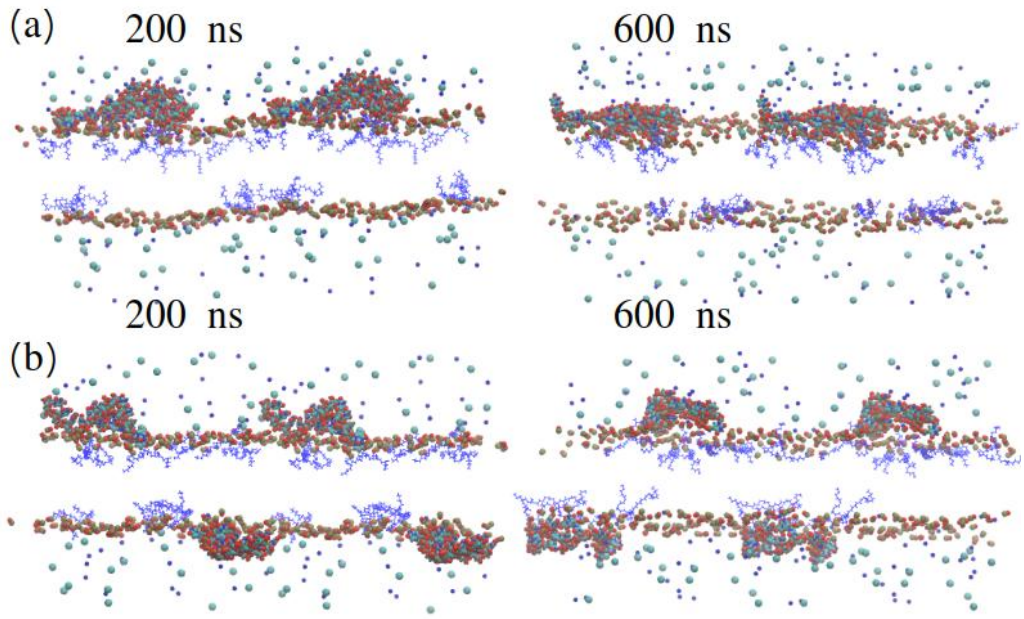

Figure S41 Snapshots of simulated systems containing with NA and 5% of DLin-MC3-DMA. (a) System with polyU and neutral DLin-MC3-DMA at 200 and 600 ns. (b) System with polyU and ionized DLin-MC3-DMA at 200 and 600 ns. Water and DOPC are omitted for the clarity. Only phospatic groups of DOPC are kept in order to show intersections of locations with polyU and shown with red-yellow colors. Visualization: blue lines - DLin-MC3-DMA, big and fat molecules on top are polyU, light blue and cyan balls are ions of salt.

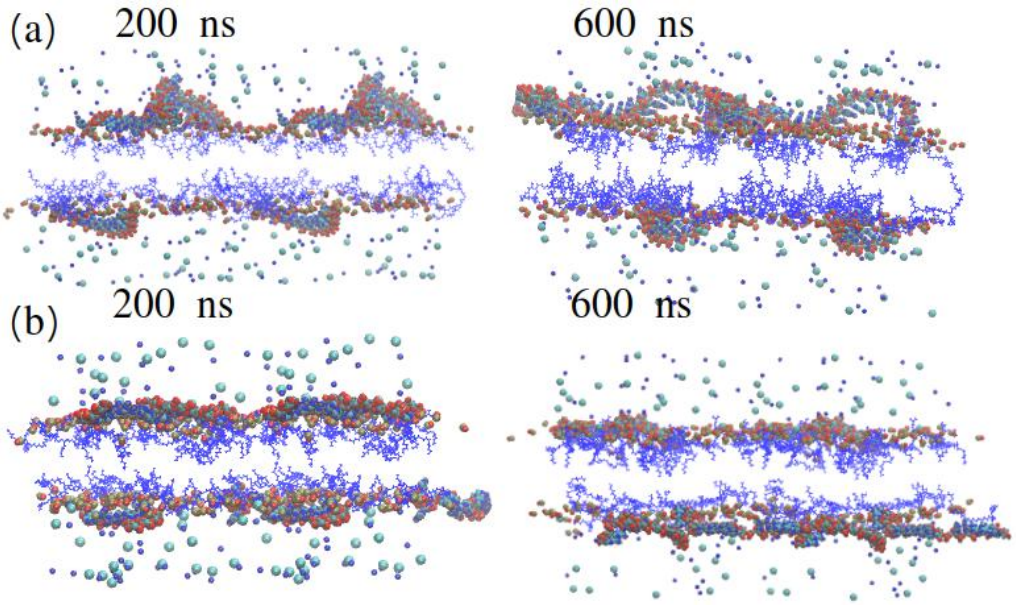

Figure S42 Snapshots of simulated systems containing with NA and 15% of DLin-MC3-DMA. (a) System with polyA and neutral DLin-MC3-DMA at 200 and 600 ns. (b) System with polyA and ionized DLin-MC3-DMA at 200 and 600 ns. Water and DOPC are omitted for the clarity. Only phospatic groups of DOPC are kept in order to show intersections of locations with polyA and shown with red-yellow colors. Visualization: blue lines - DLin-MC3-DMA, big and fat molecules on top are polyA, light blue and cyan balls are ions of salt.

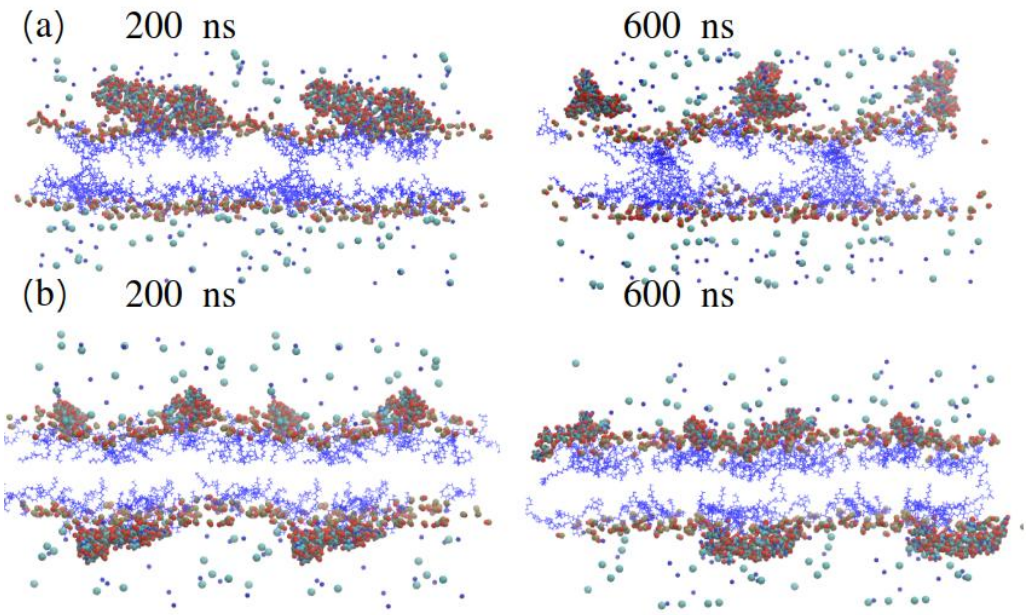

Figure S43 Snapshots of simulated systems containing with NA and 15% of DLin-MC3-DMA. (a) System with polyU and neutral DLin-MC3-DMA at 200 and 600 ns. (b) System with polyU and ionized DLin-MC3-DMA at 200 and 600 ns. Water and DOPC are omitted for the clarity. Only phospatic groups of DOPC are kept in order to show intersections of locations with polyU and shown with red-yellow colors. Visualization: blue lines - DLin-MC3-DMA, big and fat molecules on top are polyU, light blue and cyan balls are ions of salt.

3.5 Structural information about polyA and polyU

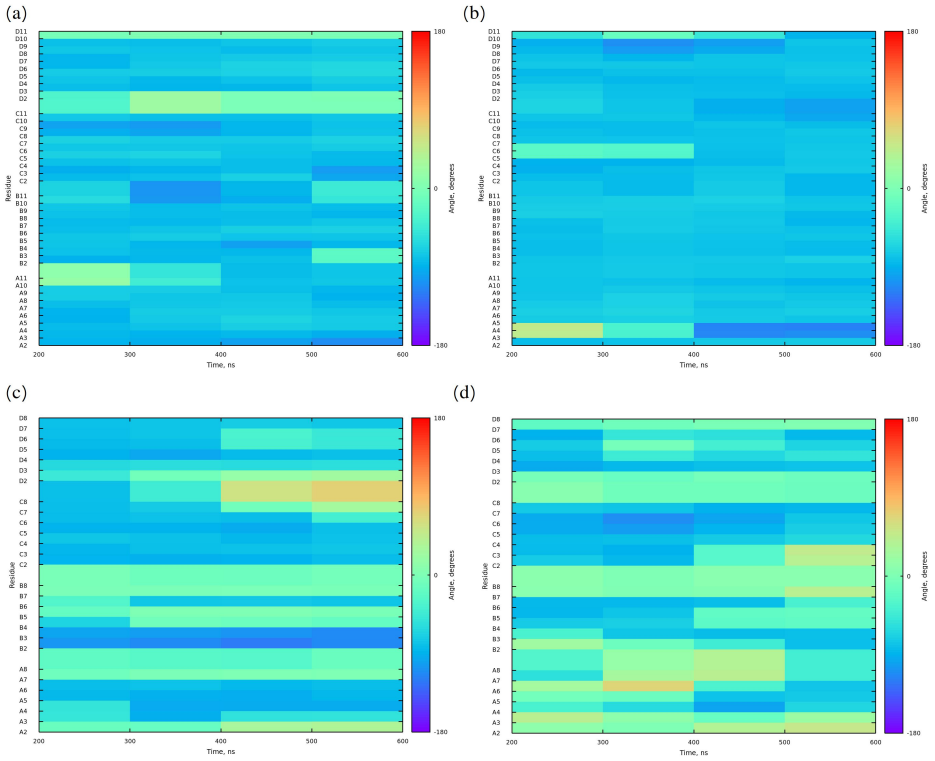

Figure S44 α dihedrals for simulations with 5% of NA. (a) System with neutral DLin-MC3-DMA and polyA. (b) System with ionized DLin-MC3-DMA and polyA. (c) System with neutral DLin-MC3-DMA and polyU. (d) System with ionized DLin-MC3-DMA and polyU. Since in simulations short chains were used on the left sides of figures letters denote different chains of NA while the numbers represent the positions in the respective chains. Dihedrals are classified according to IUPAC classification and computed using BARNABA software[6] on intervals of 100 ns starting from 200 ns.

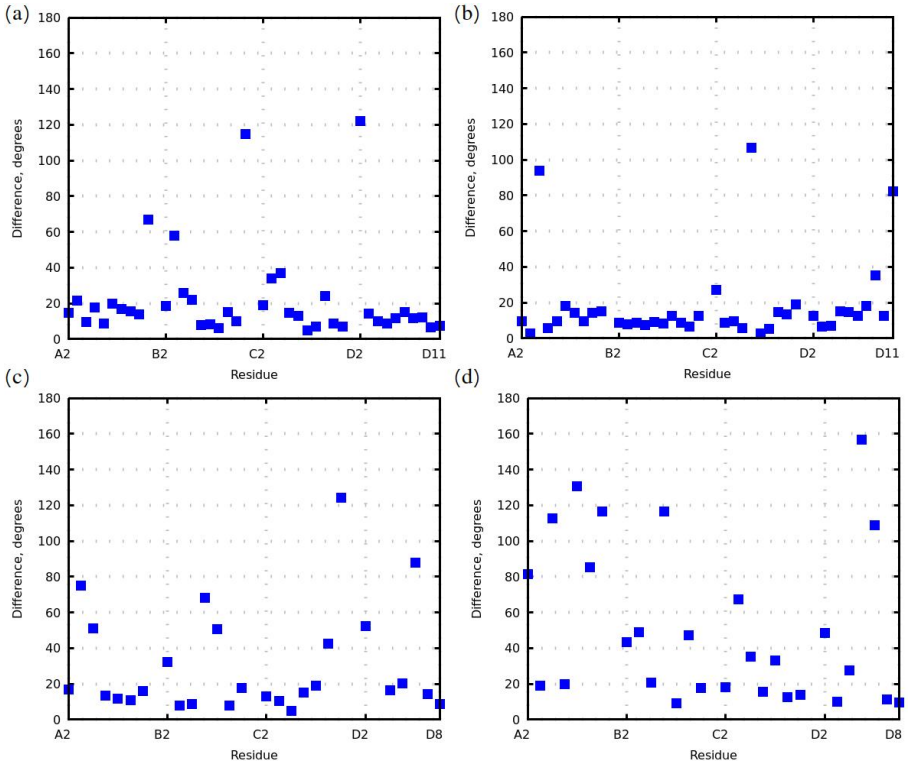

Figure S45 Difference in α dihedrals for simulations with 5% of NA. (a) System with neutral DLin-MC3-DMA and polyA. (b) System with ionized DLin-MC3-DMA and polyA. (c) System with neutral DLin-MC3-DMA and polyU. (d) System with ionized DLin-MC3-DMA and polyU. Since in simulations short chains were used on the left sides of figures letters denote different chains of NA while the numbers represent the positions in the respective chains. Difference was computed between intervals 200-300 ns, 300-400 ns, 400-500 ns, 500-600 ns.

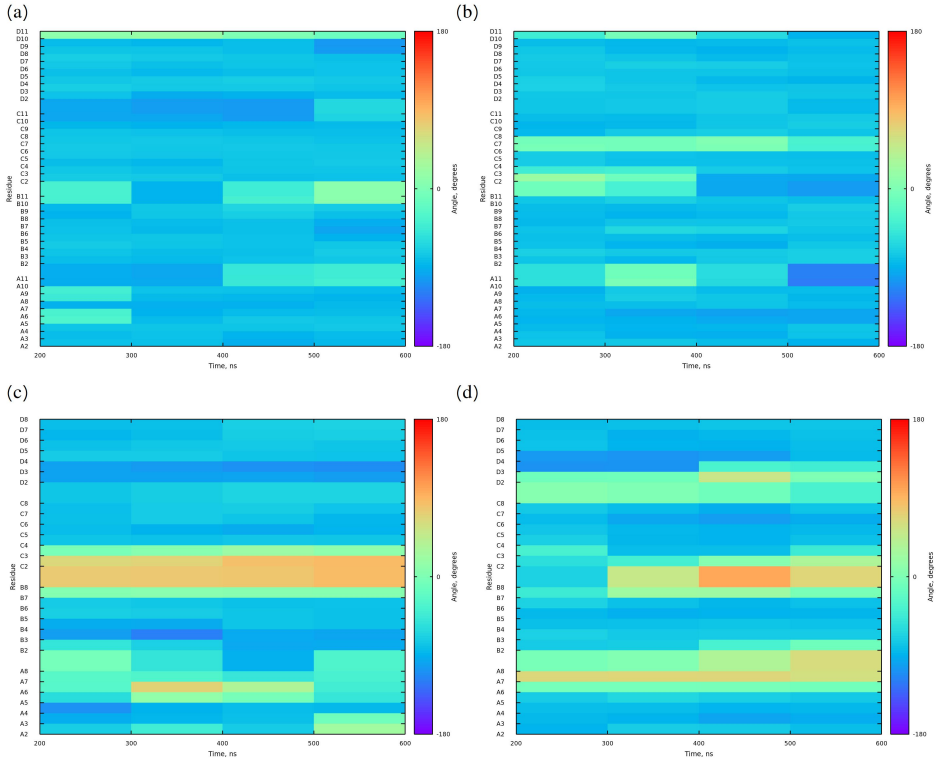

Figure S46 α dihedrals for simulations with 15% of NA. (a) System with neutral DLin-MC3-DMA and polyA. (b) System with ionized DLin-MC3-DMA and polyA. (c) System with neutral DLin-MC3-DMA and polyU. (d) System with ionized DLin-MC3-DMA and polyU. Since in simulations short chains were used on the left sides of figures letters denote different chains of NA while the numbers represent the positions in the respective chains. Dihedrals are classified according to IUPAC classification and computed using BARNABA software[6] on intervals of 100 ns starting from 200 ns.

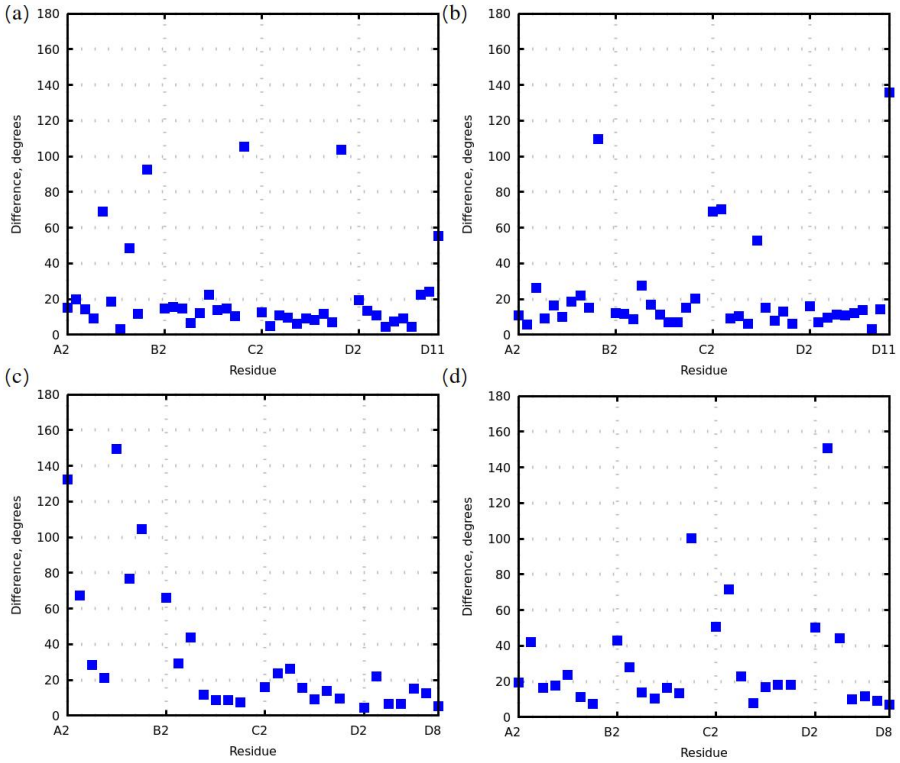

Figure S47 Difference in α dihedrals for simulations with 15% of NA. (a) System with neutral DLin-MC3-DMA and polyA. (b) System with ionized DLin-MC3-DMA and polyA. (c) System with neutral DLin-MC3-DMA and polyU. (d) System with ionized DLin-MC3-DMA and polyU. Since in simulations short chains were used on the left sides of figures letters denote different chains of NA while the numbers represent the positions in the respective chains. Difference was computed between intervals 200-300 ns, 300-400 ns, 400-500 ns, 500-600 ns.

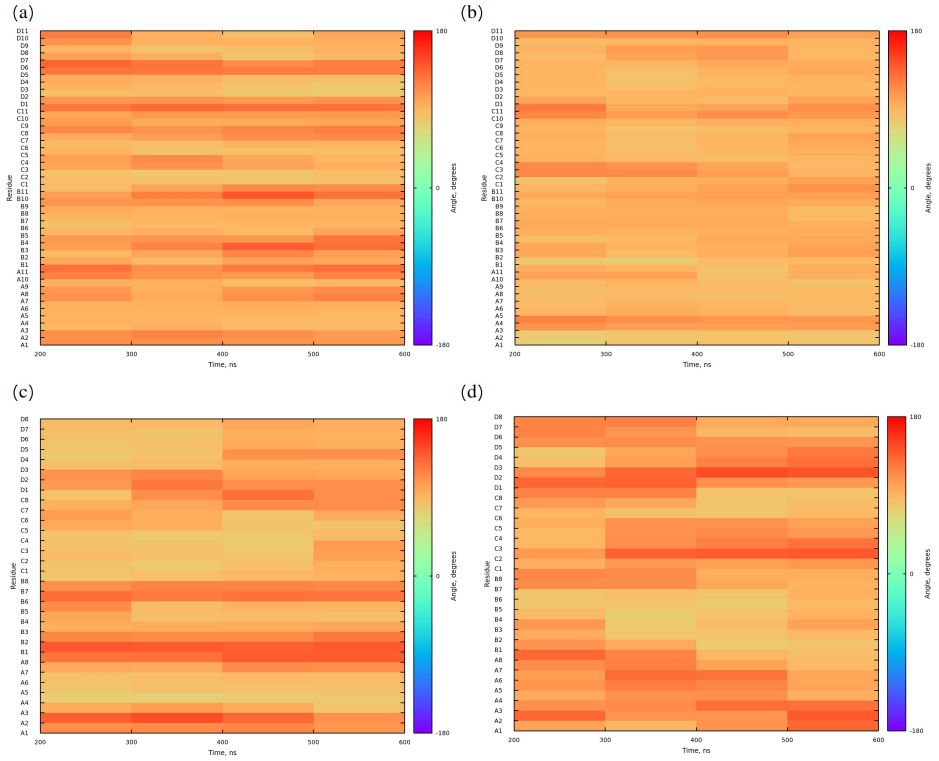

Figure S48 δ dihedrals for simulations with 5% of NA. (a) System with neutral DLin-MC3-DMA and polyA. (b) System with ionized DLin-MC3-DMA and polyA. (c) System with neutral DLin-MC3-DMA and polyU. (d) System with ionized DLin-MC3-DMA and polyU. Since in simulations short chains were used on the left sides of figures letters denote different chains of NA while the numbers represent the positions in the respective chains. Dihedrals are classified according to IUPAC classification and computed using BARNABA software[6] on intervals of 100 ns starting from 200 ns.

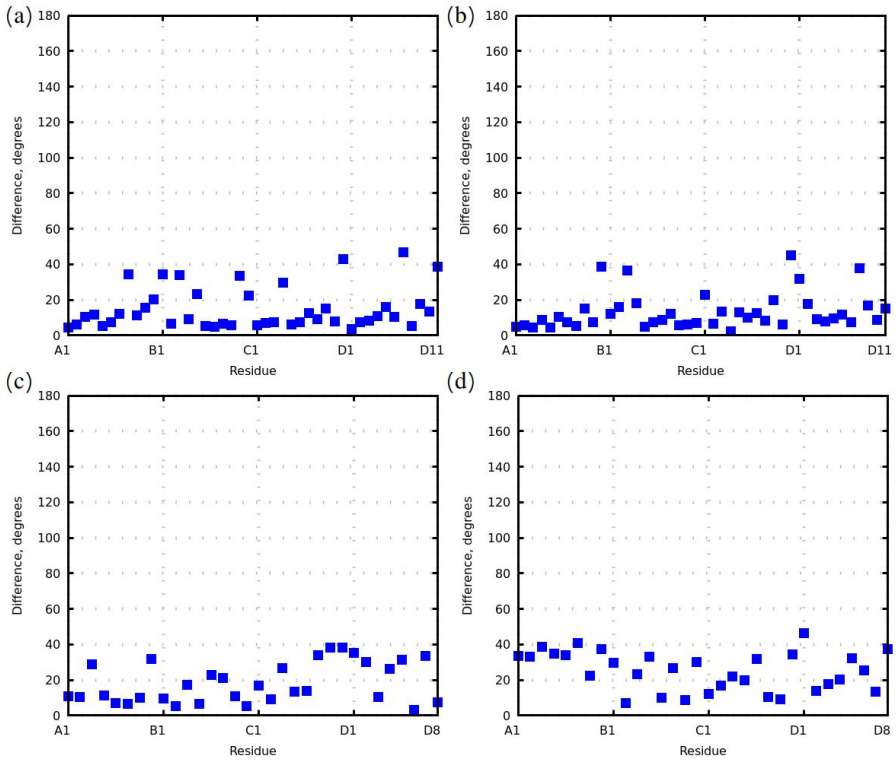

Figure S49 Difference in δ dihedrals for simulations with 5% of NA. (a) System with neutral DLin-MC3-DMA and polyA. (b) System with ionized DLin-MC3-DMA and polyA. (c) System with neutral DLin-MC3-DMA and polyU. (d) System with ionized DLin-MC3-DMA and polyU. Since in simulations short chains were used on the left sides of figures letters denote different chains of NA while the numbers represent the positions in the respective chains. Difference was computed between intervals 200-300 ns, 300-400 ns, 400-500 ns, 500-600 ns.

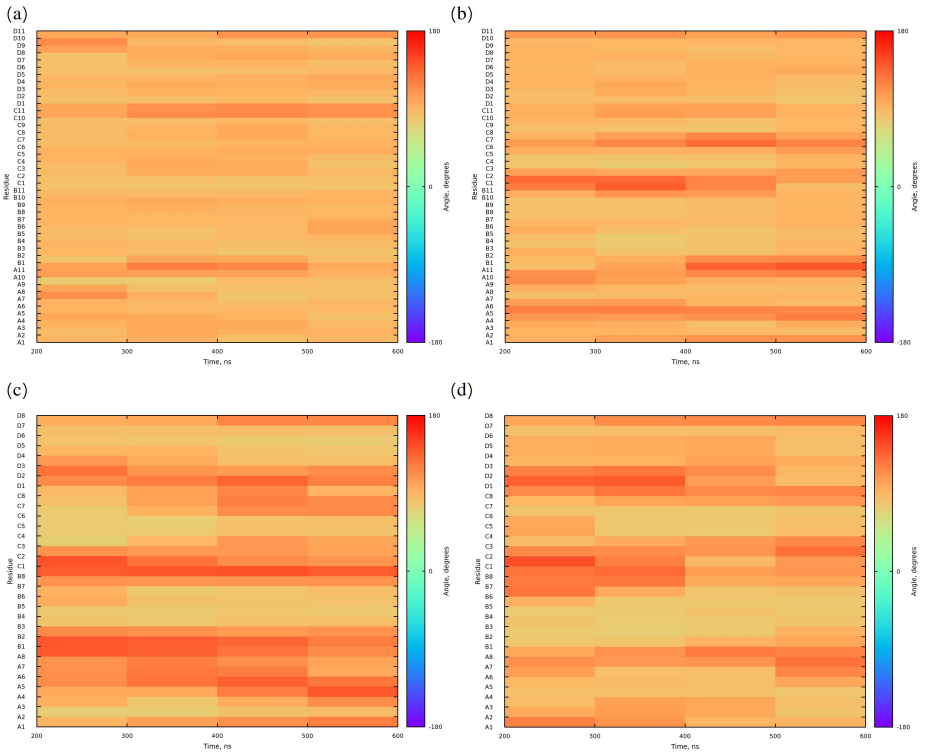

Figure S50 δ dihedrals for simulations with 15% of NA. (a) System with neutral DLin-MC3-DMA and polyA. (b) System with ionized DLin-MC3-DMA and polyA. (c) System with neutral DLin-MC3-DMA and polyU. (d) System with ionized DLin-MC3-DMA and polyU. Since in simulations short chains were used on the left sides of figures letters denote different chains of NA while the numbers represent the positions in the respective chains. Dihedrals are classified according to IUPAC classification and computed using BARNABA software[6] on intervals of 100 ns starting from 200 ns.

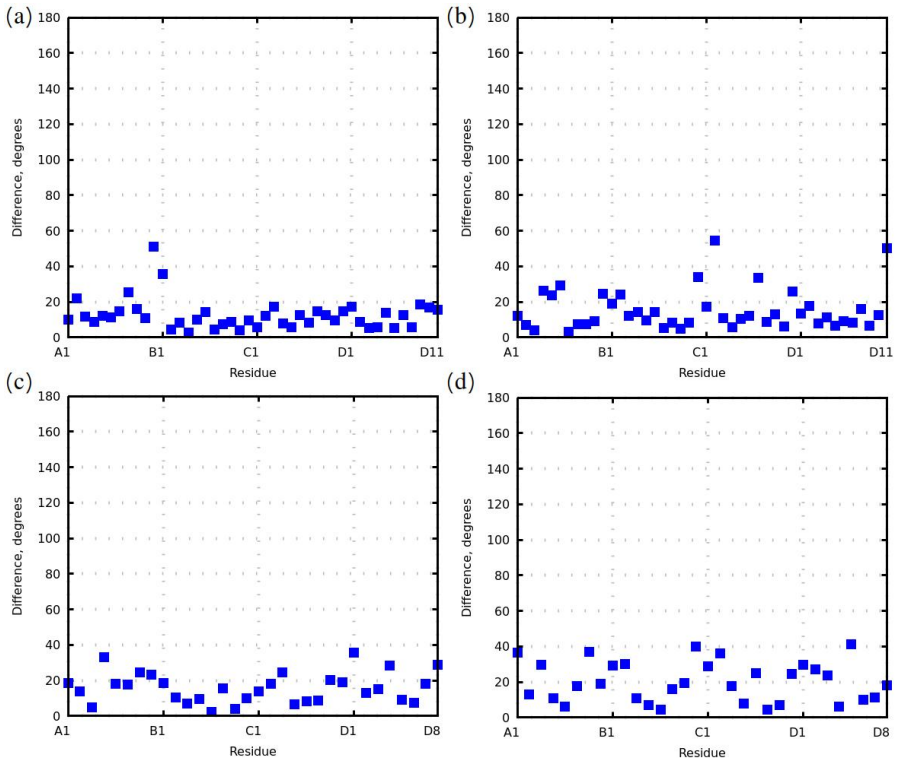

Figure S51 Difference in δ dihedrals for simulations with 15% of NA. (a) System with neutral DLin-MC3-DMA and polyA. (b) System with ionized DLin-MC3-DMA and polyA. (c) System with neutral DLin-MC3-DMA and polyU. (d) System with ionized DLin-MC3-DMA and polyU. Since in simulations short chains were used on the left sides of figures letters denote different chains of NA while the numbers represent the positions in the respective chains. Difference was computed between intervals 200-300 ns, 300-400 ns, 400-500 ns, 500-600 ns.

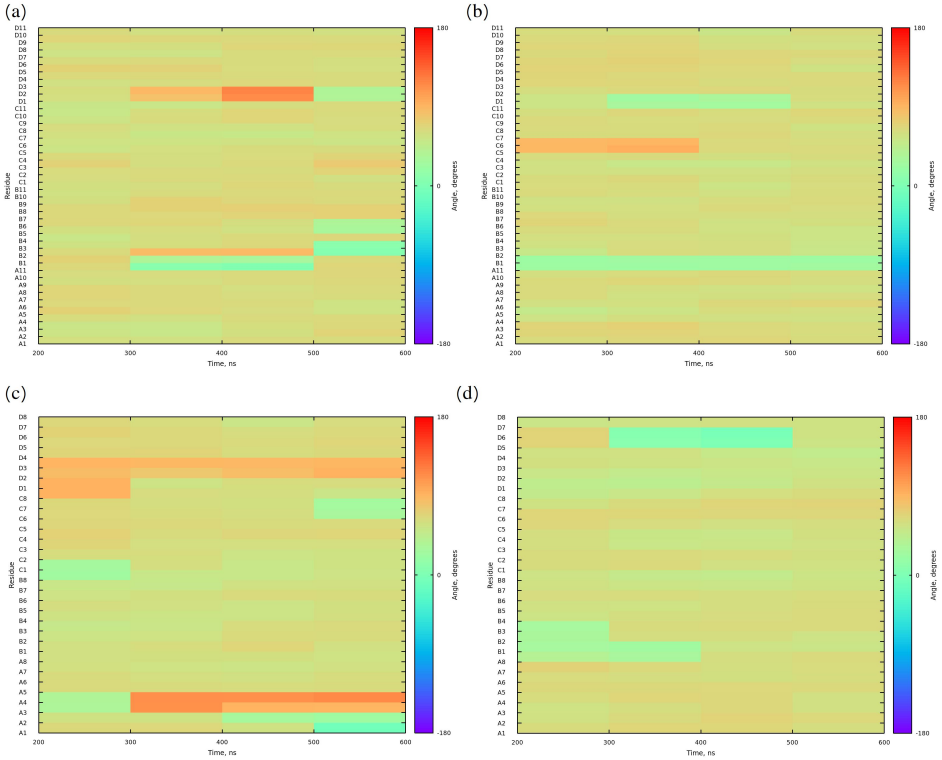

Figure S52 γ dihedrals for simulations with 5% of NA. (a) System with neutral DLin-MC3-DMA and polyA. (b) System with ionized DLin-MC3-DMA and polyA. (c) System with neutral DLin-MC3-DMA and polyU. (d) System with ionized DLin-MC3-DMA and polyU. Since in simulations short chains were used on the left sides of figures letters denote different chains of NA while the numbers represent the positions in the respective chains. Dihedrals are classified according to IUPAC classification and computed using BARNABA software[6] on intervals of 100 ns starting from 200 ns.

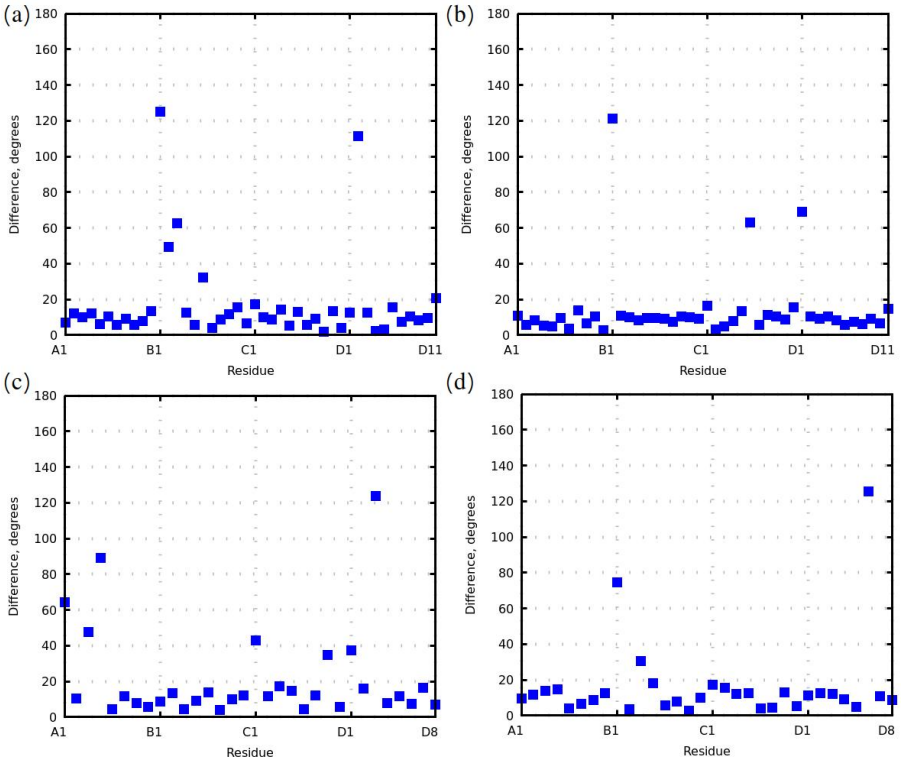

Figure S53 Difference in γ dihedrals for simulations with 5% of NA. (a) System with neutral DLin-MC3-DMA and polyA. (b) System with ionized DLin-MC3-DMA and polyA. (c) System with neutral DLin-MC3-DMA and polyU. (d) System with ionized DLin-MC3-DMA and polyU. Since in simulations short chains were used on the left sides of figures letters denote different chains of NA while the numbers represent the positions in the respective chains. Difference was computed between intervals 200-300 ns, 300-400 ns, 400-500 ns, 500-600 ns.

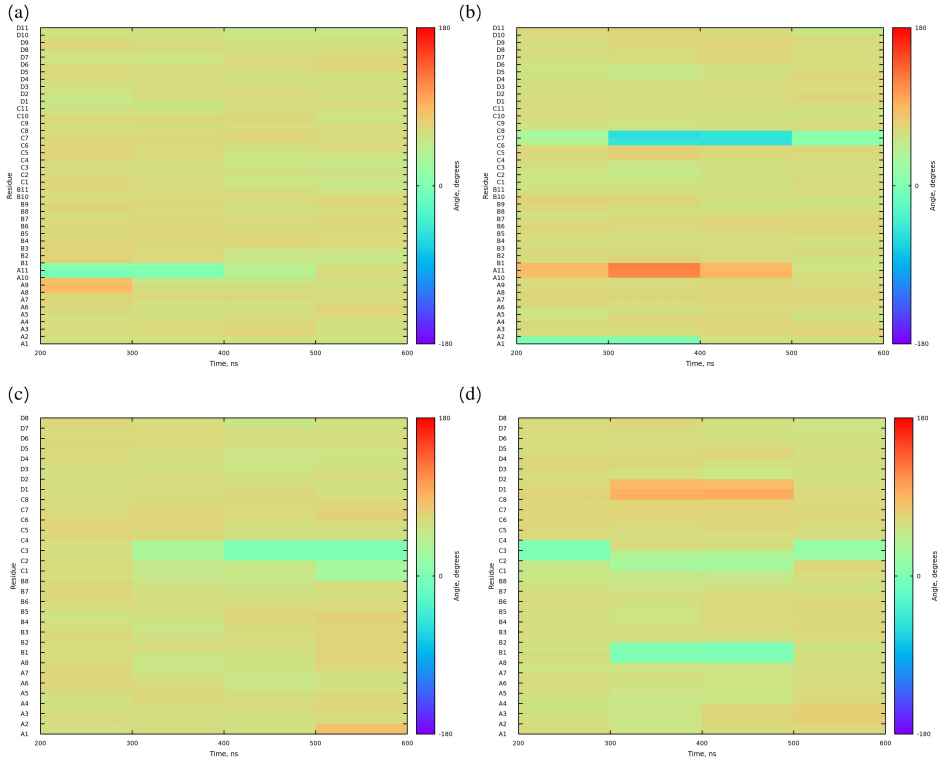

Figure S54 γ dihedrals for simulations with 15% of NA. (a) System with neutral DLin-MC3-DMA and polyA. (b) System with ionized DLin-MC3-DMA and polyA. (c) System with neutral DLin-MC3-DMA and polyU. (d) System with ionized DLin-MC3-DMA and polyU. Since in simulations short chains were used on the left sides of figures letters denote different chains of NA while the numbers represent the positions in the respective chains. Dihedrals are classified according to IUPAC classification and computed using BARNABA software[6] on intervals of 100 ns starting from 200 ns.

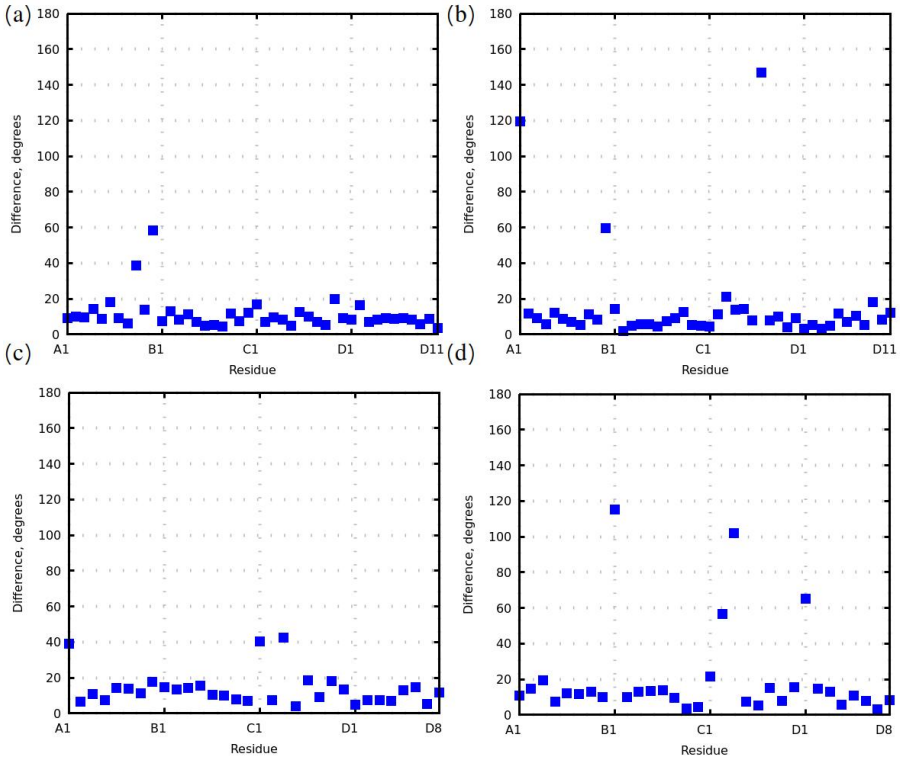

Figure S55 Difference in γ dihedrals for simulations with 15% of NA. (a) System with neutral DLin-MC3-DMA and polyA. (b) System with ionized DLin-MC3-DMA and polyA. (c) System with neutral DLin-MC3-DMA and polyU. (d) System with ionized DLin-MC3-DMA and polyU. Since in simulations short chains were used on the left sides of figures letters denote different chains of NA while the numbers represent the positions in the respective chains. Difference was computed between intervals 200-300 ns, 300-400 ns, 400-500 ns, 500-600 ns.

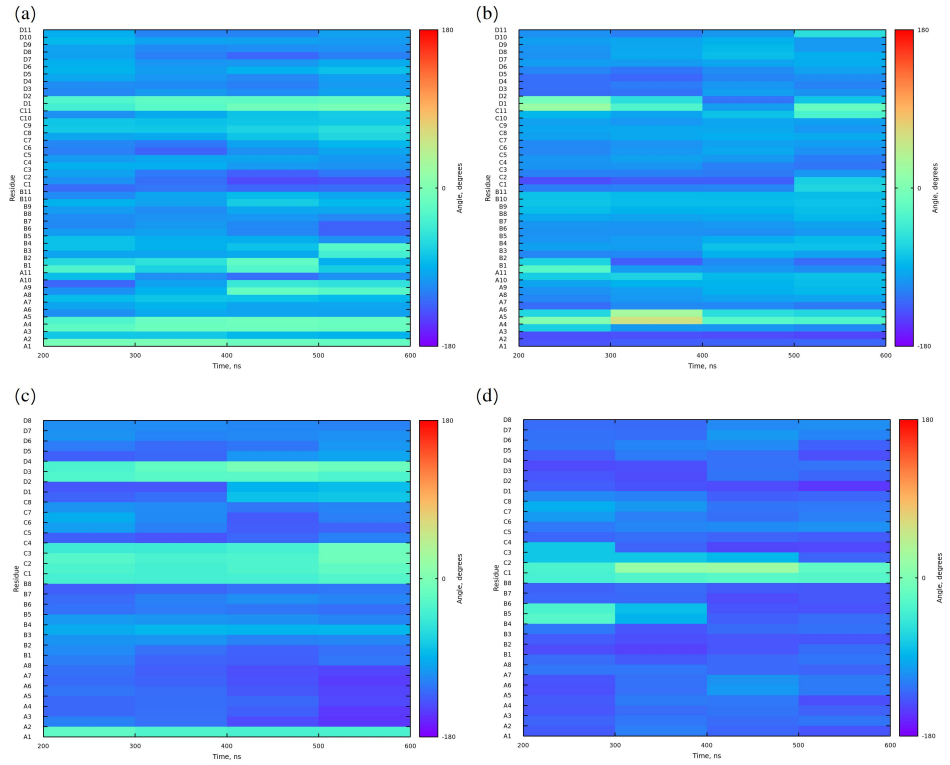

Figure S56 χ dihedrals for simulations with 5% of NA. (a) System with neutral DLin-MC3-DMA and polyA. (b) System with ionized DLin-MC3-DMA and polyA. (c) System with neutral DLin-MC3-DMA and polyU. (d) System with ionized DLin-MC3-DMA and polyU. Since in simulations short chains were used on the left sides of figures letters denote different chains of NA while the numbers represent the positions in the respective chains. Dihedrals are classified according to IUPAC classification and computed using BARNABA software[6] on intervals of 100 ns starting from 200 ns.

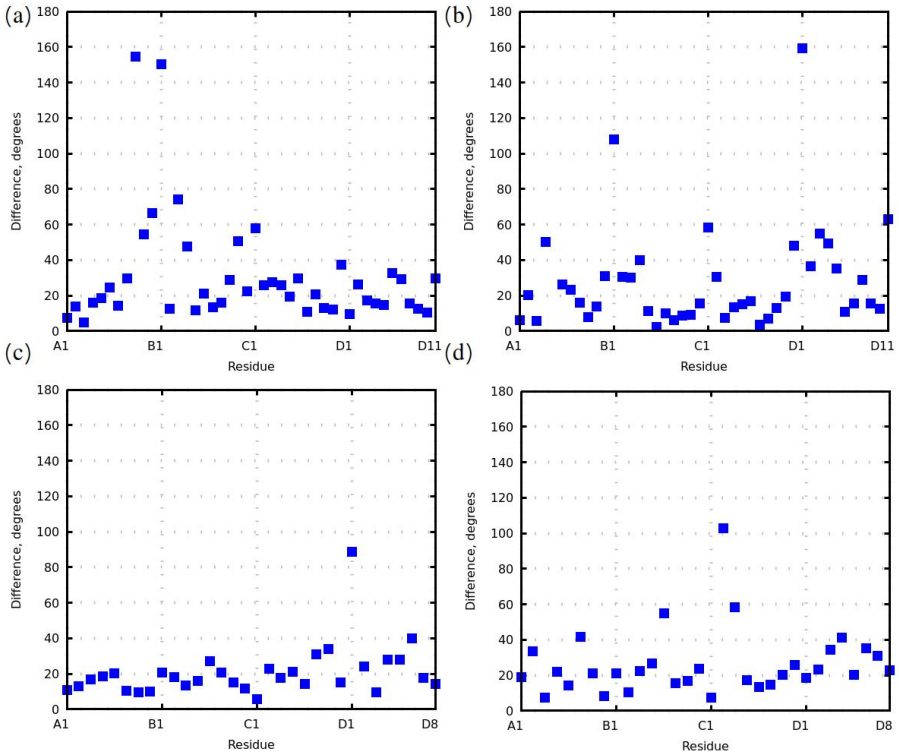

Figure S57 Difference in χ dihedrals for simulations with 5% of NA. (a) System with neutral DLin-MC3-DMA and polyA. (b) System with ionized DLin-MC3-DMA and polyA. (c) System with neutral DLin-MC3-DMA and polyU. (d) System with ionized DLin-MC3-DMA and polyU. Since in simulations short chains were used on the left sides of figures letters denote different chains of NA while the numbers represent the positions in the respective chains. Difference was computed between intervals 200-300 ns, 300-400 ns, 400-500 ns, 500-600 ns.

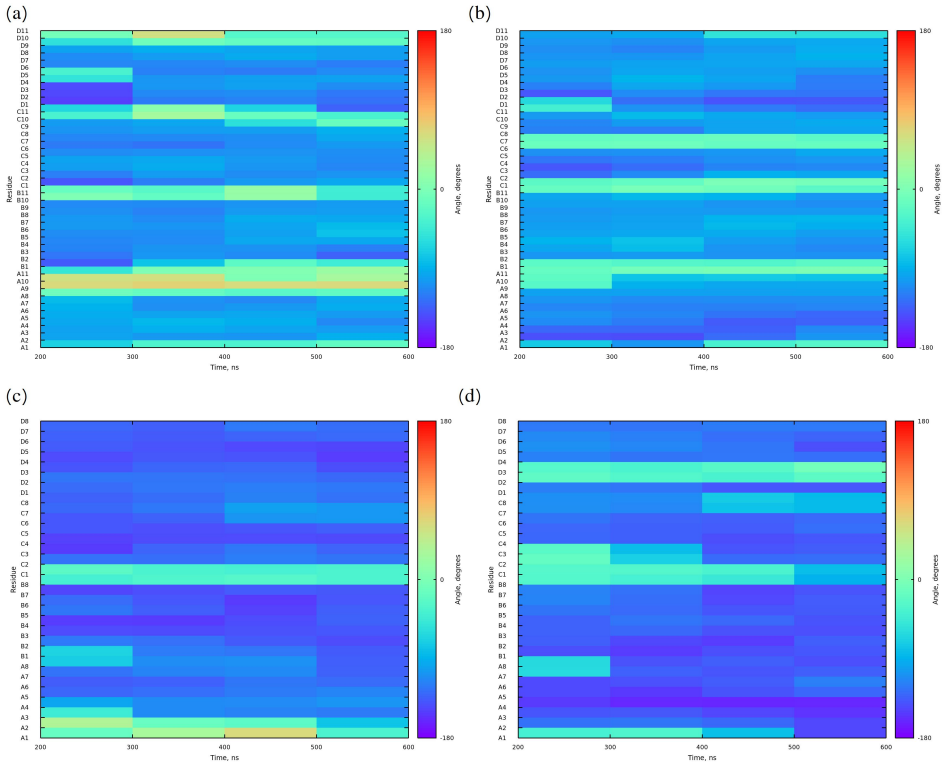

Figure S58 χ dihedrals for simulations with 15% of NA. (a) System with neutral DLin-MC3-DMA and polyA. (b) System with ionized DLin-MC3-DMA and polyA. (c) System with neutral DLin-MC3-DMA and polyU. (d) System with ionized DLin-MC3-DMA and polyU. Since in simulations short chains were used on the left sides of figures letters denote different chains of NA while the numbers represent the positions in the respective chains. Dihedrals are classified according to IUPAC classification and computed using BARNABA software[6] on intervals of 100 ns starting from 200 ns.

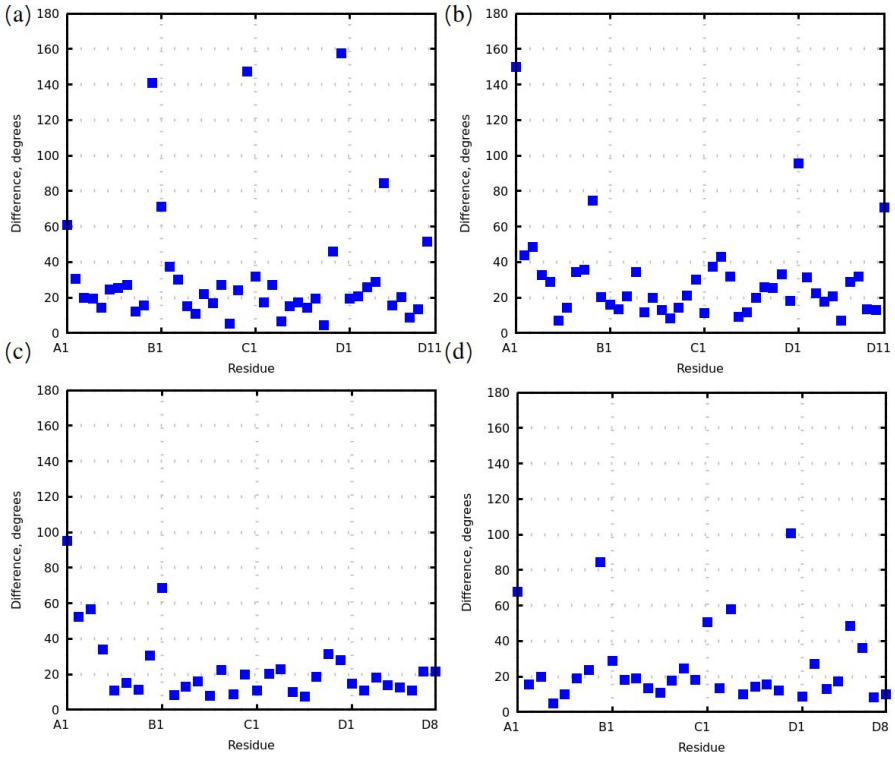

Figure S59 Difference in χ dihedrals for simulations with 15% of NA. (a) System with neutral DLin-MC3-DMA and polyA. (b) System with ionized DLin-MC3-DMA and polyA. (c) System with neutral DLin-MC3-DMA and polyU. (d) System with ionized DLin-MC3-DMA and polyU. Since in simulations short chains were used on the left sides of figures letters denote different chains of NA while the numbers represent the positions in the respective chains. Difference was computed between intervals 200-300 ns, 300-400 ns, 400-500 ns, 500-600 ns.

3.6 Partial mass density profiles

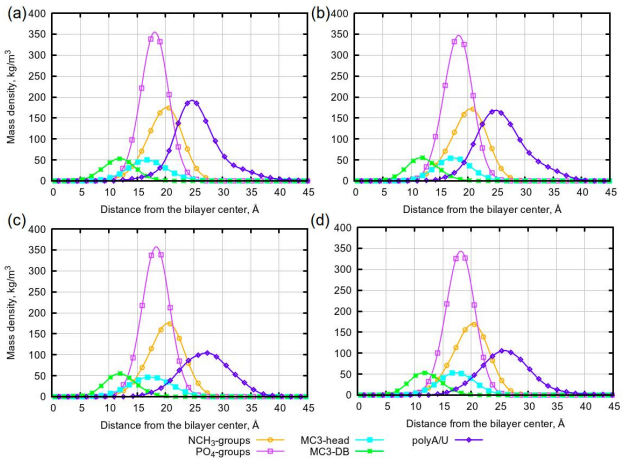

Figure S60 Partial mass density profiles for systems with 5% DLin-MC3-DMA computed over last 400 ns of simulation . (a) Neutral system with polyA. (b) Ionized system with polyA. (c) Neutral system with polyU. (d) Ionized system with polyU. NCH_3-groups are the methyl groups bonded to nitrogen in DOPC. "PO_4-groups are the phosphatic groups of phospholipids. "MC3-head" is a head group of DLin-MC3-DMA. "MC3-DB" is a region with double bonds of DLin-MC3-DMA.Partial densities for DLin-MC3-DMA are multiplied by a factor of 3 in order to make them visible.

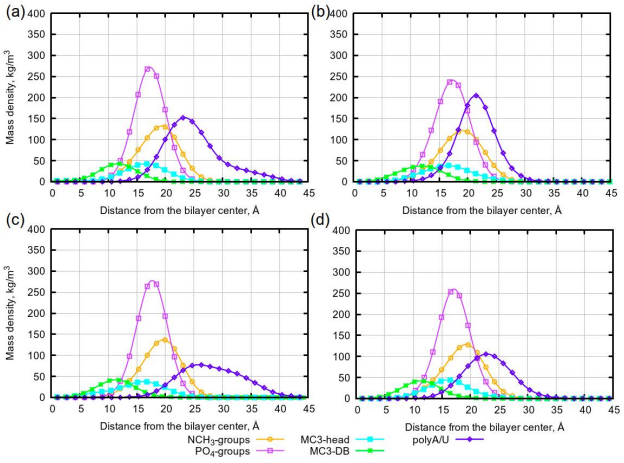

Figure S61 Partial mass density profiles for systems with 15% DLin-MC3-DMA computed over last 400 ns of simulation. (a) Neutral system with polyA. (b) Ionized system with polyA. (c) Neutral system with polyU. (d) Ionized system with polyU. NCH_3-groups are the methyl groups bonded to nitrogen in DOPC. "PO_4-groups are the phosphatic groups of phospholipids. "MC3-head" is a head group of DLin-MC3-DMA. "MC3-DB" is a region with double bonds of DLin-MC3-DMA. Partial densities for DLin-MC3-DMA are kept in their original amounts.

3.7 Radial distribution functions

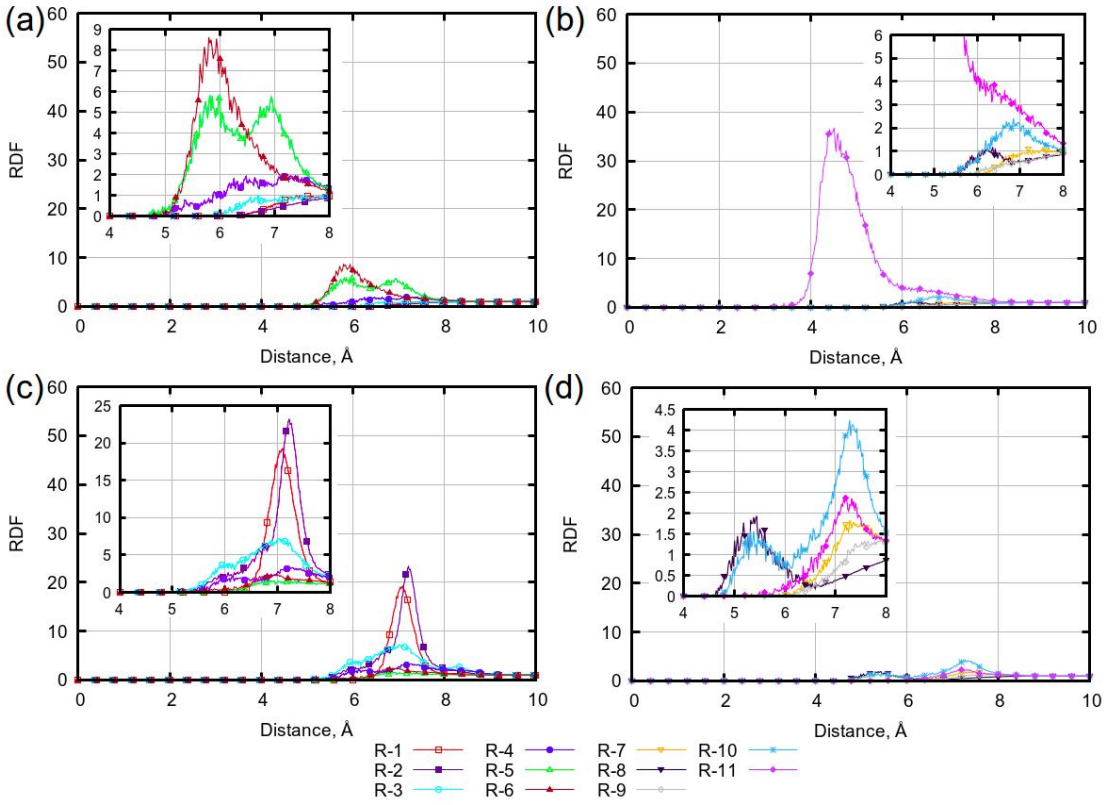

Figure S62 Radial distribution functions between centers of mass of head-groups of DLin-MC3-DMA and residues of polyA for simulations with 5% of DLin-MC3-DMA. (a) and (b) are for simulations with neutral DLin-MC3-DMA. (c) and (d) are for simulations with ionized DLin-MC3-DMA. Letter R with a number stands for a certain residue. Please note the difference in scale of the y axis.

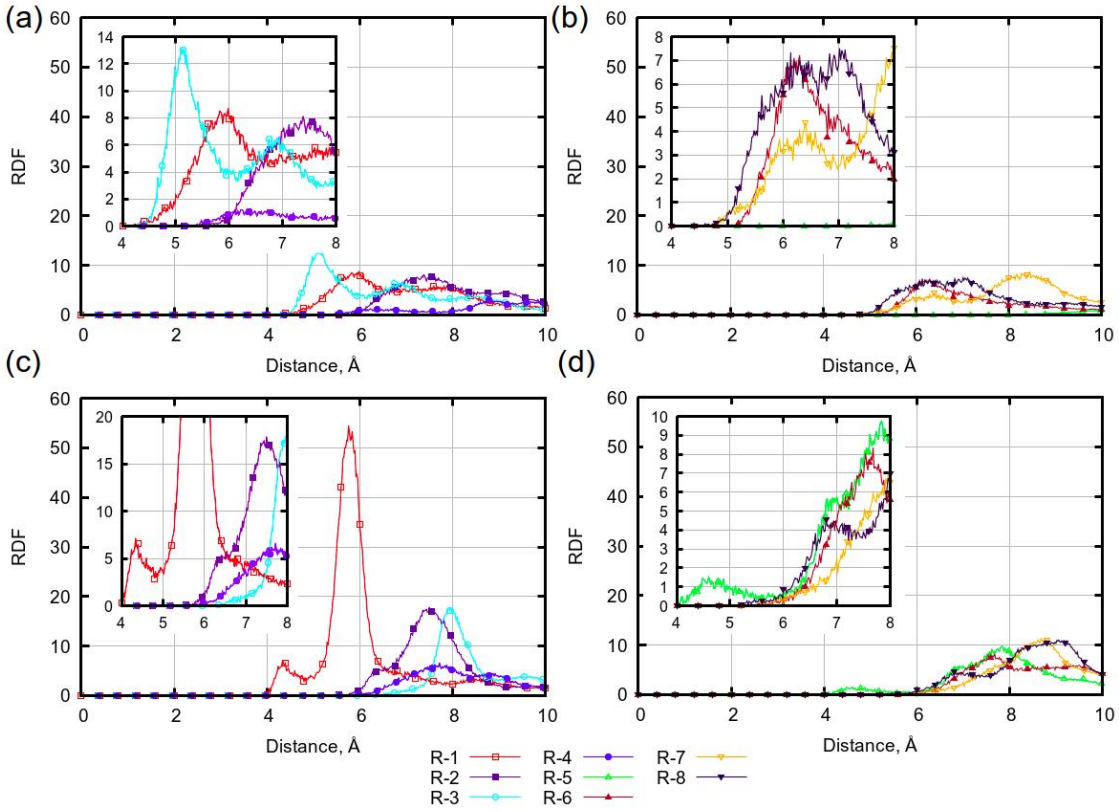

Figure S63 Radial distribution functions between centers of mass of head-groups of DLin-MC3-DMA and residues of polyU 5% of DLin-MC3-DMA. (a) and (b) are for simulations with neutral DLin-MC3-DMA. (c) and (d) are for simulations with ionized DLin-MC3-DMA. Letter R with a number stands for a certain residue. Please note the difference in scale of the y axis.

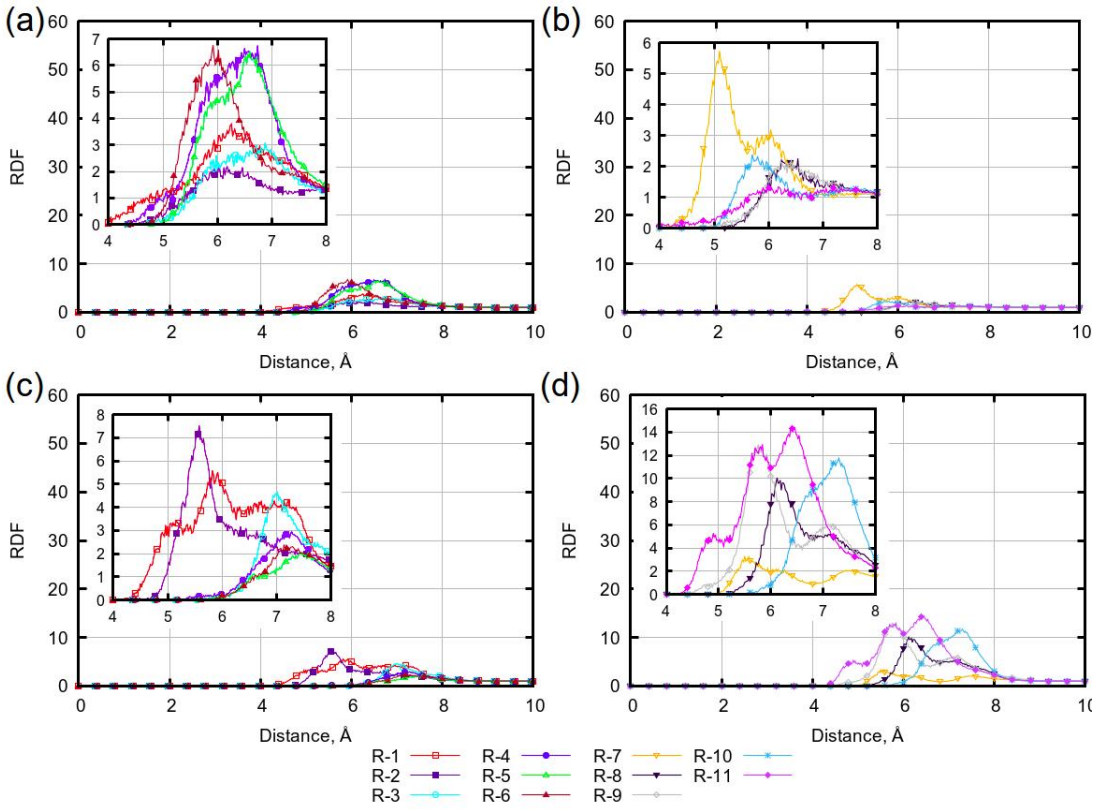

Figure S64 Radial distribution functions between centers of mass of head-groups of DLin-MC3-DMA and residues of polyA for simulations with 15% of DLin-MC3-DMA. (a) and (b) are for simulations with neutral DLin-MC3-DMA. (c) and (d) are for simulations with ionized DLin-MC3-DMA. Letter R with a number stands for a certain residue. Please note the difference in scale of the y axis.

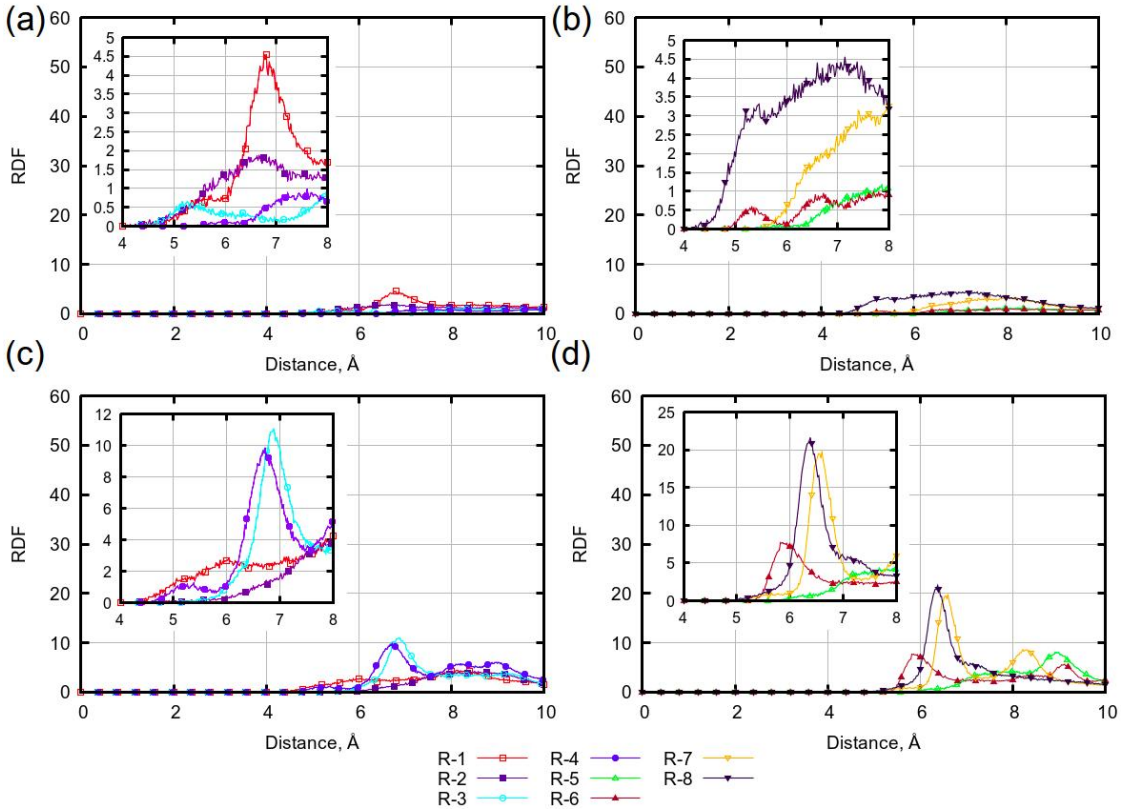

Figure S65 Radial distribution functions between centers of mass of head-groups of DLin-MC3-DMA and residues of polyU for simulations with 15% of DLin-MC3-DMA. (a) and (b) are for simulations with neutral DLin-MC3-DMA. (c) and (d) are for simulations with ionized DLin-MC3-DMA. Letter R with a number stands for a certain residue. Please note the difference in scale of the y axis.

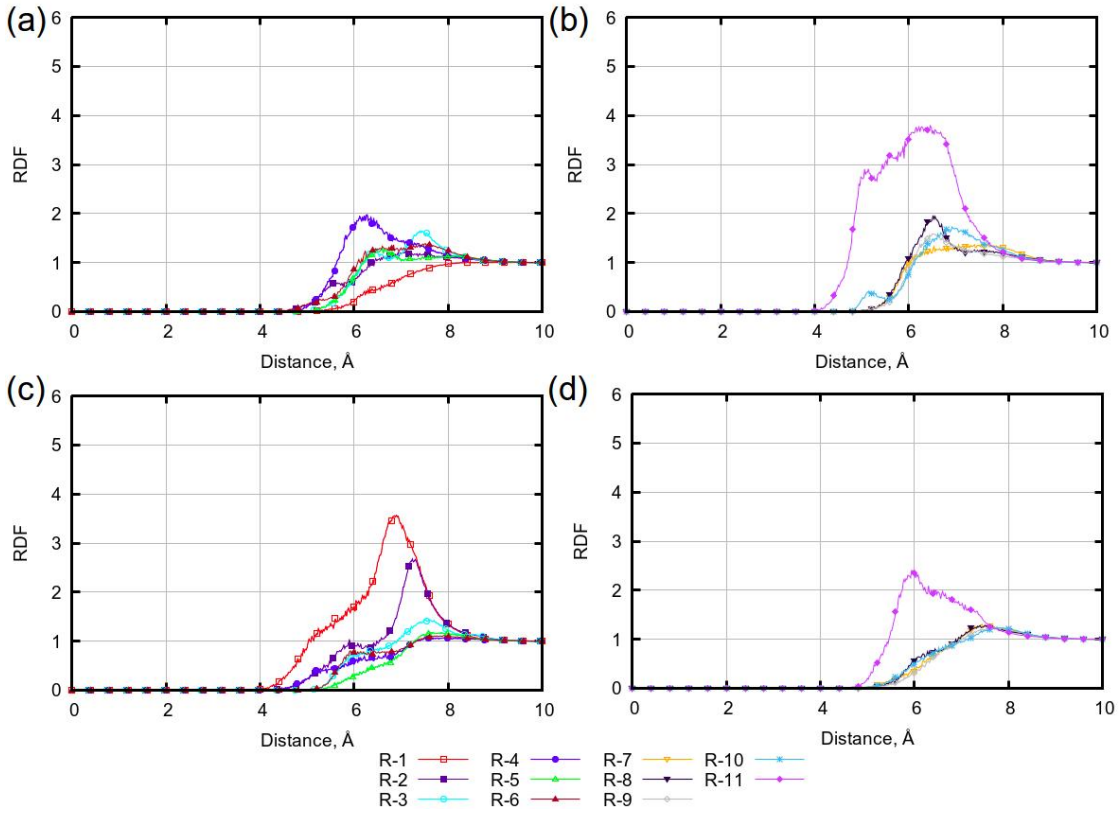

Figure S66 Radial distribution functions between centers of mass of phosphatic groups of phospholipids and residues of polyA for simulations with 5% of DLin-MC3-DMA. (a) and (b) are for simulations with neutral DLin-MC3-DMA. (c) and (d) are for simulations with ionized DLin-MC3-DMA. Letter R with a number stands for a certain residue.

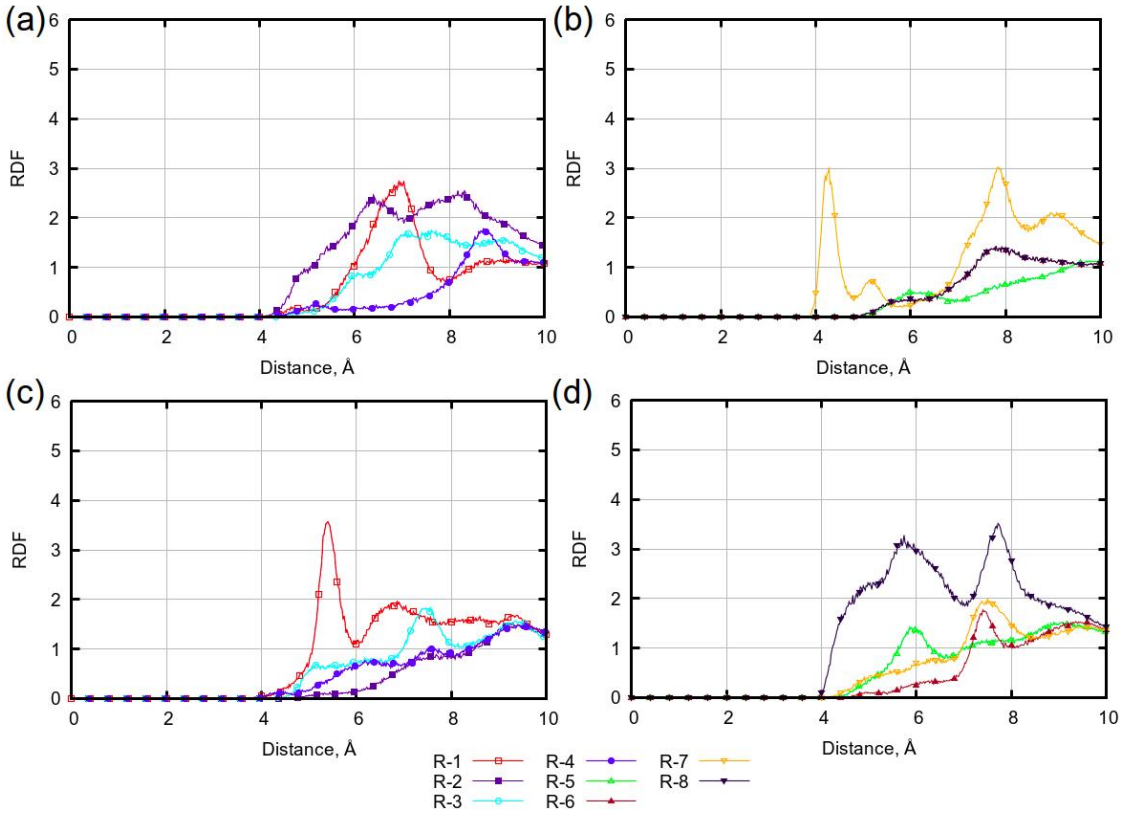

Figure S67 Radial distribution functions between centers of mass of phosphatic groups of phospholipids and residues of polyU 5% of DLin-MC3-DMA. (a) and (b) are for simulations with neutral DLin-MC3-DMA. (c) and (d) are for simulations with ionized DLin-MC3-DMA. Letter R with a number stands for a certain residue.

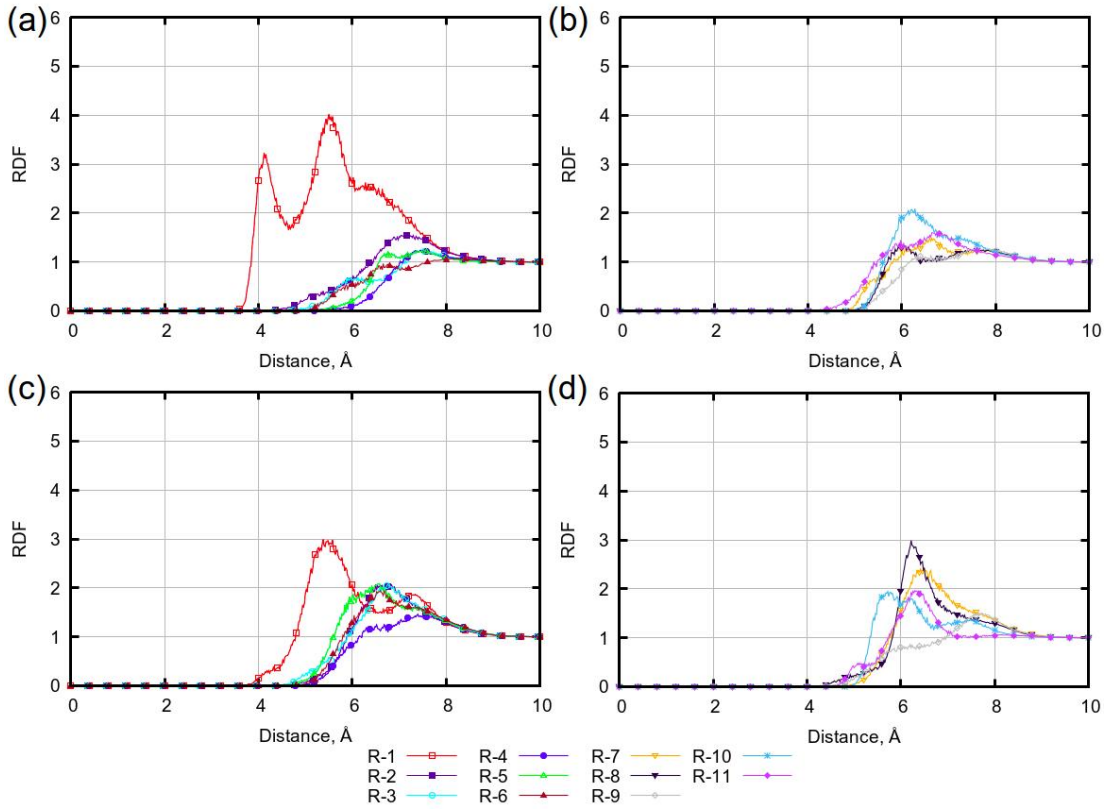

Figure S68 Radial distribution functions between centers of mass of phosphatic groups of phospholipids and residues of polyA for simulations with 15% of DLin-MC3-DMA. (a) and (b) are for simulations with neutral DLin-MC3-DMA. (c) and (d) are for simulations with ionized DLin-MC3-DMA. Letter R with a number stands for a certain residue.

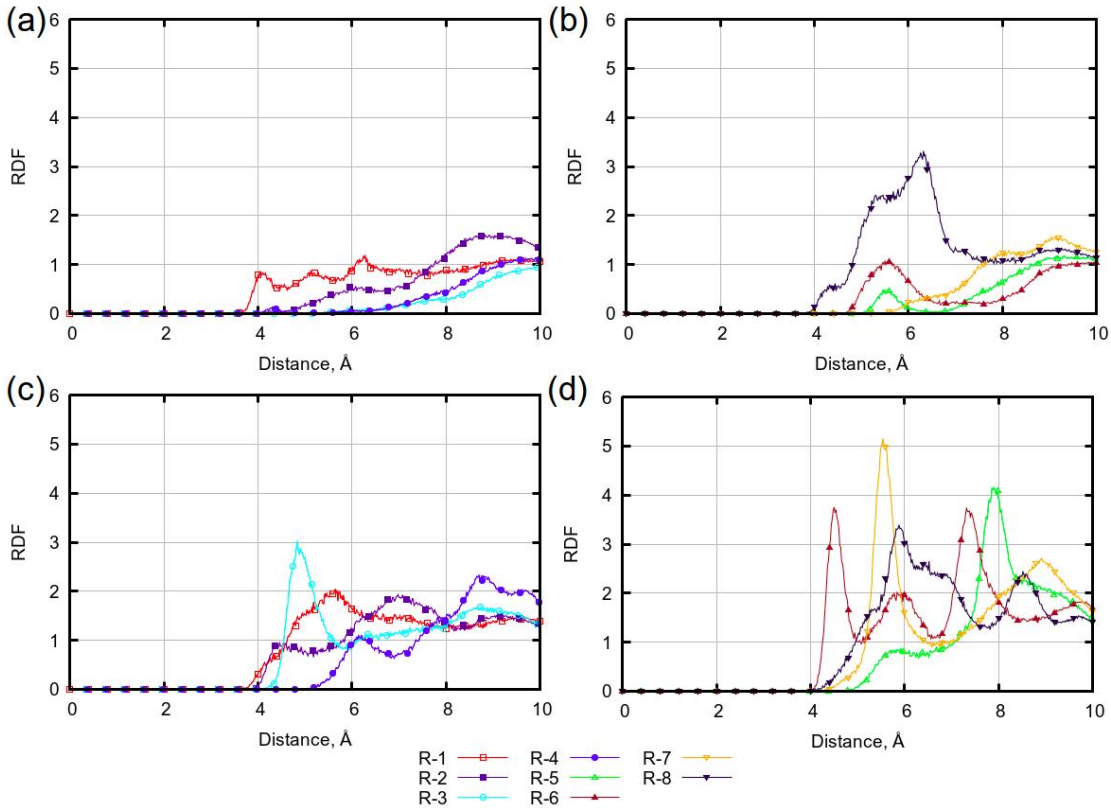

Figure S69 Radial distribution functions between centers of mass of phosphatic groups of phospholipids and residues of polyU for simulations with 15% of DLin-MC3-DMA. (a) and (b) are for simulations with neutral DLin-MC3-DMA. (c) and (d) are for simulations with ionized DLin-MC3-DMA. Letter R with a number stands for a certain residue.

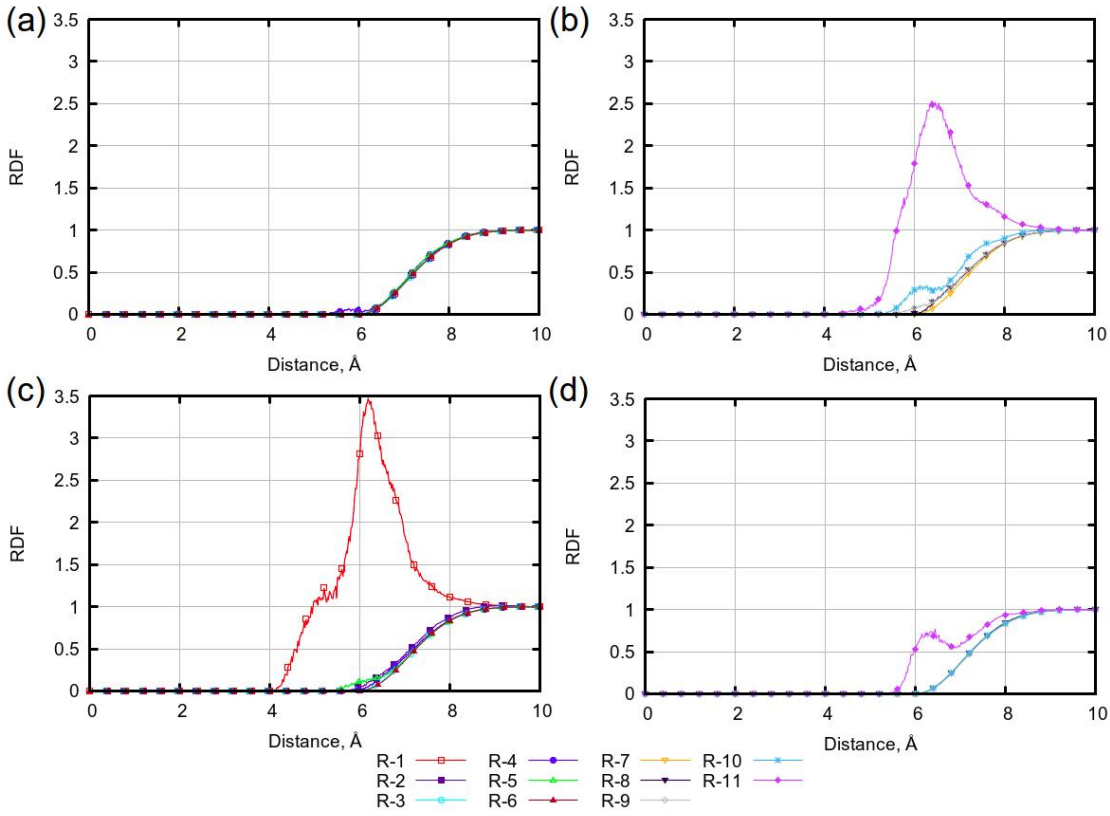

Figure S70 Radial distribution functions between centers of mass of carboxylic groups of phospholipids and residues of polyA for simulations with 5% of DLin-MC3-DMA. (a) and (b) are for simulations with neutral DLin-MC3-DMA. (c) and (d) are for simulations with ionized DLin-MC3-DMA. Letter R with a number stands for a certain residue.

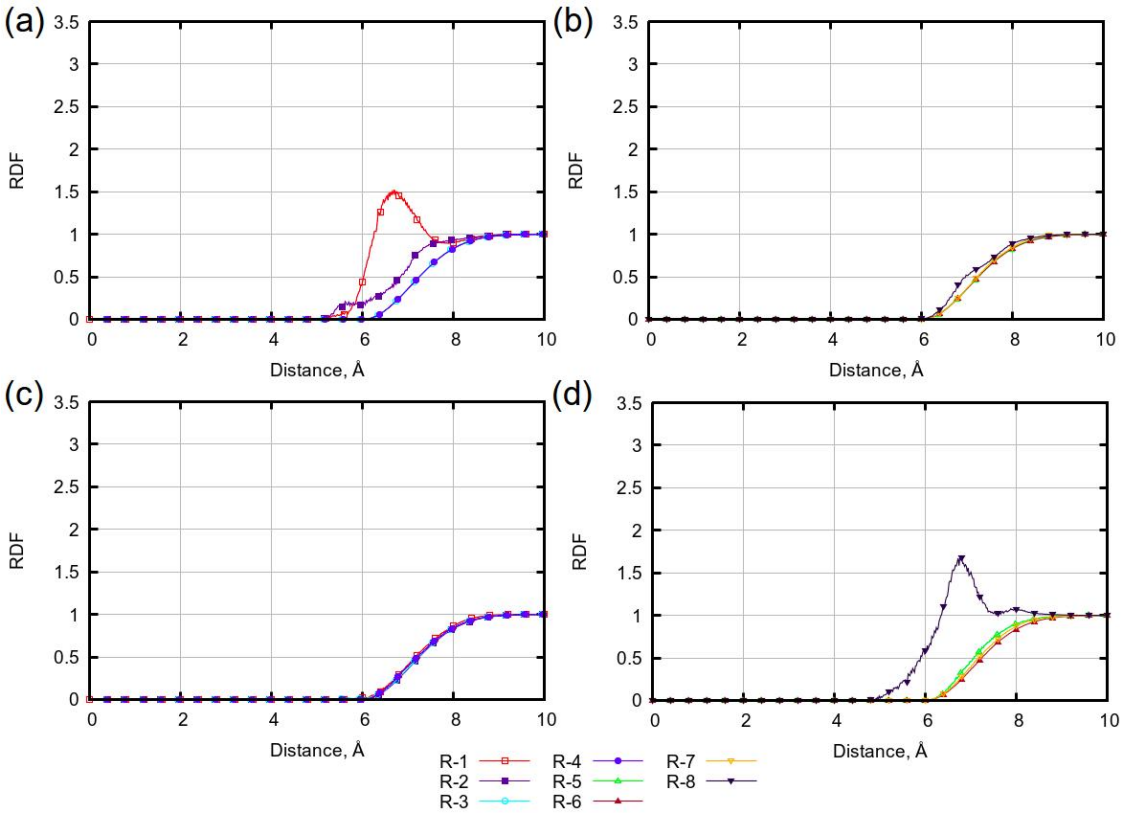

Figure S71 Radial distribution functions between centers of mass of carboxylic groups of phospholipids and residues of polyU 5% of DLin-MC3-DMA. (a) and (b) are for simulations with neutral DLin-MC3-DMA. (c) and (d) are for simulations with ionized DLin-MC3-DMA. Letter R with a number stands for a certain residue.

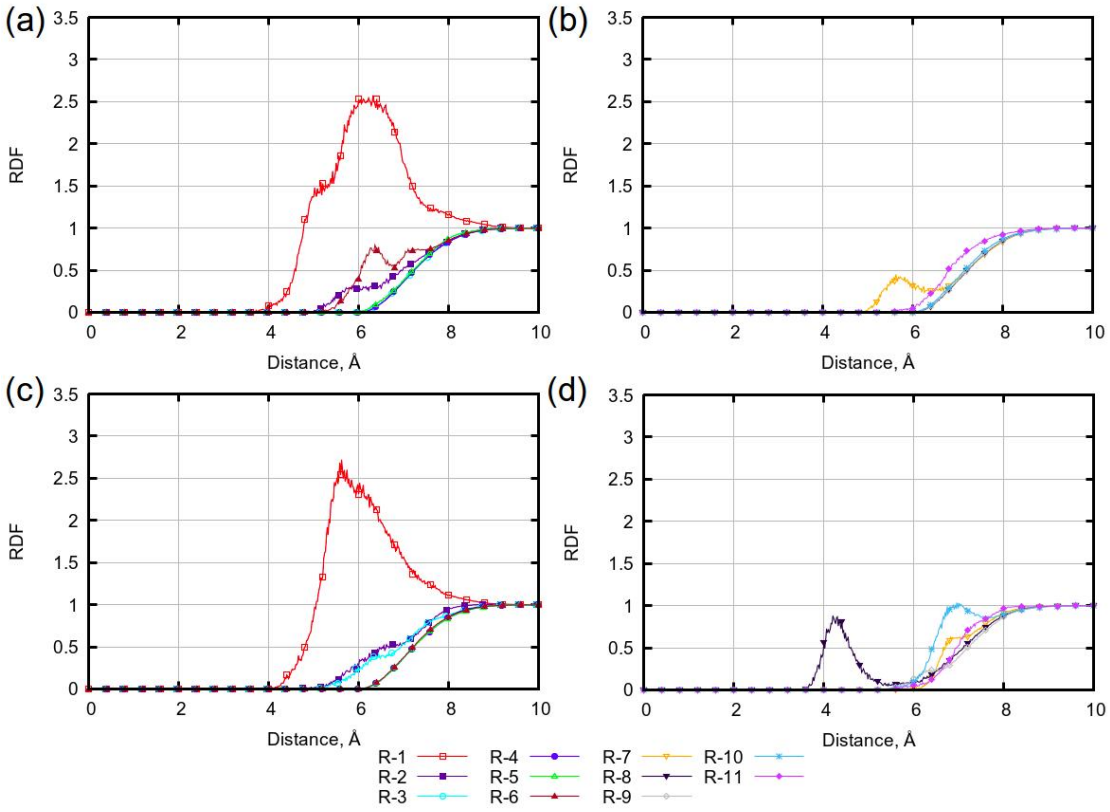

Figure S72 Radial distribution functions between centers of mass of carboxylic groups of phospholipids and residues of polyA for simulations with 15% of DLin-MC3-DMA. (a) and (b) are for simulations with neutral DLin-MC3-DMA. (c) and (d) are for simulations with ionized DLin-MC3-DMA. Letter R with a number stands for a certain residue.

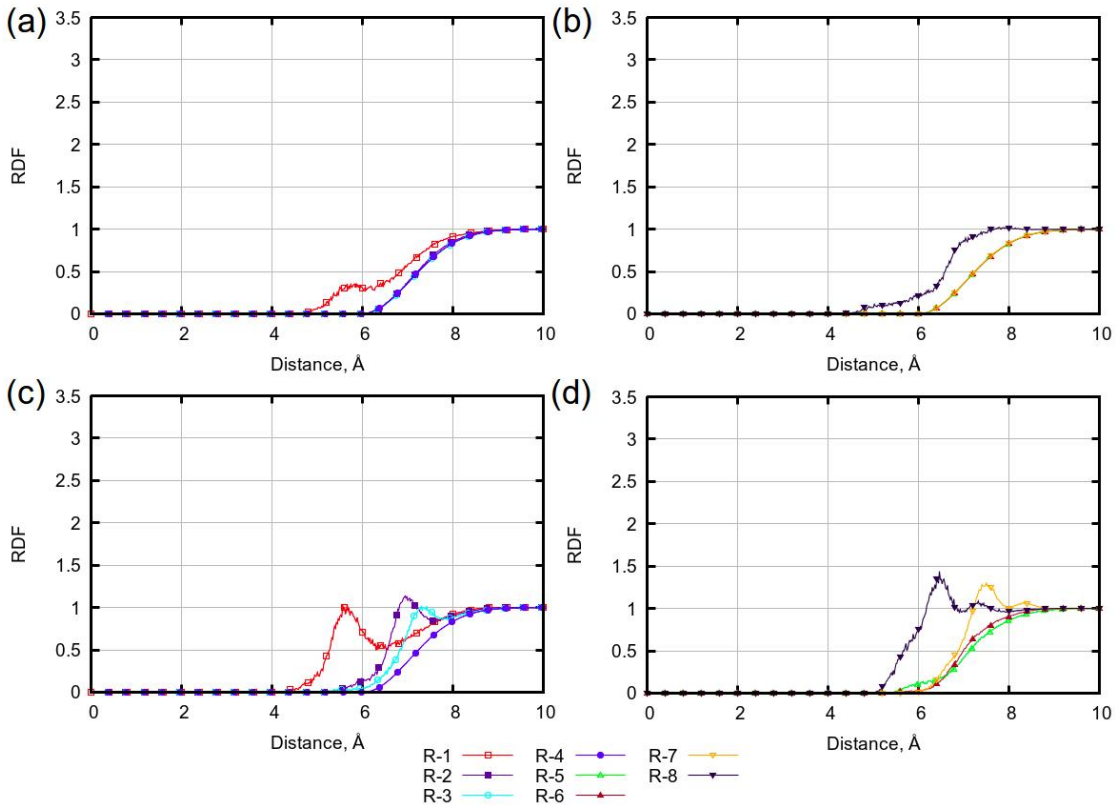

Figure S73 Radial distribution functions between centers of mass of carboxylic groups of phospholipids and residues of polyU for simulations with 15% of DLin-MC3-DMA. (a) and (b) are for simulations with neutral DLin-MC3-DMA. (c) and (d) are for simulations with ionized DLin-MC3-DMA. Letter R with a number stands for a certain residue.

3.8 Hydrogen bonding

System	DOPC-wat.	MC3-DOPC	DOPC-NA	MC3-wat.	MC3-NA	NA-wat.
5% (neut.)	1221 ± 5	0 ± 0	-	6 ± 1	-	-
5% (char.)	1218 ± 5	5 ± 1	-	10 ± 1	-	-
5% (neut., polyA)	1201 ± 5	0 ± 0	2 ± 1	7 ± 1	0 ± 1	419 ± 15
5% (char., polyA)	1200 ± 5	6 ± 1	7 ± 1	8 ± 1	1 ± 1	418 ± 15
5% (neut., polyU)	1179 ± 5	0 ± 0	6 ± 1	8 ± 1	0 ± 0	254 ± 12
5% (char., polyU)	1213 ± 5	2 ± 1	5 ± 1	9 ± 1	3 ± 1	285 ± 15
15% (neut.)	1116 ± 5	0 ± 0	-	20 ± 1	-	-
15% (char.)	1073 ± 5	15 ± 1	-	26 ± 1	-	-
15% (neut., polyA)	1072 ± 5	0 ± 0	7 ± 1	17 ± 1	0 ± 0	409 ± 15
15% (char., polyA)	1038 ± 5	16 ± 1	6 ± 1	26 ± 1	4 ± 1	412 ± 15
15% (neut., polyU)	1101 ± 5	0 ± 0	0 ± 1	20 ± 1	0 ± 0	270 ± 12
15% (char., polyU)	1053 ± 5	17 ± 1	11 ± 1	25 ± 1	2 ± 1	263 ± 12

Table S18 Hydrogen bonds in simulated systems computed at the distance of 0.35 nm.

Notes and references

[1] V. F. Sears, *Neutron News*, 1992, **3**, 26–37.

[2] M. Y. Arteta, T. Kjellman, S. Bartesaghi, S. Wallin, X. Wu, A. J. Kvist, A. Dabkowska, N. Székely, A. Radulescu, J. Bergenholtz and L. Lindfors, *Proceedings of the National Academy of Sciences*, 2018, **115**, E3351–E3360.

[3] R. S. Armen, O. D. Uitto and S. E. Feller, *Biophysical Journal*, 1998, **75**, 734–744.

[4] A. I. Greenwood, S. Tristram-Nagle and J. F. Nagle, *Chemistry and Physics of Lipids*, 2006, **143**, 1–10.

[5] W.-J. Sun, R. M. Suter, M. A. Knewtson, C. R. Worthington, S. Tristram-Nagle, R. Zhang and J. F. Nagle, *Phys. Rev. E*, 1994, **49**, 4665–4676.

[6] S. Bottaro, G. Bussi, G. Pinamonti, S. Reißer, W. Boomsma and K. Lindorff-Larsen, *Rna*, 2019, **25**, 219–231.